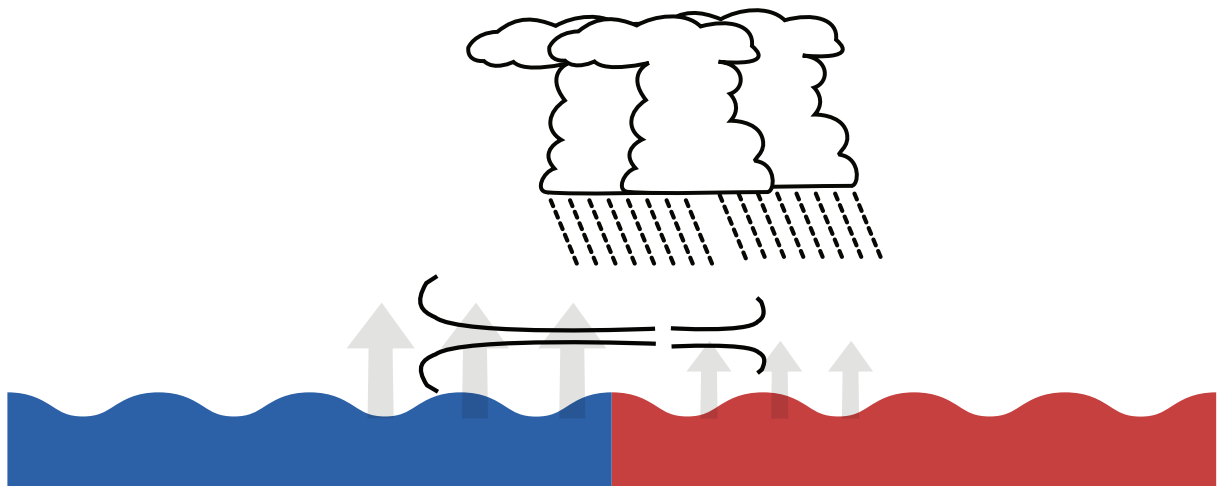




Sensitivity of Resolved Convection to Ocean and Land Surfaces in the Tropical Atlantic and Amazon Basin



Laura Giulianna Paccini Peña

Hamburg 2022

Hinweis

Die Berichte zur Erdsystemforschung werden vom Max-Planck-Institut für Meteorologie in Hamburg in unregelmäßiger Abfolge herausgegeben.

Sie enthalten wissenschaftliche und technische Beiträge, inklusive Dissertationen.

Die Beiträge geben nicht notwendigerweise die Auffassung des Instituts wieder.

Die "Berichte zur Erdsystemforschung" führen die vorherigen Reihen "Reports" und "Examensarbeiten" weiter.

Anschrift / Address

Max-Planck-Institut für Meteorologie
Bundesstrasse 53
20146 Hamburg
Deutschland

Tel./Phone: +49 (0)40 4 11 73 - 0
Fax: +49 (0)40 4 11 73 - 298

name.surname@mpimet.mpg.de
www.mpimet.mpg.de

Notice

The Reports on Earth System Science are published by the Max Planck Institute for Meteorology in Hamburg. They appear in irregular intervals.

They contain scientific and technical contributions, including PhD theses.

The Reports do not necessarily reflect the opinion of the Institute.

The "Reports on Earth System Science" continue the former "Reports" and "Examensarbeiten" of the Max Planck Institute.

Layout

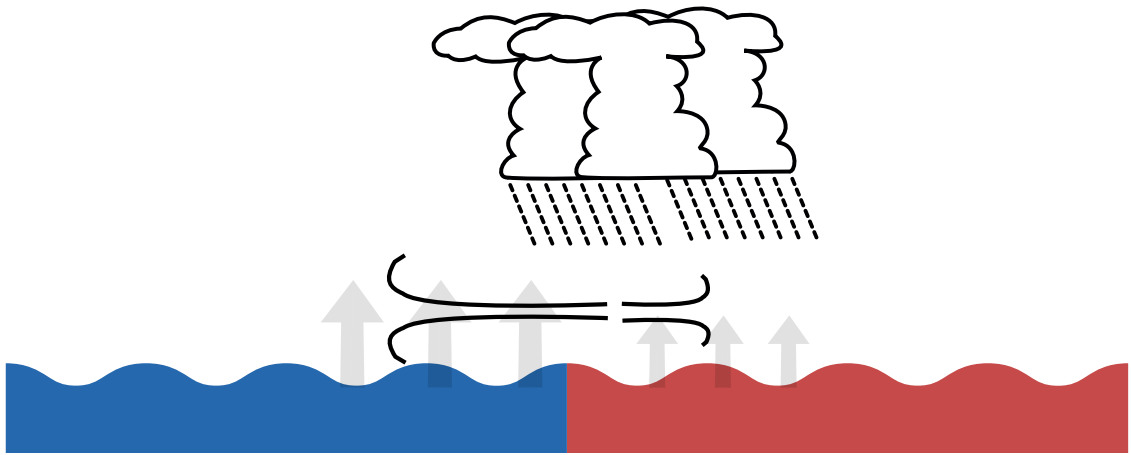
*Bettina Diallo and Norbert P. Noreiks
Communication*

Copyright

*Photos below: ©MPI-M
Photos on the back from left to right:
Christian Klepp, Jochem Marotzke,
Christian Klepp, Clotilde Dubois,
Christian Klepp, Katsumasa Tanaka*



Sensitivity of Resolved Convection to Ocean and Land Surfaces in the Tropical Atlantic and Amazon Basin



Laura Giulianna Paccini Peña

Hamburg 2022

Laura Julianna Paccini Peña

aus Lima, Peru

Max-Planck-Institut für Meteorologie
The International Max Planck Research School on Earth System Modelling
(IMPRS-ESM)
Bundesstrasse 53
20146 Hamburg

Tag der Disputation: 9. Dezember 2021

Folgende Gutachter empfehlen die Annahme der Dissertation:

Dr. Cathy Hohenegger
Prof. Dr. Bjorn Stevens

Vorsitzender des Promotionsausschusses:

Prof. Dr. Hermann Held

Dekan der MIN-Fakultät:

Prof. Dr. Heinrich Graener

Laura Giulianna Paccini Peña

Sensitivity of Resolved Convection to Ocean and Land
Surfaces in the Tropical Atlantic and Amazon Basin

ABSTRACT

Surface interactions modulate precipitating convection in the tropics. However, convective parameterizations fail in representing tropical precipitation and its interactions with the surface. In recent years, the increased use of "storm-resolving" simulations has shown promising improvements on the simulation of precipitation. In this dissertation, we investigate the sensitivity of resolved convection to its underlying surface from seasonal timescales over ocean to diurnal variations over land in the tropical Atlantic sector.

Over ocean, we tackle the interaction of resolved convection and the sea surface temperature (SST) related to the Atlantic Meridional Mode (AMM) with uncoupled and coupled simulations. We investigate whether the explicit representation of convection leads to i) a robust precipitation response to the AMM and ii) a weaker coupling with SST in contrast to simulations that parameterize convection. We show that the precipitation response to the AMM can be interpreted as a meridional shift of the mean-state precipitation towards the warmer hemisphere. Simulations with explicit (E-CON) and parameterized (P-CON) convection exhibit a similar shift, of about 1° , despite of their distinct mean-state precipitation. In contrast, E-CON exhibits stronger mean-state surface winds which translates into greater wind-driven latent heat flux, and can potentially produce stronger changes in the SST anomalies. We test this hypothesis with coupled simulations. Both the precipitation and SST anomalies respond differently to the AMM during its decay from May to July. In May, the shift of the mean-state precipitation in E-CON is consistent with the uncoupled simulations demonstrating a robust precipitation response to the AMM; whereas the P-CON simulations exhibit a displacement of 2° . Moreover, the cooling of SST is stronger in E-CON than in P-CON. This is influenced by wind-driven latent heat flux anomalies, which are larger in E-CON and lead to a stronger cooling by 0.5 to 1.5K. The wind-driven latent heat flux explains a significant part of the total SST cooling in E-CON (67%) as compared to P-CON (48%), which agrees with the proposed hypothesis.

Over land, we investigate whether improvements in the representation of precipitation with explicit convection can be attributed to the representation of organized convective systems in the Amazon. We identify that the distribution of precipitation intensity and the diurnal cycle are the precipitation features with major improvements by the E-CON simulations. Light and high intensity precipitation rates are particularly well reproduced by E-CON, whereas they remain biased in P-CON. The E-CON simulations, unlike P-CON, also reproduce the heterogeneous times of maximum precipitation, with most regions featuring their maximum rain in the afternoon (18h-20h), but others depicting a rain peak overnight. The precipitation associated with organized convective systems display overnight precipitation peaks between 1h-6h in E-CON, which enables the representation of heterogeneous times of maximum precipitation as in observations. Moreover, the simulated diurnal evolution of the size and intensity of organized convective systems is consistent with their observed life cycle. We show that E-CON simulates a realistic diurnal cycle of organized convective systems, which helps to improve the overall representation of the precipitation diurnal cycle.

ZUSAMMENFASSUNG

Oberflächeninteraktionen modellieren die niederschlagsbringende Konvektion in den Tropen. Konvektive Parametrisierungen versagen jedoch bei der Darstellung tropischer Niederschläge und ihren Wechselwirkungen mit der Oberfläche. In den letzten Jahren hat der verstärkte Einsatz von Sturmauflösenden Simulationen vielversprechende Verbesserungen bei der Simulation von Niederschlägen gezeigt. In dieser Dissertation untersuchen wir die Empfindlichkeit der aufgelösten Konvektion gegenüber der darunter liegenden Oberfläche von saisonalen Zeitskalen über dem Ozean bis hin zu tageszeitlichen Schwankungen über dem Land im tropischen Atlantiksektor.

Über dem Ozean beschäftigen wir uns mit der Wechselbeziehung von explizit aufgelöster Konvektion mit der Meeresoberflächentemperatur (engl. *sea surface temperature*; SST) im Kontext des Atlantischen Meridionalen Modus (AMM) in gekoppelten und entkoppelten Simulationen. Wir untersuchen ob explizit aufgelöste Konvektion i) zu einer robusten Darstellung der Niederschläge in Reaktion auf den AMM führt und ii) weniger stark an SST gekoppelt ist im Vergleich mit Simulationen mit parametrisierter Konvektion. Wir zeigen, dass die Reaktion des Niederschlags auf den AMM als meridionale Verlagerung des mittleren Niederschlags hin zur wärmeren Hemisphäre interpretiert werden kann. Sowohl Simulationen mit expliziter (E-CON), als auch solche mit parametrisierter Konvektion (P-CON) zeigen die gleiche Verlagerung um etwa 1° , obwohl sie sich in der mittleren Menge des Niederschlags unterscheiden. In den E-CON Simulationen herrschen im Vergleich zu P-CON stärkere Bodenwinde, die zu größeren, wind-getriebenen Flüssen von latenter Wärme führen und das Potential haben stärkere SST-Anomalien hervorzurufen. Diese Hypothese testen wir mit gekoppelten Simulationen. Niederschlag und SST-Anomalien reagieren beide unterschiedlich auf den Abklang des AMM zwischen Mai und Juli. Die Verschiebung des mittleren Niederschlags im Monat Mai ist in E-CON in Übereinstimmung mit den entkoppelten Simulationen und zeigt eine belastbare Reaktion des Niederschlags auf den AMM – in P-CON hingegen verschiebt sich der Niederschlag um 2° . Außerdem ist die Kühlung der Meeresoberfläche in E-CON 0.5 bis 1.5 K stärker als in P-CON. Wind-getriebene Flüsse latenter Wärme, die in E-CON stärker ausgeprägt sind, sind der Auslöser für dieses Verhalten. Diese Wärmeflüsse erklären einen signifikanten Teil der Absenkung der SST (67%; im Vergleich zu 48% in P-CON), was mit der vorgeschlagenen Hypothese übereinstimmt.

Über Land untersuchen wir, ob Verbesserungen der Darstellung globaler Niederschläge auf die Verbesserung der Darstellung von organisierten Konvektionssystemen im Amazonasbecken zurückzuführen ist. Wir stellen fest, dass die Bereiche, die die größten Verbesserungen durch explizite Konvektion erfahren, die Verteilung der Intensität des Niederschlags und die Darstellung des Tageszyklus sind. E-CON bildet Leicht- und Starkregenereignisse besonders gut ab. In P-CON bleibe diese auch bei hoher Auflösung verzerrt. E-CON Simulationen bilden auch – anders als P-CON – die verschiedene Zeitliche Verteilung von Regen gut ab, der in den meisten Regionen nachmittags (18 bis 20 Uhr), andernorts aber bevorzugt nachts fällt. Niederschläge, die mit organisierten konvektiven Systemen assoziiert sind, zeigen in E-CON nächtliche Niederschlagsspitzen zwischen 1 und 6 Uhr. Diese Darstellung von maximalem Niederschlag zu verschiedenen Tageszeiten steht im Einklang mit Beobachtungen. Auch die Entwicklung von Größe und Stärke der organisierten konvektiven System im Tagesverlauf stimmt mit ihrem in der

Natur beobachtetem Lebenszyklus überein. Wir zeigen, dass E-CON einen realistischen Tag-Nacht-Zyklus organisierter konvektiver Systeme simuliert, was zu eine besseren Darstellung des Tag-Nacht-Zyklusses insgesamt führt.

PUBLICATIONS RELATED TO THIS DISSERTATION

Appendix A:

Paccini, L., Hohenegger, C. & Stevens, B. (2021). "Explicit versus parameterized convection in response to the Atlantic Meridional Mode", *Journal of Climate* 34(9), pp.3343-3354. <https://doi.org/10.1175/JCLI-D-20-0224.1>

Appendix B:

Paccini, L., Hohenegger, C. & Stevens, B. (2021). "Atmosphere-ocean coupling related to the Atlantic Meridional Mode in simulations with explicit and parameterized convection"

Appendix C:

Paccini, L., Stevens, B. & Hohenegger, C. (2021). "Value of storm-resolving simulations for the representation of Amazon rainfall", *In preparation*

ACKNOWLEDGMENTS

First, I would like to thank my supervisors Cathy and Bjorn, for all their support through these years. Having such great scientists as mentors was an honor to me. Many thanks to Cathy for her disposition to provide detailed advice and feedback as many times as necessary. Thanks to Bjorn for his patience to explaining things, but especially, I am very grateful for his constant encouragement.

I thank Martin Claussen for the enjoyable discussions during the panel meetings. Thanks to Daniel Klocke and Guido Cioni for introducing me to the ICON world and assisting me on the multiple technical obstacles I encountered. I also thank my work group, especially Leonore, Geet, Hauke S., Jiawei, Junhong and Julia for their feedback and constructive comments during our Wednesday meetings.

The role of the IMPRS-office team is beyond "regular administrative matters" and I'm very grateful to them. Many thanks to Antje, Connie and Michaela, for their great support since I arrived in Hamburg. Special thanks to Angela Gruber for being so caring and supportive, especially during hard times.

I am very grateful for having met great friends during my stay in Hamburg. I truly appreciate all moments of fruitful discussions at work, enjoyable joint-lunches, pleasant coffee breaks and the many activities outside work. Thanks to my office-mates Hauke S. and Hernan, who literally accompanied me during this journey, thanks for the nice talks and shared quick-breaks. I especially thank Diego for organizing splendid outings and activities. Thanks also to Violeta, David, Jiawei, Mateo, Geet, Pin-hsin, Katherine, Sally, Emily and Hans, for the nice hikings, picnics, lunches and dinners. Special thanks to Diego and Leo, for their encouragement and emotional support through these years, but particularly the last months.

I am most grateful to my family, for their love and unending support. To my parents, to whom I dedicate this thesis. To my sister and brother, for the joyful video-calls that cheered me up every time. And finally, thank you, Bryam. I am infinitely grateful for having you in my life and especially for the enormous support these past months.

CONTENTS

I UNIFYING TEXT

1	INTRODUCTION	2
1.1	Moist convection in the tropics	2
1.2	Surface-precipitation interactions in the tropical Atlantic	3
1.2.1	Over ocean	3
1.2.2	Over land	4
2	SIMULATING TROPICAL PRECIPITATION	6
2.1	Long-standing biases	6
2.2	Insights from a new generation of climate models	7
2.3	Research questions	8
2.4	Modeling strategy	9
3	SUMMARY OF RESULTS	10
3.1	Atmospheric response to the Atlantic Meridional Mode	10
3.2	Atmosphere-ocean coupling in the decay of the Atlantic Meridional Mode	12
3.3	On the representation of the Amazon rainfall by storm-resolving simulations	14
4	CONCLUSIONS AND OUTLOOK	17
4.1	Response to research questions	17
4.2	Unexpected findings	18
4.3	Challenges and opportunities	18
4.3.1	Beyond a realistic simulation	19

II APPENDICES

A	APPENDIX	22
A.1	Introduction	24
A.2	Data and methods	25
A.2.1	Observations	25
A.2.2	Simulations	28
A.3	Sensitivity of precipitation to imposed SST	30
A.3.1	Mean state	30
A.3.2	Response to the AMM-SST pattern	31
A.3.3	Shift in the climatology	33
A.4	Implications for ocean-atmosphere coupling	35
A.5	Summary and conclusions	38
B	APPENDIX	41
B.1	Introduction	44
B.2	Data and methods	45
B.2.1	Observations	45
B.2.2	Model and experimental set-up	45
B.3	Mean state	46
B.4	Atmospheric response	47
B.5	Decay of SST anomalies and the role of wind-driven latent heat flux	49
B.6	Conclusions and final remarks	51

C	APPENDIX	54
B.1	Introduction	56
B.2	Data and methodology	57
B.2.1	Observations	57
B.2.2	CMIP6	57
B.2.3	ICON-NWP	57
B.3	Representation of precipitation	58
B.3.1	Geographic distribution	58
B.3.2	Frequency and intensity	60
B.3.3	Diurnal cycle	61
B.4	Organized convective systems	62
B.4.1	Size and intensity	63
B.4.2	Diurnal cycle	64
B.5	Summary and conclusion	65
	BIBLIOGRAPHY	69

ACRONYMS

AMM	Atlantic Meridional Mode
CMIP	Coupled Model Intercomparison Project
CMORPH	Climate prediction center MORPHing technique
GCM	General Circulation Model
HadISST	Hadley Centre Global Sea Ice and Sea Surface Temperature
ICON	ICO-saedral Non-hydrostatic
ITCZ	Inter-Tropical Convergence Zone
NCEP	National Centers for Environmental Prediction
NWP	Numerical Weather Prediction
SST	Sea Surface Temperature
TRMM	Tropical Rainfall Measuring Mission

Part I

UNIFYING TEXT

INTRODUCTION

Rain is grace; rain is the sky
descending to the earth; without
rain, there would be no life.

(John Updike)

1.1 MOIST CONVECTION IN THE TROPICS

The process of rising air is what we commonly understand by convection, in simple terms. Atmospheric moist convection arises in response to thermal instability, induced by the solar radiation. Over the Earth, the tropics are where most convective activity occurs given the abundant solar energy they receive. As a result, a belt of cumulus clouds and precipitation, manifestation of moist convection, stands out in the tropics.

Convection in the tropics has global effects. Tropical convection regulates the atmospheric temperature by releasing latent heat against radiative cooling (Manabe and Strickler, 1964). Deep precipitating convection drives the rising motion near the Equator setting a global circulation (i.e. the Hadley circulation) for the redistribution of energy towards high latitudes. Precipitating convection also undergoes water-phase changes and releases great heat amounts in the atmosphere, which perturbs the large-scale circulation (Gill, 1980) even in the short-term (e.g. Kiladis and Weickmann, 1992). In this way, tropical convection and associated precipitation play an important role in determining global weather and climate.

Not only global, but regional and especially local effects of tropical rainfall are important for living beings. The tropics cover around 40% of the Earth's surface and host very vulnerable populations, including over 40% of the human population and over 60% of the total biodiversity (Penny et al., 2020). Tropical populations depend on precipitation for subsisting and development. For instance, floods and droughts can damage agriculture, affecting societies and economies (e.g. Marengo and Espinoza, 2016; Gao et al., 2019). Entire ecosystems also rely on tropical rain and even small changes of precipitation can alter the hygric niche of species (Boyle et al., 2020).

Because of the global and local effects of rain in the tropics, great interest has been devoted to studying tropical rain and the influencing factors determining its location, timing, intensity and frequency. Studies based on observations and on a hierarchy of numerical simulations have documented precipitation variability and its interaction with the environment. For instance, over tropical oceans, changes in the spatial distribution of precipitation have been linked to changes in the sea surface temperature (SST) from seasonal to decadal timescales (e.g. Deser et al., 2010). Over land, tropical precipitation is also affected by SST variations albeit their effects are the result of complex interactions, including remote effects (e.g. Fontaine and Janicot, 1996; Nobre and Shukla, 1996; Lucena et al., 2011). Variations of precipitation over land are notably stronger at short timescales in contrast to the ocean. For instance, during the Amazon dry season, daytime precipitation is influenced by land-atmosphere interactions; whereas nocturnal rain is modulated by propagating systems (Ghate and Kollias, 2016). Land surface heterogeneities such as

vegetation and elevated topography can also induce meso and local scale circulations affecting the diurnal cycle of precipitation.

Given the complex interactions of precipitating convection across spatio-temporal scales and different surface environments, it is difficult to fully understand the tropical precipitation system. The inability of conventional climate models to adequately represent tropical precipitation and its various interactions adds to this problem. Therefore, in this dissertation, we study how the interaction of convection and its underlying surface could affect precipitation by using numerical simulations where convection is explicitly resolved.

In the following section, I present two detailed examples of how tropical precipitation can interact with the ocean surface at a seasonal timescale, and over land at diurnal timescales. These comprise the tropical Atlantic ocean and tropical South American regions which are also the focus of analysis in this dissertation.

1.2 SURFACE-PRECIPIATION INTERACTIONS IN THE TROPICAL ATLANTIC

1.2.1 Over ocean

Variability in the SST directly affects the spatial distribution of precipitation over the ocean. The leading mode of coupled ocean-atmosphere variability in the tropical Atlantic is the Atlantic Meridional Mode (AMM; e.g. Nobre and Shukla, 1996; Chiang and Vimont, 2004). The AMM is a mode of inter-annual variability which depicts the strongest signal during March-May (boreal spring) season. The spatial structure of the AMM features a meridional dipole of SST anomalies. In the case of a positive AMM, positive SST anomalies of about 0.5K to 0.8K are placed up to 30°N; whereas negative anomalies of about 0.3K to 0.5K are located at about 10°S (see red contours in Fig.1.1a). Opposite conditions characterize the negative phase of the AMM.

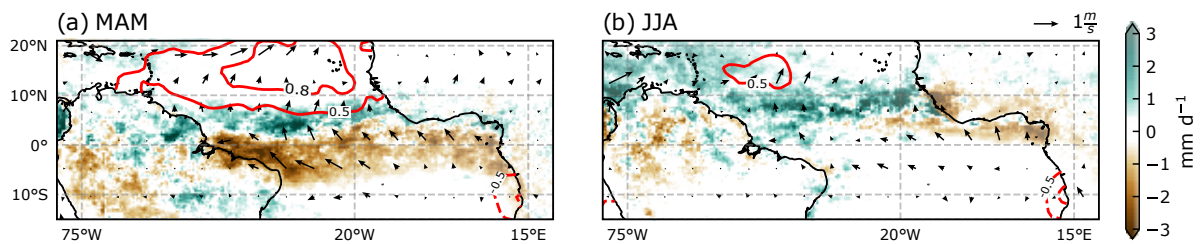


Figure 1.1: Composite of positive Atlantic Meridional Mode (AMM) strong¹events (1998-2013) from (a) its peak signal in boreal spring (MAM) to (b) its decay in boreal summer (JJA). The variables shown are: precipitation (TRMM ; shading), SST (HadISST; contours) and surface wind anomalies (NCEP reanalysis; vectors).

The inter-hemispheric difference of SST modifies the pressure gradient in the boundary layer (Lindzen and Nigam, 1987) which drives a cross-equatorial surface wind flow towards the warmer hemisphere (e.g. Nobre and Shukla, 1996; Chiang et al., 2002; Chiang and Vimont, 2004; Hu and Huang, 2006) (see vectors in Fig.1.1a). The tropical precipitation band, also known as the Inter-tropical Convergence Zone (ITCZ), is meridionally displaced towards the warmer hemisphere (see shaded precipitation anomalies in Fig.1.1a). Changes in the confluence of surface winds over the ocean (Nobre and Shukla,

¹ See Section 3 and Appendix A for more details.

1996) and precipitation anomalies over the neighbouring continents (e.g. Hastenrath and Greischar, 1993) have provided evidences of the meridional ITCZ shift in observations. Regions such as the Sahel in Africa, and the Northeast of Brazil can experience drought episodes during a positive AMM; whereas wet spells have been noticed in the northern Amazon. The effects of the AMM are also perceived in boreal summer, although the signal of SST anomalies and cross-equatorial wind are reduced (Fig. 1.1b). Past studies have linked the effects of the AMM in boreal spring on the next season by preconditioning the ocean-atmosphere environment. Positive AMM events can enhance precipitation over the Caribbean (Taylor et al., 2002, see also Fig. 1.1) and favor the occurrence of hurricanes in the north tropical Atlantic (Vimont and Kossin, 2007).

The coupled variability of the AMM and associated precipitation are not correctly represented by climate models (e.g. Amaya et al., 2017; Myers et al., 2018). Even when isolating the atmospheric response from the ocean forcing, the agreement among models in the precipitation response to the AMM is not robust (Wang and Carton, 2003). Moreover, such assessment is done qualitatively and a metric that quantifies the precipitation response to the AMM (i.e. the meridional precipitation shift) is missing.

One of the reasons why climate models cannot represent the coupled variability of the AMM is their inability to realistically simulate the AMM driving mechanisms (e.g. Amaya et al., 2017; Myers et al., 2018). In the following, I briefly explain each of them.

During the development of the AMM, ocean-atmosphere interactions are at play. The AMM is triggered during boreal winter by stochastic forcing of the surface winds in the subtropical north Atlantic (Nobre and Shukla, 1996; Chiang and Vimont, 2004). Following on the example of the positive AMM, a weakening of the surface winds reduces the latent heat flux, reducing evaporation and favoring a warming of the sea surface. This mechanism, known as the wind-evaporation-SST feedback (Xie and Philander, 1994), drives the growing of the SST anomaly in boreal spring and its southward propagation towards its decay in summer (e.g. Hu and Huang, 2006; Amaya et al., 2017). Amaya et al. (2017) estimated that the change of SST anomalies in the positive AMM from spring to summer, can be explained only by latent heat flux anomalies with good approximation. Another mechanism involves the radiative effect of low clouds (Evan et al., 2013; Myers et al., 2018). Strato-cumulus clouds over the west coast of Africa (at 20°N) are suppressed by warm temperatures, which in turn allow the solar radiation to heat the surface given the reduced amount of clouds. Ship-based observations (Tanimoto and Xie, 2002) and idealized studies (Evan et al., 2013) agree that such radiative effect can delay the Newtonian cooling by about 30% to 40%. A third mechanism is related to the interaction of surface winds and latent heat flux with changes in the mixed layer depth (e.g. Rugg et al., 2016; Kataoka et al., 2019). In a positive AMM, weaker trade winds in the north tropical Atlantic reduce the turbulent flux in the mixed layer, while the reduced evaporation increases buoyancy in the ocean. As a result, the mixed layer depth gets shallower and allows the short wave radiation to amplify the warming.

Several studies have acknowledged the effects of the described mechanisms on the AMM. However, their relative roles in the development of the AMM are still uncertain and require further study.

1.2.2 *Over land*

Land surfaces are distinct from the ocean because of their lower heat capacities, which lead to quicker responses. An example that evidences such difference, is the pronounced diurnal cycle over land. The diurnal cycle of precipitation is primarily modulated by

the solar heating. The incoming solar radiation and warming of the surface, quickly destabilizes the boundary layer after sunrise. As a result, convection develops during the day from small shallow clouds to a deep convective stage that produce precipitation in the late afternoon.

The time of maximum precipitation over land can be influenced by local and mesoscale processes that are induced by the surface (e.g. Janowiak et al., 2005). For instance, elevated topography can influence the precipitation diurnal cycle through thermal circulations (e.g. Junquas et al., 2018). Likewise, land-sea (e.g. Mori et al., 2004) or land-river (e.g. Wu et al., 2021) contrasts can have the same effect by inducing subsidence over water in the afternoon. Land surface heterogeneities also enable the maintenance and propagation of organized convective systems, for instance, through low-level jets (e.g. Anselmo et al., 2020). These provide moisture to such convective systems overnight, which allows longer life spans. The related nocturnal precipitation can delay the onset of convection by cooling and drying the boundary layer overnight; whereas the nocturnal extensive cloud cover can weaken convection by blocking the solar radiation in the following morning (Rickenbach, 2004).

The Amazon basin is an important region that gathers such interactions. Especially during its rainy season, the Amazon atmosphere is very close to saturation and thus, very sensitive to processes on many spatial scales (Betts et al., 2009). As a result, the precipitation diurnal cycle in the Amazon exhibits a spatial variability. Precipitation peaks overnight in the eastern slope of the Andes (e.g. Chavez and Takahashi, 2017; Junquas et al., 2018) and near the Amazon river (e.g. Tanaka et al., 2014) in response to thermally driven circulations. Precipitation peaks at different times in the afternoon and night relate to the propagation of organized convective systems (e.g. Burleyson et al., 2016).

Organized convective systems account for about 50% of the total Amazon rain, especially during boreal summer and spring (e.g. Feng et al., 2021). These systems typically originate near the northeast coast of South America (Greco et al., 1990; Garreaud and Wallace, 1997) and over the central Amazon (Rehbein et al., 2018; Anselmo et al., 2020).

The relationship of diurnal characteristics of Amazon rainfall and organized convection have been mostly studied thanks to observations and satellite data (e.g. Greco et al., 1990; Rickenbach, 2004; Rehbein et al., 2018; Anselmo et al., 2020). These data have made it possible to monitor convection and its spatio-temporal variability. However, less progress has been achieved in understanding the mechanisms of organized convection and its interactions at different scales.

As described in this section, many processes involving the interaction of convection with the large-scale and different surfaces are still not well understood. One of the reasons why, is the inability of climate models to represent such processes. In the following section I provide a general overview of how moist convection is represented by these models.

SIMULATING TROPICAL PRECIPITATION

All models are wrong but some models are useful.

(George E.P. Box)

Beyond the scientific interest of understanding how processes in the climate system occur and interact with each other, the ultimate goal of simulating the climate, and in particular precipitation, is our necessity to know how it is going to change.

Commonly, the representation of tropical precipitation relies on general circulation models (GCMs). These, given their coarse resolution, have to simplify diverse processes through the use of parameterizations. The parameterization of moist convection is, precisely, one important simplification in the representation of atmospheric processes. Its overall purpose is "to formulate the statistical effects of cumulus convection without predicting each individual cloud" (Arakawa, 2004), thus representing the average effects of convection.

2.1 LONG-STANDING BIASES

Years of development in convective parameterizations have shown little progress on improving the representation of tropical rain (Arakawa, 2004). Long-standing systematic biases like the overestimation of light rain frequency and the too-early diurnal precipitation maximum are observed in state-of-the-art climate models (Fiedler et al., 2020). As a consequence, tropical rain bands are still misrepresented regarding their spatial distribution and intensity over ocean and land. Unrealistic features such as the double ITCZ, too intense rain over oceans and too little over regions like the Amazon, are especially pronounced biases in summer seasons (Fig. 2.1).

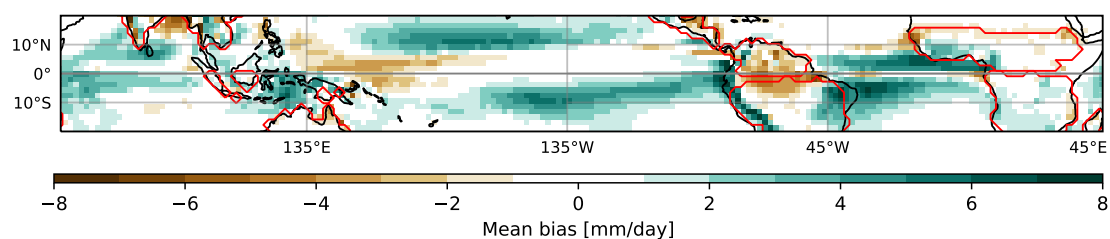


Figure 2.1: Mean bias of CMIP6 summer-time precipitation (December to February in the southern hemisphere, June to August in the northern hemisphere) against TRMM precipitation. The bias is calculated for the climatology of 2000-14. The red contour indicates monsoon regions over land. Adapted from Fiedler et al. (2020)

Not surprisingly, projections of regional seasonal precipitation due to climate change remain highly uncertain (Kent et al., 2015). Moreover, the latest report of the Intergovernmental Panel on Climate Change (Masson-Delmotte et al., 2021) states that most tropical regions display no change in the observed heavy precipitation due to limited

information or low agreement among models; whereas for all tropical regions there is low confidence in the antropogenic contribution to changes in heavy rain.

Most of the biases in present-day climate precipitation and the uncertainties for climate projections have been related to problems in the parameterization schemes, including convection (e.g. Sherwood et al., 2014). In particular, one of the reasons why biases over ocean and land might stem from errors in the convective parameterizations is related to their over-sensitivity to the surface forcing (e.g. Hirota et al., 2011; Oueslati and Bellon, 2015; Siongco et al., 2017). For instance, convective parameterizations over ocean have been found to be too sensitive to SST and produce precipitation that collocates high-intensity rain over high SST at a degree not seen in observations (Biasutti et al., 2006). Likewise over land, the high sensitivity of convective schemes to surface fluxes is directly related to an early onset of convection, affecting the representation of the diurnal cycle of precipitation over land (e.g. Betts and Jakob, 2002; Bechtold et al., 2004; Marsham et al., 2013).

Given the long persistence of precipitation biases and better computational resources, it becomes questionable to keep on improving such convective schemes; whose basic assumptions do not hold anymore (Jones and Randall, 2011).

2.2 INSIGHTS FROM A NEW GENERATION OF CLIMATE MODELS

With the exponential growth of computational power, the use of high-resolution climate modeling has become more feasible over the last decades. The so-called storm-resolving models are run over kilometer-scale grid spacing, enabling the explicit representation of moist convection on the model grid (e.g. Stevens et al., 2020).

The use of these models for climate research has been mostly conducted over limited domain regions, given their high computational cost (Prein et al., 2015). Over tropical regions, studies in the framework of the Cascade Project ¹ have investigated the role of mesoscale and synoptic scale organization on the evolution the Madden-Julian Oscillation (e.g. Holloway et al., 2013) over the Indian and West Pacific Oceans. Likewise over land, studies have focused on regional phenomena like the representation of the West African Monsoon (Marsham et al., 2013) and land-sea processes related to diurnal convection over the maritime continent (Love et al., 2011). More recent projects have investigated the representation of the Atlantic ITCZ (Klocke et al., 2017; Senf et al., 2018) and mesoscale organization in tropical West Africa (Peters et al., 2019). In the last years, global storm-resolving simulations have provided insights on the interaction of storm-resolving scales with the large scale circulation systems at sub-seasonal scales (e.g. Satoh et al., 2019; Stevens et al., 2019; Judt and Rios-Berrios, 2021).

Positive results have been found in all the above mentioned studies, which identify systematic improvements in the representation of precipitation with respect to its spatial distribution, organization, precipitation intensity and diurnal cycle. Whilst the improvements of such precipitation features are related to the representation of convection rather than the small grid spacing (e.g. Hohenegger et al., 2020; Judt and Rios-Berrios, 2021), the use of high-resolution is advantageous. Surface heterogeneities such as topography are important forcings for deep convection; therefore by resolving fine-scale variations in the surface it makes it possible to better capture convective processes.

Apart from the benefits of kilometer-scale grids on enabling a better representation of small-scale processes, the use of explicit convection has intrinsic advantages. Storm-

¹ <https://catalogue.ceda.ac.uk/uuid/e327069454b1483cb7c1d7e1df916461>

resolving simulations allow the interaction of convection with its environment, unlike convective parameterizations that are determined by environmental conditions. This is a great advantage for representing processes that are commonly ignored. These processes include the development of convection from shallow to deep convection and to organized systems, that propagate and can promote new convection. An important property of such processes is the convective memory. This can be understood as the effects of earlier convection in modifying current convection (Colin et al., 2019), hence enabling a more realistic representation of convection.

Storm-resolving models provide a new tool for studying the effects and interactions between convection and its environment, which are poorly understood (Stevens and Bony, 2013, see also Section 1.2). The sensitivity of storm-resolving simulations to modes of SST variability in tropical oceans remains unexplored. Likewise, the representation of precipitation and its interaction with mesoscale phenomena has received little attention in tropical South America.

2.3 RESEARCH QUESTIONS

Therefore, in this dissertation, we investigate how convection in storm-resolving simulations (i.e. explicit convection) interacts with its environment. In particular, how it responds to the underlying surface. In this regard, we study the sensitivity of explicit convection to the ocean and land surfaces, at different timescales, and pose the following research questions:

1) How does explicit convection interact with sea surface temperature anomalies?

We approach this question at a seasonal timescale in the context of the AMM, from two different perspectives: the effect of SST on precipitation and the effect of explicit convection on the SST. In particular we ask:

i) Does the explicit representation of convection lead to a robust precipitation response to the AMM?

ii) Does the explicit representation of convection lead to a weaker coupling with the sea surface temperature?

For question i) we address the sensitivity of the precipitation in response to the AMM by comparing uncoupled and coupled simulations. For question ii), we define the coupling as the change in the SST anomaly per change in the wind-driven latent heat flux, given the importance of surface winds for the evolution of SST anomalies in the tropical Atlantic.

Given the over-sensitivity of convective parameterizations to high SST values, we expect simulations with explicit convection to respond less strongly to SST anomalies both in the precipitation response and in terms of the coupling with SST.

2) Does the representation of organized convective systems by explicit convection improve the representation of the precipitation diurnal cycle in the Amazon?

In this case we tackle the interaction of resolved convection and the land surface in a more indirect way. We focus on the effect of atmospheric processes, induced by the land surface (Section 1.2.2), on the diurnal cycle of precipitation.

Storm-resolving simulations have shown systematic improvements in the representation of the precipitation diurnal cycle (Stevens et al., 2020; Kendon et al., 2021). The hypothesis we want to test is whether such improvement can be attributed to a more

realistic representation of observed physical processes; in particular, the influence of convective systems on the precipitation diurnal cycle.

2.4 MODELING STRATEGY

In order to address the research questions, we follow a common modeling strategy in our experiments. We perform two types of simulations which differ in their spatial resolution and treatment of convection.

First, global simulations are integrated at a coarse resolution of 40km, with the convective parameterization switched on. These are named P-CON simulations. Second, the P-CON simulations serve as boundary and initial conditions to nested domains, which increase their spatial resolution by a factor of two (up to 5km), covering the tropical Atlantic sector (25°S - 25°N ; 85°W - 25°E). These have the convective parameterization switched off and are called E-CON simulations.

SUMMARY OF RESULTS

To answer the research questions in Section 2.2, we conducted three studies as detailed in the Appendices. Appendix A and B address question 1, and question 2 is tackled in Appendix C. In this section I summarize the main findings.

3.1 ATMOSPHERIC RESPONSE TO THE ATLANTIC MERIDIONAL MODE

As described in Section 1, modes of SST variability such as the AMM influence the distribution of precipitation in the tropical Atlantic. By using uncoupled simulations we focus on the atmospheric response to the AMM. The aim is to investigate whether the representation of convection influences the precipitation and surface wind responses to the AMM.

As a first step, we design the experimental set-up based on analysis from observations. We isolate the strongest AMM events as those that exceed one standard deviation of the AMM-index¹ time series. It is found that the strongest positive and negative AMM events are very similar among them in terms of their SST pattern and corresponding precipitation response. We then build SST composites from the defined strong events, which serve to prescribe the pattern of the positive and negative AMM.

Following the modelling approach described in Section 2.4, we perform three pairs of experiments which differ in the prescribed SST: a control case with the climatological SST from MAM season and the AMM patterns from positive and negative composites. The simulation pairs only differ in the atmospheric initial conditions, in order to reduce atmospheric noise. The simulations are integrated for 92 days.

Our results show that we can interpret the precipitation response to the AMM as a northward shift of the mean-state precipitation towards the warmer hemisphere (Fig.3.1a,b). A meridional shift of about 1° explains most of the response ($r = 0.75$, Fig.3.1c) for both E-CON and P-CON experiments, as well as for observations (TRMM). This response is consistent with cross-equatorial surface winds between 5°S - 5°N , featuring weaker trade winds in the warmer hemisphere as observed in our simulations and past studies (e.g. Hastenrath and Greischar, 1993; Chiang et al., 2002; Chiang and Vimont, 2004).

The similarity between the E-CON and P-CON responses to the AMM is surprising given their distinct mean-state precipitation. The P-CON simulations exhibit high sensitivity to SST by placing more precipitation over warmer areas in the eastern basin, unlike the E-CON simulations. Nonetheless, the main precipitation response to the AMM (i.e. the meridional displacement of the ITCZ) remains independent from such differences in the zonal distribution of precipitation. These results are overall similar for the case of the negative AMM.

We further examine the atmospheric response to the AMM by focusing on the surface winds, which are generally stronger in the E-CON simulations. The stronger surface winds are consistent with a stronger pressure gradient. The latter is related to a stronger radiative cooling, which is the result of a moister boundary layer and drier free troposphere in E-CON as compared to P-CON simulations.

¹ We use the AMM index proposed by Chiang and Vimont (2004).

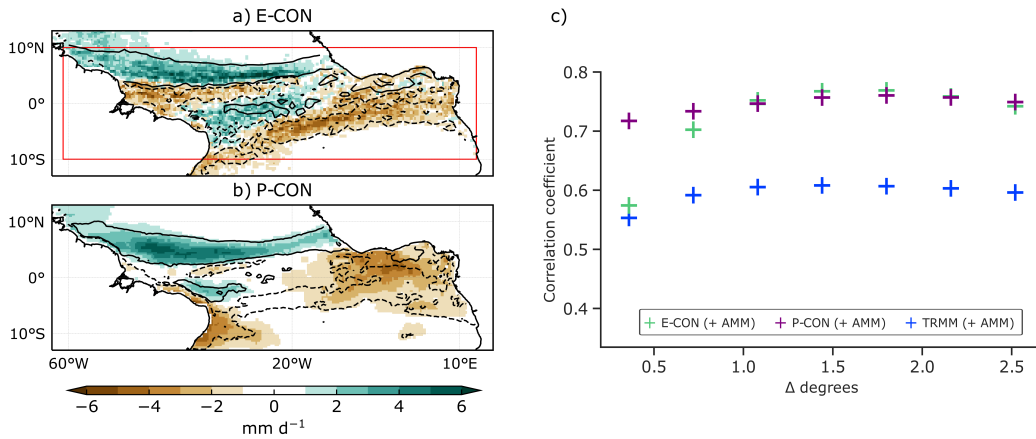


Figure 3.1: Precipitation response to the positive AMM in (a) E-CON and (b) P-CON from the AMM experiments (shaded) and from shifting the mean-state precipitation by one degree northward (only 1 mm d^{-1} contour). (c) Correlation of precipitation anomaly maps obtained from shifting the mean-state precipitation by different degrees in latitude for E-CON (green), P-CON (purple), and observations (blue). All data have been interpolated onto the coarser grid of P-CON. The region for the correlation is computed over the ocean grids bounded by the red-outlined box in (a).

Surface wind anomalies related to the AMM are also stronger in E-CON than P-CON. The distinct surface wind anomalies can impact the surface enthalpy flux (sum of the latent and sensible heat fluxes) and ultimately influence the SST change if all the other terms in the surface energy budget remain unchanged. By considering this assumption it is possible to infer how SST may change given the anomaly of the surface enthalpy flux (δF_h). Since F_h is mostly² controlled by the surface winds, we estimate its wind-driven anomaly as: $\delta F_h = (\delta V/V) F_h$, where F_h is the surface enthalpy flux (defined positive upward) and V is the wind at 10m, both from the control experiments; δV is the surface wind anomaly between the AMM and control experiments. All these terms are averaged over March-May.

Negative wind anomalies, which are larger in E-CON than P-CON, lead to negative values of δF_h in the northern hemisphere. The reduced F_h suggests a stronger ocean warming in E-CON than P-CON, given our sign convention and considering the mean March-May response. Based on these results, we hypothesize that simulations with explicit convection would lead to a stronger change in the SST anomaly given the stronger wind-driven surfaces fluxes.

² F_h is also influenced by air-sea differences of humidity and temperature, but these are negligible in our experiments.

3.2 ATMOSPHERE-OCEAN COUPLING IN THE DECAY OF THE ATLANTIC MERIDIONAL MODE

Motivated by the results of the uncoupled simulations, we further investigate how the coupling with SST depends on the representation of convection. In this second study we focus on the evolution of the positive AMM from its peak signal in May towards its decay in July.

In order to perform simulations with an interactive ocean surface, we introduce a slab-ocean configuration into the atmospheric ICON-NWP model. This is done by adapting the Fresh-water lake model (Flake, Mironov et al., 2010) to a one-layer slab scheme over ocean grids. According to the experimental design detailed in Section 2.4, we then conduct 3-member ensemble simulations of a control case (with the climatology SST) and the positive AMM (with the composite pattern). Simulations are initialized in mid-April and integrated for 100 days.

We analyse the evolution of the AMM in two parts by focusing on: i) the precipitation response to the AMM in May, given the similar SST anomaly between E-CON and P-CON and ii) the coupling with SST, defined as the change in the SST anomaly due to the wind-driven latent heat flux.

First, during the peak time of the AMM (May) we observe a different shift in the mean-state precipitation between the E-CON and P-CON simulations. The E-CON simulations have the highest correlation in the northward shift at about 1° (Fig. 3.2), consistent with the results of uncoupled simulations (Fig. 3.1a). It is also striking how well the E-CON simulations match the observations after including a simple slab-ocean in the experimental set-up. In contrast, the precipitation response of P-CON simulations appears to be more sensitive to the SST anomaly by showing a preferred displacement of about 2° northward.

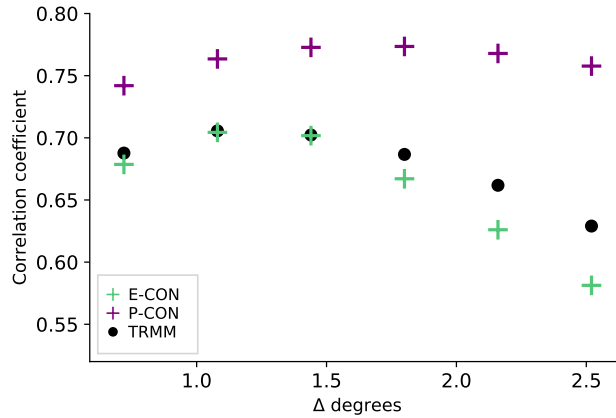


Figure 3.2: Correlation of precipitation anomaly maps in May obtained from shifting the mean-state precipitation by different degrees in latitude for E-CON (green), P-CON (purple), and observations (blue). All data have been interpolated onto the coarser grid of P-CON. The region for the correlation is computed over the ocean region bounded by the red-outlined box in Fig. 3.1a.

We hypothesize that the distinct displacements of the Atlantic ITCZ by E-CON and P-CON simulations are the result of different SSTs in the mean-state. The P-CON simulations generally exhibit warmer SSTs as compared to E-CON both in the control and AMM simulations, which can be explained by the larger incoming short wave radiation

related to less cloud cover. Given that simulations with parameterized convection tend to collocate precipitation over high SST (e.g. Biasutti et al., 2006), more precipitation would be enhanced over larger areas of high SST ($>29^{\circ}\text{C}$) and favor a widening of the ITCZ.

In the second part, we focus on the decay of SST anomalies (δSST) towards boreal summer. The anomalies are defined as the difference between the AMM and the control experiment. We observe that the cooling shown by δSSTs is stronger in the E-CON simulations (Fig. 3.3 a,c). In particular, we focus the analysis on the region bounded by the red box in Fig. 3.3. Following a similar procedure as in Section 3.1., we derive the wind-driven anomaly of the latent heat flux since it is the largest term in the surface heat fluxes. Then we estimate its contribution to the total δSST change (Fig. 3.3 b,d) as determined by the energy budget in the mixed layer:

$$\partial(\delta\text{SST}_{total}) = (\delta\text{LHF} + \delta\text{SHF} + \delta\text{LW} + \delta\text{SW}) \frac{\partial t}{h\rho C_p} \quad (3.1)$$

where $\partial(\delta\text{SST}_{total})$ is the total change of δSST from July with respect to May and is the result of adding May-July averages of: latent heat flux anomalies (δLHF), itself decomposed by the wind (V) and air-sea humidity difference (Δq) components as: $\delta\text{LHF} = (\delta V/V) \text{LHF} + (\delta\Delta q/\Delta q) \text{LHF}$; sensible heat flux anomalies (δSHF), net long-wave radiation anomalies at the surface (δLW) and net short-wave radiation anomalies at the surface (δSW); all of which are in W m^{-2} . Note that we refer to the anomalies as the difference between the AMM and control experiments. The mixed layer depth, h is 30m, ∂t is the time in seconds from May to July, and ρC_p is the volumetric heat capacity of water.

Given the positive wind anomalies during May-July, stronger positive anomalies in the wind-driven latent heat flux translate into a greater cooling in the E-CON simulations from 0.5K (east of 35°W) to 1.5K (west of 35°W) than P-CON (Fig. 3.3b, d). The averaged SST cooling due to wind-driven δLHF in the red box of Fig. 3.3b,d represents about 67% of the total δSST change (red box on Fig. 3.3a) in the E-CON simulations, and about 48% in P-CON. The exposed differences between E-CON and P-CON denotes a greater influence of the surface winds on the SST changes in the E-CON simulations.

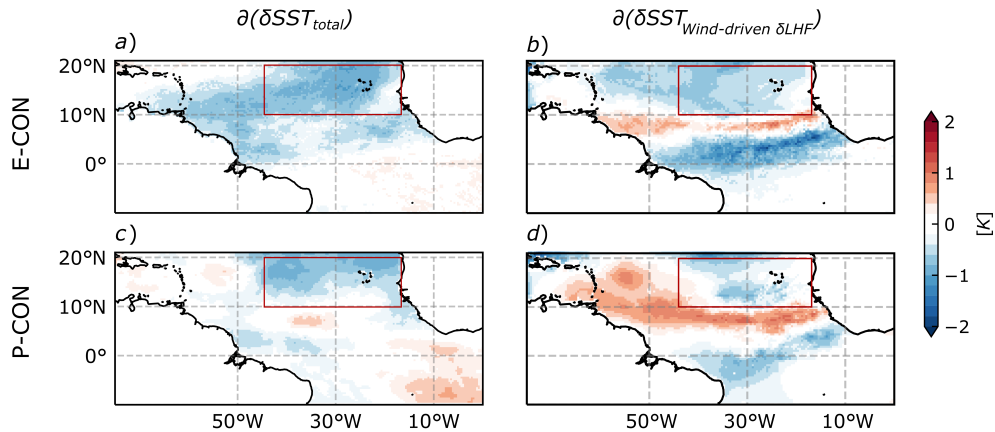


Figure 3.3: (a,c) Total change of SST anomalies ($\partial(\delta\text{SST}_{total})$) from July with respect to May and (b,d) change of SST anomalies only due to the wind-driven latent heat flux ($\partial(\delta\text{SST}_{wind-driven \delta\text{LHF}})$). The analysis is focused over the region enclosed by the red-outlined box (45°W - 15°W ; 10°N - 20°N).

The remaining change in δSST can be explained by Δq -driven δLHF and δSW , which considerably favor the cooling in P-CON unlike E-CON over the region of interest. As a result, differences in the total δSST are reduced between E-CON and P-CON (Fig. 3.3a, c).

Our results demonstrate that the atmosphere-ocean coupling is sensitive to the representation of convection during the decay of the AMM, in terms of the precipitation and SST responses. We show that simulations with explicit convection exhibit i) a robust precipitation response to the AMM in May and ii) a stronger change of the SST anomalies influenced by stronger wind anomalies, which agrees with the proposed hypothesis from the uncoupled simulations.

3.3 ON THE REPRESENTATION OF THE AMAZON RAINFALL BY STORM-RESOLVING SIMULATIONS

In this third study we turn the attention to tropical land precipitation, and also move from seasonal timescales to diurnal variations. The aim is to investigate whether improvements in the representation of Amazon precipitation can be attributed to the representation of organized convective systems.

We use 8-member ensemble simulations of E-CON and P-CON according to the set-up of the uncoupled simulations (Section 2.4) and focus the analysis in March, which is one of the months with most convective activity (e.g. Rehbein et al., 2018). Additionally, we conduct 2-member ensemble runs of E-CON at 2.5km grid spacing over a domain that covers the entire Amazon.

As a first step, we assess the overall representation of Amazon rainfall in terms of its mean, spatial distribution, frequency of intensity and diurnal cycle. We compare our set of simulations with the Climate Prediction Center Morphing Method (CMORPH; Xie et al., 2017) dataset as observations.

The major improvements in the Amazon are found in the representation of the distribution of precipitation intensity and the spatial variability of the diurnal cycle. These are overall similar between 2.5 km and 5 km E-CON simulations.

The E-CON simulations display a distribution of precipitation intensity much closer to observations than P-CON (Fig.3.4). Rain rates between 2 mm d^{-1} to 20 mm d^{-1} are slightly underestimated in E-CON; whereas it is consistently overestimated by simulations with parameterized convection as previously documented (e.g. Flato et al., 2014; Fiedler et al., 2020). Higher intensity rates ($>25 \text{ mm d}^{-1}$), which are especially underestimated by the P-CON ensemble, are very well reproduced in the E-CON simulations. The 2.5 km E-CON simulations are very close to the observed 11-year climatology up to 100 mm d^{-1} . Discrepancies for higher intensities may be related to the smaller ensemble of days in the 2.5 km E-CON (62 days) compared with observations.

The second major improvement is found in the representation of the diurnal cycle. The spatial variability of peaking precipitation time over the whole Amazon is reasonably captured by the E-CON simulations (Fig. 3.5a,b,c); in particular, overnight precipitation peaking at 1h-6h (local time) in the central and northeast Amazon. Such nocturnal precipitation has been related to mature organized convective systems formed near the coast (e.g Garstang et al., 1994) or inland (e.g Rehbein et al., 2018). The P-CON simulations are able to reproduce the afternoon precipitation peak (18h-20h); however, its spatial distribution is rather homogeneous (Fig.3.5d). Nocturnal precipitation peaks are captured near elevated topography.

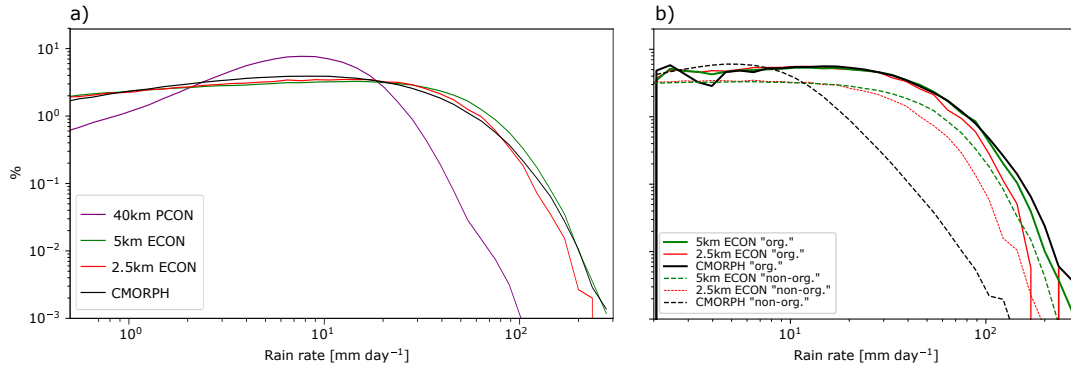


Figure 3.4: (a) Distribution (%) of daily precipitation intensity greater than 0 mm d⁻¹ over the Amazon basin for observations (black line) and simulations (colored lines). (b) Distribution (%) of daily precipitation intensity in organized convective systems (solid lines, "org.") and non-organized precipitation (dashed "non-org."). Values are binned in a logarithmic scale.

Next, we associate the representation of organized convective systems with the improved representation of high-intensity rain and the spatial variability of the diurnal cycle. Given that P-CON simulations are not able to reproduce such precipitation features we exclude them from further analysis. The organized convective systems are defined as 8-way connected precipitation grid points with rain rates greater than 2mm h⁻¹ and a total area equal to or greater than 10000km². The thresholds are chosen from references of observed values (Rehbein et al., 2018; Feng et al., 2021).

The defined organized systems by the E-CON simulations reveal some differences in contrast to observations. The E-CON simulations tend to produce smaller convective systems than observed. The median area for CMORPH is 19223km², whereas for E-CON it is 14411km². Also, organized precipitation in the E-CON simulations displays more intense rain than observations. The mean value intensity per area is about twice in E-CON than CMORPH.

Nonetheless, by comparing the distribution of precipitation intensity and diurnal cycle of the organized convective systems in E-CON against observations, we obtain a closer similarity.

Intensity rates from 5 mm d⁻¹ to 100 mm d⁻¹ coincide remarkably well between observations and the E-CON simulations, especially in the 5km E-CON ensemble (Fig. 3.4b). We also note the intensity distribution of non-organized precipitation in observations is similar to that of the total precipitation in P-CON (Fig. 3.4a).

The spatial distribution of precipitation peaks associated with the organized convective systems in E-CON (Fig. 3.5f,g) agrees with observations (Fig. 3.5e). Overnight precipitation that peaks between 1h-6h are identified over the central and northeast Amazon, the regions where P-CON cannot capture the time of maximum precipitation. By contrast, non-organized precipitation commonly features its maximum in the late afternoon (Fig. 3.5 h, i, j), as commonly observed over land.

Analysis of the diurnal cycle of organized convective systems in E-CON with respect to variations in their size and intensity, also provides a good representation of their life cycle (Fig. C.7). The maximum intensity is shown in the afternoon, when systems begin to organize and display a rather small size. Later on, overnight, the organized systems

have a maximum peak in size and feature less intense rain, associated with their mature phase and dissipation (e.g. Rickenbach, 2004; Rehbein et al., 2018).

Our results show the value of storm-resolving simulations for linking the representation of atmospheric processes, such as organized convective systems, with improvements in the representation of land precipitation.

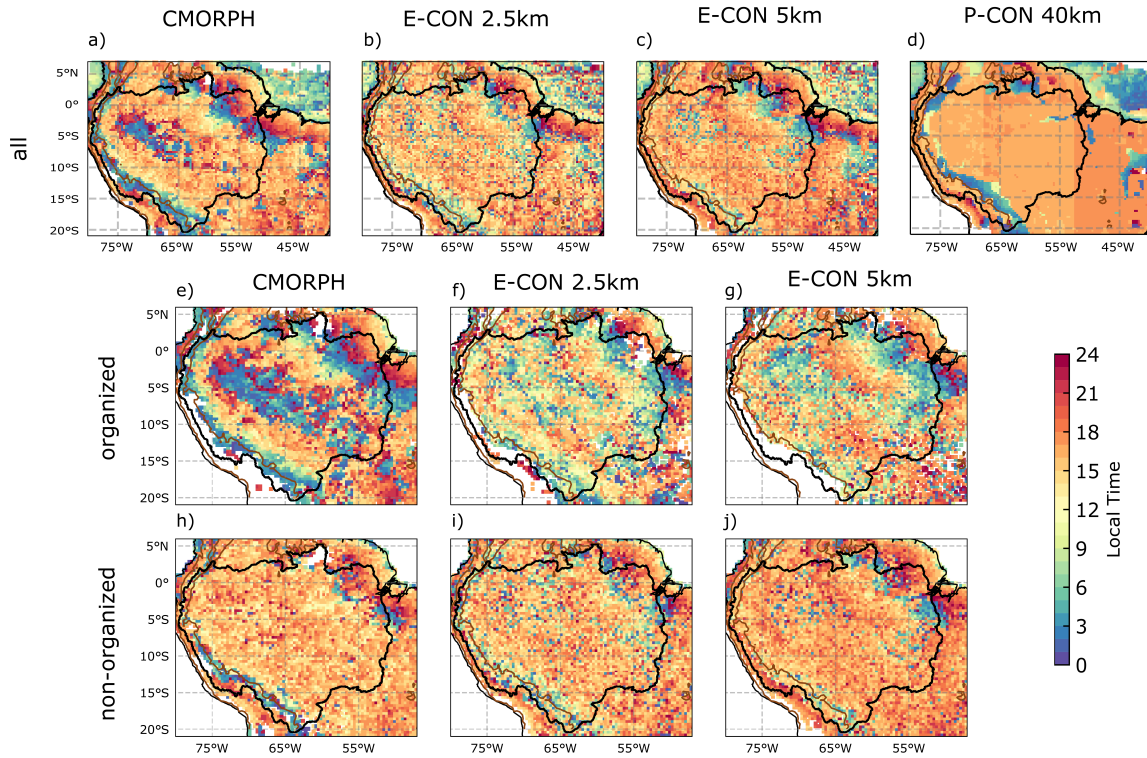


Figure 3.5: Time of maximum diurnal precipitation in March for (a, b, c, d) all precipitation and subdivided by (e, f, g) organized convective systems labelled as "organized" and (h, i, j) non-organized precipitation labelled as "non-organized". The boundaries of the Amazon basin are defined in black contours, topography at 1000m is shown in brown contours. Columns represent observations (CMORPH) and model output as indicated.

CONCLUSIONS AND OUTLOOK

Science progresses not because scientists as a whole are passionately open-minded but because different scientists are passionately closed-minded about different things.

(Henry Bauer)

4.1 RESPONSE TO RESEARCH QUESTIONS

In this dissertation we have investigated how the explicit representation of convection interacts with the ocean and land surfaces in the tropical Atlantic sector, from seasonal to diurnal timescales. The research questions are addressed in Section 3, in the context of the Atlantic Meridional Mode (AMM) and the Amazon diurnal precipitation. On the basis of our main findings we answer the outlined research questions as follows:

1) How does explicit convection interact with sea surface temperature anomalies?

We investigated the interaction of resolved convection with the ocean surface from two perspectives. For each case we conclude:

i) The explicit representation of convection leads to a robust precipitation response to the AMM when its signal is strongest. The precipitation response to the AMM is the displacement of the ITCZ towards the warmer hemisphere as a result of the related gradient of SST anomalies, which induces cross-equatorial surface winds. We show that such response to the AMM can be interpreted as a 1° meridional shift of the mean-state precipitation towards the warmer hemisphere. This response is consistent when we isolate the atmospheric response in uncoupled simulations and when we use coupled simulations. The sensitivity of the precipitation response to SST is less strong than simulations with parameterized convection and closer to observations.

ii) Our results indicate that the explicit representation of convection can lead to a stronger atmosphere-ocean coupling in contrast to parameterized convection. The argument is based on the stronger cooling in simulations with explicit convection during the decay of the AMM, which is influenced by a larger imprint of the surface winds via latent heat flux anomalies. The impact of the larger imprint is twofold. First, considering only the cooling of SST due to wind-driven latent heat flux, we estimate a larger cooling (from 0.5 to 1.5K) in simulations with explicit convection. This is consistent with the larger anomalies of surface winds in response to the decay of the AMM. Second, the cooling of SST anomalies due to wind-driven latent heat flux explains 67% of the total SST cooling (19% more than in simulations with parameterized convection).

2) Does the representation of organized convective systems by explicit convection improve the representation of the precipitation diurnal cycle in the Amazon?

Simulations with explicit convection at 2.5km and 5km grid spacing reproduce the diurnal cycle of organized convective systems, which explains most of the overnight precipitation peaks in observations. In organized convective systems, the precipitation maximum occurs from 1h to 6h over central and northeast Amazon, wherein parameterized convection fails to simulate the timing of diurnal precipitation. Storm-resolving simulations also capture diurnal variations of the size and intensity of organized convective systems, which are consistent with their observed life-cycle. The explicit representation of convection lead to a realistic diurnal cycle in organized convective systems, hence improving the overall representation of precipitation diurnal cycle in the Amazon.

4.2 UNEXPECTED FINDINGS

Our first study concerning oceanic convection, is the first to investigate the sensitivity to modes of SST variability in storm-resolving simulations covering the entire tropical Atlantic basin. Some of the results were in line with our hypotheses, but others unforeseen.

In the uncoupled simulations, the precipitation response to the AMM was surprisingly similar between simulations with explicit and parameterized convection. Both displace the ITCZ by the same distance even though they show a different mean-state precipitation (Fig. A.4) associated with different sensitivities to SST (Fig. A.5). Nonetheless, coupled simulations with parameterized convection exhibit a larger displacement of the mean-state precipitation; whereas simulations with explicit convection confirm the results of the uncoupled experiments. The robust response of explicit-convection simulations and its similarity with observations, suggest that uncoupled simulations might be masking deficiencies of convective parameterization in the response of precipitation to SST anomalies.

Whilst we anticipated differences in the SST coupling due to the surface winds, we did not expect a great influence from the clouds. Simulations with explicit convection tend to produce more cloud cover than those with parameterized convection. This showed an impact on the mean-state conditions by favoring the warming in simulations with parameterized convection. Moreover, strato-cumulus clouds over the west coast of Africa did not show a clear response to AMM, which could have influenced the rapid cooling of the SST anomalies in our simulations (e.g. Evan et al., 2013; Myers et al., 2018). These results point out the importance of the representation of clouds and their influence on the short wave radiation, for a more realistic interaction with the ocean surface.

4.3 CHALLENGES AND OPPORTUNITIES

One of the assumptions in our coupled simulations was the homogeneous spatial distribution of the mixed layer depth. However, the mixed layer depth features an horizontal gradient where the larger depths are found in the west ocean basin and the shallowest at the east (Foltz et al., 2013). Also, the mixed layer depth responds and feeds back on the SST anomalies, especially on the east basin (e.g. Rugg et al., 2016). A possible extension of our work with coupled simulations, would be to investigate the interaction of surface wind anomalies with an interactive mixed layer. Implications of such a study

would be of relevance for other modes of variability in which ocean dynamics play an important role (e.g. Atlantic Niño).

The study of the Amazon rainfall and the diurnal variation of organized convective systems brings out promising results. Our results suggest a good representation of their life-cycle, including the development of deep convection in the afternoon towards its dissipation on the following day. The mature stage of organized convective systems features convective and stratiform regions, which imply different structures in the vertical latent heating profile and effects on the large-scale circulation (Schumacher et al., 2004). A possible research direction could be to further investigate whether the storm-resolving simulations can also correctly represent the stratiform component of organized convective systems and its effects on the large-scale circulation. And if not, investigate which microphysical properties would require better parameterizations or changes to be used at kilometre-scales.

4.3.1 *Beyond a realistic simulation*

I had the opportunity to collaborate¹ in a study where the latest generation of climate models (CMIP6) were evaluated in terms of the representation of tropical precipitation (Fiedler et al., 2020). One of the conclusions of this study is that the uneven progress in simulating tropical rain may be the result of improving parameterization schemes by overfitting, which no longer compensate errors elsewhere in the model. This means that model development has been mostly focused on the final result rather than on the physical processes towards it. The result of such approach is a slow progress on simulating climate (Jakob, 2010).

A new generation of climate models is becoming more affordable thanks to advances in supercomputer power, with evident faster progress than the parameterization of moist convection in GCMs (e.g. Satoh et al., 2019; Stevens et al., 2020). Yet, high-resolution modelling is far from being the solution for biases in simulating tropical precipitation, or climate in general, but it does enable improvements in the representation of physical processes. Storm-resolving resolutions still face issues on accurately representing some aspects of precipitation, given that convection is not resolved completely (Kendon et al., 2021). Moreover, several processes like microphysics, atmospheric turbulence and radiative transfer still need to be parameterized given their sub-kilometre scales. New challenges are open to adapt those schemes formerly developed for coarse resolution models, hopefully without the overfitting approach.

The great advantage, or real added-value of such new generation of climate models, is the opportunity of understanding, from a new perspective, the process behind the result. Studies like those presented in this dissertation are still needed to identify the strengths and weaknesses of storm-resolving models, towards a better understanding of the coupled climate system. Projects such as the Next Generation Earth Modelling Systems (NextGems²), which ambitiously aims to simulate 30 years of the coupled land-ocean-atmosphere climate system, must be seen as exciting opportunities for better understanding climate processes and rediscovering the physics of nature.

¹ My contribution to this article was with the elaboration of Fig.9 and Fig.S7, and discussion in Section 4a

² <https://nextgems-h2020.eu>

Part II

APPENDICES

APPENDIX

The work in this appendix has been published with minor modifications as:

Paccini, L., Hohenegger, C. & Stevens, B. (2021). "Explicit versus parameterized convection in response to the Atlantic Meridional Mode", *Journal of Climate* 34(9), pp.3343-3354. <https://doi.org/10.1175/JCLI-D-20-0224.1>

The contributions of the authors to this paper are as follows:

The original idea was conceived the by BS and CH. LP performed the simulations and analysis. The manuscript was mainly written by LP with contributions of CH and BS. CH helped with the experiment design, discussions and reviewed the manuscript. BS discussed the results and reviewed the manuscript. All authors proofread draft versions of the paper.

Explicit versus parameterized convection in response to the Atlantic Meridional Mode

Laura Paccini¹, Cathy Hohenegger¹ and Bjorn Stevens¹

¹Max Planck Institute for Meteorology, Bundesstraße 53, 20146 Hamburg, Germany

Received: 28 March 2020 / Accepted: 8 February 2021 / Published online: 25 March 2021

This study investigates whether the representation of explicit and parameterized convection influences the response to the Atlantic Meridional Mode (AMM). The main focus is on the precipitation response to the AMM-SST pattern, but possible implications for the atmospheric feedback on SST are also examined by considering differences in the circulation response between explicit and parameterized convection. Based on analysis from observations, SST composites are built to represent the positive and negative AMM. These SST patterns, in addition to the March-May climatology, are prescribed to the atmospheric ICON model. High-resolution simulations with explicit (E-CON) and coarse-resolution simulations with parameterized (P-CON) convection are used over a nested tropical Atlantic and a global domain, respectively. Our results show that a meridional shift of about 1° in the precipitation climatology explains most of the response to the AMM-SST pattern, both in simulations with explicit and with parameterized convection. Our results also indicate a linearity in the precipitation response to the positive and negative AMM in E-CON, in contrast to P-CON. Further analysis of the atmospheric response to the AMM reveals that anomalies in the wind-driven enthalpy fluxes are generally stronger in E-CON than in P-CON. This suggests that SST anomalies would be amplified more strongly in coupled simulations using an explicit representation of convection.

A.1 INTRODUCTION

Convective parameterizations are one of the main simplifications in the representation of atmospheric processes and, despite decades of development, still show difficulties in adequately representing precipitation, particularly in the tropics (e.g. Arakawa, 2004; Flato et al., 2014; Fiedler et al., 2020). Over the Atlantic basin, tropical precipitation is misrepresented both in terms of its intensity and spatial distribution. General circulation models (GCMs) tend to misplace the Atlantic Inter-Tropical Convergence Zone (ITCZ) farther south of its observed position (e.g. Biasutti et al., 2006; Richter and Xie, 2008) and to favor precipitation over the east or west Atlantic coast, rather than the central Atlantic as it is observed in the annual mean (Siongco et al., 2015). Biases such as these call into question the representation of the coupling of convection to its environment, particularly SST, with obvious implications for understanding variability and climate change. In this study, we investigate whether the representation of convection influences the response of precipitation to changes in SST.

Over the tropical Atlantic, an important mode of coupled variability is the Atlantic Meridional Mode (AMM, e.g. Nobre and Shukla, 1996; Chiang and Vimont, 2004; Xie and Carton, 2004). A positive AMM displays warmer than normal SSTs north of the equator, up to 30°N, and cooler than normal south of the equator. Opposite features occur during the negative AMM phase. This inter-hemispheric difference in SST changes the boundary layer pressure gradient (Lindzen and Nigam, 1987), which drives anomalous cross-equatorial surface winds towards the warmer hemisphere (e.g. Chiang and Vimont, 2004). As a consequence of the anomalous SST gradient and cross-equatorial winds, the ITCZ is meridionally displaced (e.g. Chiang et al., 2002; Chiang and Vimont, 2004). This change in the precipitation pattern also affects the neighboring continents. For instance, positive AMM events are related to dry spells in Northeast Brazil and to wet periods in the Northern Amazon and West Africa (e.g. Nobre and Shukla, 1996). The precipitation response over land, nevertheless, is not a sole response to the AMM but a result of the combined effect with other modes of variability such as ENSO (e.g. Giannini et al., 2004; Lucena et al., 2011). In contrast, the shift of the ITCZ in the Atlantic basin is the local atmospheric response to AMM-like SST perturbations (Chang et al., 2000; Wang and Carton, 2003; Chiang and Vimont, 2004) and can be considered the main response to the AMM.

Ocean-atmosphere interactions also play an important role in the AMM development. Positive SST anomalies in the north tropical Atlantic (i.e. positive AMM) are related to weakened trade winds north of the equator. This change in the surface winds suppresses evaporative heat loss, thus favoring a warming of the sea surface. Conversely, negative SST anomalies are related to a strengthening of the surface winds, which leads to surface cooling. This positive feedback, known as the Wind – Evaporation – SST (WES) feedback (Xie and Philander, 1994), has been recognized as a driving mechanism of the AMM (e.g. Amaya et al., 2017). The WES feedback is most pronounced in the northwestern tropical Atlantic and it is stronger during boreal spring when the AMM is more prominent (e.g. Chang et al., 2001; Chiang et al., 2002; Hu and Huang, 2006; Foltz et al., 2012; Amaya et al., 2017).

Current GCMs do not represent correctly the coupled SST - precipitation variability in the AMM, since they struggle to reproduce its main driving mechanisms (e.g. Amaya et al., 2017) and do not show a robust atmospheric response to the AMM. Even in atmospheric-only models, the precipitation response to the AMM is far from unanimous. For instance, Wang and Carton (2003) evaluated the atmospheric response to modes of

variability in the tropical Atlantic using a set of uncoupled simulations from various GCMs. They found that only two out of six models represented precipitation and wind anomalies as large as those in observations in response to the AMM mode. Past modelling studies, however, have not evaluated other aspects of the response to the AMM such as the ITCZ displacement.

The inconsistent precipitation response among GCMs may be explained by the different representations of convection and what this implies for their coupling to SST perturbations. Generally, parameterized convection is overly sensitive to the surface temperature (e.g. Hirota et al., 2011; Oueslati and Bellon, 2015; Siongco et al., 2017) as evidenced by a tendency of GCMs to collocate high precipitation over high SST (Biasutti et al., 2006) to a degree that is not seen in observations. Since convection schemes fail to robustly represent changes in precipitation in response to tropical SST perturbations, it becomes relevant to explore this matter with models that do not parameterize convection. Fortunately, advances in computing allow the use of simulations with explicit convection integrated at convection-permitting resolution of a few kilometers on large domains (Holloway et al., 2012; Marsham et al., 2013; Klocke et al., 2017; Satoh et al., 2019; Stevens et al., 2019). However, the influence of explicit convection in response to SST modes of variability remains unexplored.

In this study, we use both uncoupled convection-permitting simulations, as well as coarser-resolution simulations with parameterized convection over the tropical Atlantic and neighbouring continents. This allows us to study how precipitation and associated circulation respond to AMM-SST patterns. We assess this coupling from two directions: first the atmospheric response and then its potential feedback on SST. In this latter case, we examine whether differences between explicit and parameterized convection in the surface winds response to the AMM could suggest a distinct change in SST via changes in the magnitude of the surface enthalpy flux, something which would have implications for the representation of modes of variability in the tropics.

This paper is organized as follows. Section 2 is divided into observations and model simulations. First, we present data from observations which are then used to analyze AMM events. This analysis is necessary to determine the SST patterns representative of the AMM that will serve the experimental design. Second, we introduce the model and describe the experimental set-up. In section 3, we discuss the main features of the precipitation distribution represented by explicit and parameterized convection, as well as the response to the AMM patterns. Section 4 further explores the possible implications of the atmospheric response, in particular, wind-driven surface fluxes, for changes in SST through the WES feedback. Summary and conclusions are given in section 5.

A.2 DATA AND METHODS

A.2.1 Observations

A.2.1.1 Data

For the observational analysis of the AMM mode we study the 1950-2013 period. We use monthly SST data from the Hadley Centre Sea Ice and Sea Surface Temperature dataset (HadISST, Rayner et al., 2003), which is provided on a 1° spatial resolution. Surface winds at 10 m are taken from the National Centers for Environmental Prediction–National Center for Atmospheric Research (NCEP–NCAR) reanalysis dataset (Kalnay et al., 1996) and have a 2.5° spatial grid. Further analysis of the precipitation response to the AMM

in observations is performed with data from the Global Precipitation Climatology Project (GPCP, Adler et al., 2003) for the period 1979-2013 at a grid spacing of 2.5° . In addition, we use the TRMM-3B42 V7 rainfall product from the Tropical Rainfall Measuring Mission (Huffman et al., 2007) on a 0.25° spatial grid.

To identify AMM events, we use the AMM-SST index proposed by Chiang and Vimont (2004) which is based on NCEP-NCAR Reanalysis. According to their approach, a maximum covariance analysis (MCA) is applied to SST and 10 m wind anomalies over the tropical Atlantic ($21^\circ\text{S} - 32^\circ\text{N}$, $74^\circ\text{W} - 15^\circ\text{E}$). The time series of the AMM index is then constructed by projecting the spatial pattern of the leading MCA mode onto the SST. This study focuses on March to May (MAM) season (Fig. A.1), as it is the time when the AMM signal is strongest (e.g. Chiang and Vimont, 2004; Amaya et al., 2017).

A.2.1.2 Building AMM composites

Due to limited computational resources we are unable to simulate the whole 64 year period for this study, and hence need to build composites of SST patterns representative for positive and negative AMM phases. Since the AMM displays interannual variability with positive and negative events at different intensities (Fig. A.1), we build composites based on strong events in an effort to better capture the recurrent features of the AMM. The latter are defined by a threshold of 1 unit in the normalized AMM index, equivalent to 1 standard deviation of the time series (Fig. A.1). Strong events are defined as those whose seasonal mean index exceeds this threshold. We then construct from these a composite of strong negative (12 events) and positive (14 events) AMM.

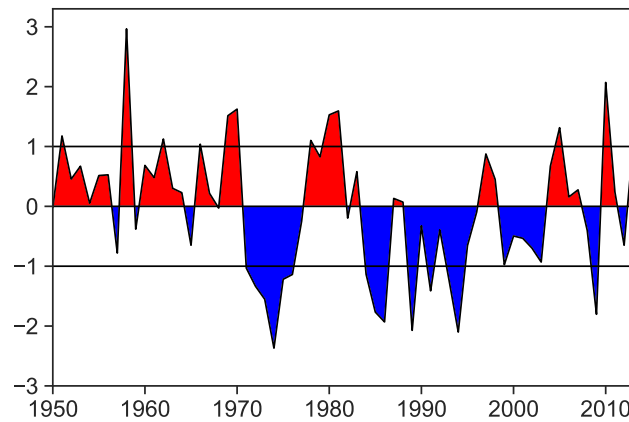


Figure A.1: Seasonal mean of the normalized AMM - SST index for March to May (MAM) season, based on the index proposed by Chiang and Vimont (2004). Red shaded areas refer to positive AMM and the blue ones, to negative AMM. The black lines indicates the threshold for the strong AMM events.

Figure A.2 shows the spatial pattern of the AMM composites. In addition to precipitation and SST anomalies, surface wind anomalies are also shown, since the AMM is strongly related to the cross-equatorial winds response (e.g. Nobre and Shukla, 1996; Chiang et al., 2002). The SST pattern depicts an anti-symmetric dipole with stronger anomalies (up to 0.8 K) over the north tropical Atlantic near the West Africa coast around 10°N . In the southern hemisphere, a maximum anomaly of 0.5 K is observed around 10°S . The cross-equatorial wind anomalies are associated with a shift of the mean precipitation which expresses itself as a positive anomaly from about 4°N to 10°N for the case of a

positive AMM; and a negative anomaly for the case of a negative AMM. Over land, the dipole precipitation anomalies are visible along the coast of South America, but details are hard to notice due to the coarse (2.5°) grid spacing. The shift of precipitation is more evident over west of 20°W in the tropical Atlantic. Analysis of individual events show much more variability east of 20°W , which is why significant precipitation anomalies in the eastern basin are hardly visible. Due to these characteristics, we separate the Atlantic basin into a west ($75^\circ\text{W} - 20^\circ\text{W}$) and an east ($20^\circ\text{W} - 15^\circ\text{E}$) basin for later analysis. The comparison between positive and negative AMM composites show overall opposite symmetric characteristics. The pattern correlation of both AMM composites for SST and precipitation anomalies are -0.95 and -0.88 , respectively.

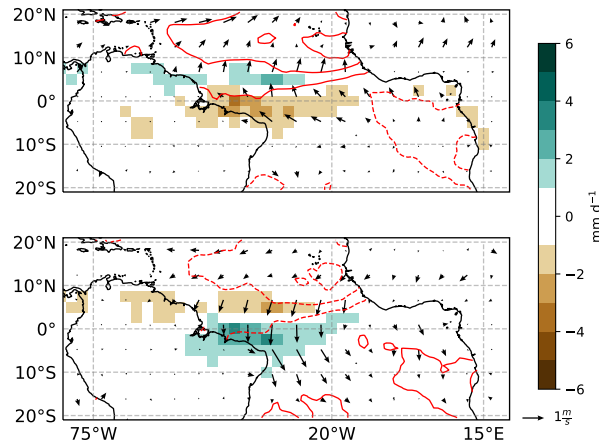


Figure A.2: Positive (upper panel) and negative (lower panel) composites of strong AMM events based on SST data for the 1950-2013 SST period. Precipitation anomalies (shaded) are from GPCP dataset (1979-2013); SST anomalies (positive solid red line, negative red dashed line. Intervals each 0.3K starting at 0.2K) from HadISST and surface wind anomalies from NCEP reanalysis. The 20°W longitude separates west and east Atlantic basin.

Even though the composites seem to display the expected features associated with AMM events as found in previous studies (e.g. Chiang and Vimont, 2004), we further assess their representativeness as compared to specific years. To do this, we compute the pattern correlation of SST and precipitation anomalies among single events (Fig. A.3). Here, we only consider the common period with the available precipitation data (1979 - 2013). The resulting correlation heatmaps are arranged according to the AMM index from the greatest (top and left side) to the lowest (bottom and right side) values. The SST patterns are highly correlated within the stronger AMM events (darker colors over the heatmap corners). Likewise in the case of precipitation, correlation among strong events is greater than among those events with an AMM index between -0.5 to $+0.5$. In general, the correlation values for precipitation are lower than that for SSTs. This could be due to more variability in precipitation, especially over land. Nonetheless, the highest correlation among the AMM events are within the so-defined strong events for both SST and precipitation. The built composites, thus, illustrate well the main patterns of positive and negative AMM.

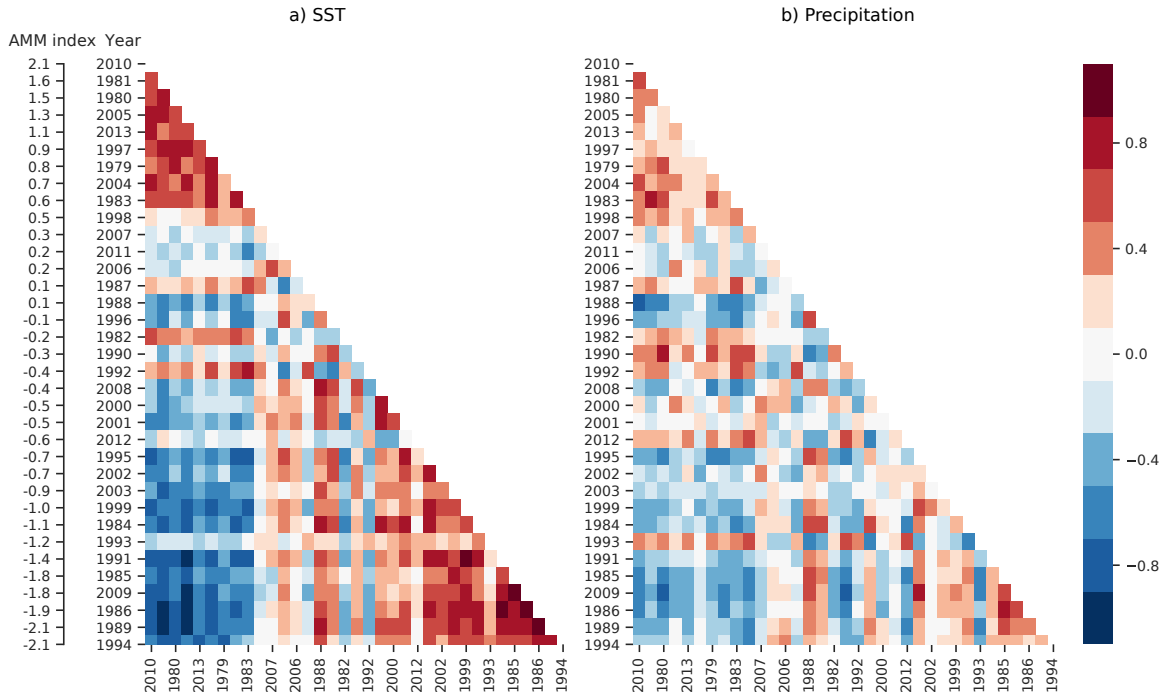


Figure A.3: Correlation heatmaps of (a) SST and (b) precipitation anomalies for the 1979-2013 common period. The years are ordered from the greatest value of the AMM index to the lowest value.

A.2.2 Simulations

A.2.2.1 Model

Simulations are performed with the ICOSahedral Non-hydrostatic (ICON) model (Zängl et al., 2015) in the Numerical Weather Prediction (NWP) configuration, version 2.3.03. Physical parameterizations are as described in Klocke et al. (2017) and Hohenegger et al. (2020) except that, depending on the grid spacing (see next section), we switch on the parameterization of convection. Convection is parameterized using a bulk mass-flux scheme, which is an implementation based on the Bechtold (2017) modifications to the Tiedtke (1989) convection scheme.

Simulations are initialized from the operational analyses from the European Centre for Medium-Range Weather Forecasts and Integrated Forecast System (ECMWF - IFS) except for SST, which is taken from the HadISST dataset. We use the ICON tools 2.3.1 for remapping the IFS and HadISST data onto the model grid. Grids and external parameters (like orography and land properties) are obtained via the Online Grid Generator tool provided by the German Meteorological Service (DWD).

A.2.2.2 Experimental set-up

We conduct the simulations using two representations of moist convection. In the first case, convection is parameterized and the simulation is referred to as "P-CON". P-CON is run over the global domain with a horizontal grid spacing of about 40 km and 90 vertical levels, with the model top at 75 km. In the second configuration the convection scheme is turned off at a convection-permitting resolution, allowing the model to explicitly

Table A.1: List of the main characteristics of the experiments. TA = Tropical Atlantic.

Experiment	SST condition]	Convection	Domain	Spatial Resolution
E-CON (Clim)	Climatology SST	Explicit	Nested TA	5km
P-CON (Clim)		Parameterized	Global	40km
E-CON (+AMM)	Positive AMM SST	Explicit	Nested TA	5km
P-CON (+AMM)		Parameterized	Global	40km
E-CON (-AMM)	Negative AMM SST	Explicit	Nested TA	5km
P-CON (-AMM)		Parameterized	Global	40km

resolve convection. This simulation is called "E-CON". Due to the computational cost, we were unable to perform high resolution explicit convection simulations at a global scale. Instead, we performed a one-way nesting approach where the P-CON 40 km global simulation provides boundary conditions to nested E-CON domains. Three E-CON nests are applied in which only the horizontal grid spacing is successively step-wise refined from 20 km to 10 km and to 5 km over the tropical Atlantic. The refined domains bound the regions: $95^{\circ}\text{W}-35^{\circ}\text{E}$, $35^{\circ}\text{S}-35^{\circ}\text{N}$; $90^{\circ}\text{W}-30^{\circ}\text{E}$, $30^{\circ}\text{S}-30^{\circ}\text{N}$ and $85^{\circ}\text{W}-25^{\circ}\text{E}$, $25^{\circ}\text{S}-25^{\circ}\text{N}$, respectively. Due to the different grid spacing, the model dynamic time-step varies from 360 s to 45 s. Time-stepping in the physical parameterizations, such as the cloud-cover time interval, is set to 1080 s in the coarsest resolution and to 900 s for the finest resolution.

To address the concern that the nesting approach might unduly constrain the results, we performed additional simulations using a 20 km grid spacing. The simulations showed no significant difference in terms of overall ITCZ structure, resulting ITCZ shift and wind response between a global 20 km E-CON and a nested 20 km E-CON simulation. Hence we find no evidence that the use of a limited domain can spuriously impact the results, at least for the investigated aspects.

In total 12 simulations are performed. P-CON and E-CON start with the same initial conditions and afterwards, boundary conditions in E-CON are forced by the P-CON simulation that used the same SST pattern. For each configuration of convection we conduct a pair of simulations for three cases as shown in Table A.1. For the control experiments, the MAM SST climatology from 1950 - 2013 is prescribed in the simulations. For the AMM experiments, we imposed the SST patterns from the positive and the negative AMM composites (see previous section). In every case the applied SST is held constant in time. The simulation pairs differ only in their start dates, one is started with the ECMWF - IFS initial conditions of 27 February 2017 at 00UTC, the other one with the initial conditions of 1 March 2017 at 00UTC. The simulation pairs are used to help assess the influence of internal variability on the results, where each pair of E-CON simulation is driven by its respective P-CON simulation. Simulations are integrated for three months in stand-alone mode. The analysis is performed for the period between 11 March and 31 May, thus allowing 10 days for the simulations to spin up.

A.3 SENSITIVITY OF PRECIPITATION TO IMPOSED SST

A.3.1 Mean state

We examine the main features of the precipitation as simulated using the climatological SST (control experiments). The mean precipitation amount is 3.5 mm d^{-1} for E-CON and 3.6 mm d^{-1} for P-CON over the $20^{\circ}\text{S} - 20^{\circ}\text{N}; 75^{\circ}\text{W} - 15^{\circ}\text{E}$ domain. Values are also similar when only land is considered (3.8 mm d^{-1} and 3.6 mm d^{-1} , respectively). Differences are more marked over the ocean: 2.9 mm d^{-1} for E-CON and 3.4 mm d^{-1} for P-CON. For this reason and because we are interested in the implications for SST coupling, further analysis is focused on this region.

As shown in Fig. A.4, both the simulations with parameterized (P-CON) and explicit (E-CON) convection display a double precipitation band which is more pronounced over the west basin. The main difference between E-CON and P-CON, however, is that the precipitation features in P-CON are confined closer to the neighboring continents. E-CON simulates a more zonally elongated distribution, with both bands expanding up to about 15°W , but precipitation maximizing north of the equator (Fig. A.4a). The northern band reaches a maximum at about 3°N , whereas the southern band peaks near 4°S . For P-CON, precipitation bands are not as zonally extensive and stay confined westward of 20°W (Fig. A.4b). Both (north and south) bands show high precipitation amounts over the eastern coast of South America at about 3°N and 6°S , respectively. Additionally, P-CON displays a second peak of precipitation over the Gulf of Guinea, which is absent in E-CON. Such distinct features of E-CON and P-CON are mostly an effect of the representation of convection, since they persist when coarsening the grid spacing of E-CON to the resolution of P-CON. Moreover, the fact that the main precipitation band extends towards the central basin, in principle, is closer to observations in E-CON than in P-CON. However, one has to be careful to not overinterpret this comparison because our simulations are based on fixed SST composites, rather than changing observed SST.

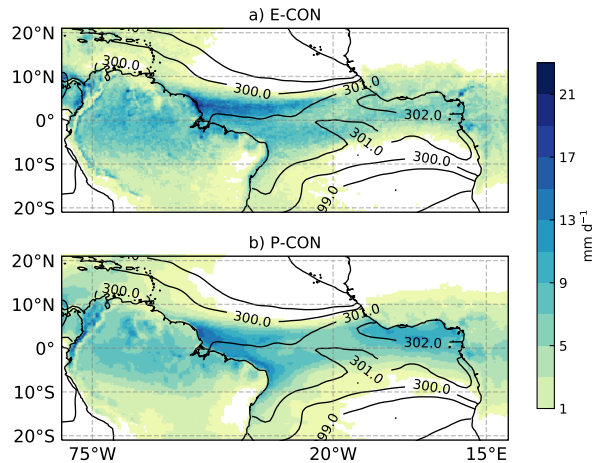


Figure A.4: Mean precipitation (shaded) and prescribed SST climatology (contours) of the three month run for (a) E-CON and (b) P-CON simulations interpolated onto the coarser grid of P-CON.

By plotting the precipitation versus SST over the ocean, it becomes apparent that the coastal confinement of precipitation over the Gulf of Guinea in the P-CON simulations is likely the result of P-CON having a stronger sensitivity to SST. Figure A.5 shows this

clearly, as the precipitation associated with SSTs larger than 301.5 K is much greater for P-CON than it is for E-CON. This is consistent with the predisposition of GCMs relying on convective parameterizations to favour convection over the local SST maximum (Biasutti et al., 2006). Coarsening the grid spacing of E-CON to that of P-CON also leads to an overestimation of precipitation at high SST. This is expected since, by coarsening the grid spacing, the triggering of convection becomes more difficult, which favors convection over high SST regions. Moreover, the well-known pick-up of precipitation with SST is more evident in E-CON at about 300 K. For P-CON, precipitation increases more gradually beginning already at 299 K. This results in a larger area of light precipitation ($< 3 \text{ mm d}^{-1}$) in the case of P-CON (Fig. A.4b and right panel in Fig. A.5), which is an expression of the well-known drizzle problem of convective parameterizations (Dai, 2006).

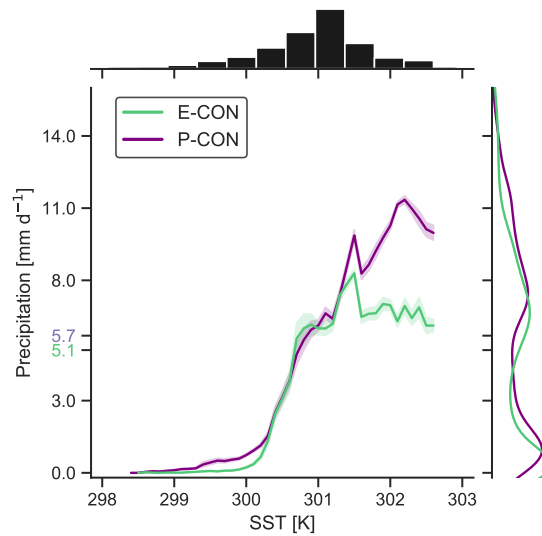


Figure A.5: Average precipitation associated with SST over the deep tropical Atlantic ($10^{\circ}\text{S} - 10^{\circ}\text{N}$, $75^{\circ}\text{W} - 15^{\circ}\text{E}$). Bins of 0.1 K are used for SST. Mean values of precipitation over the ocean area are highlighted for E-CON (green) and P-CON (purple) simulations. The shaded areas denote the 95% confidence intervals of the simulated values. The histogram of SST and kernel density estimate of precipitation are displayed on the upper and right side of the plot, respectively.

A.3.2 Response to the AMM-SST pattern

Figure A.6 shows the precipitation, surface wind and SST anomalies relative to the control experiments for the cases with positive (a,d) and negative (b,e) AMM-SST patterns. In addition, the zonal mean precipitation over the west basin (c,f) is displayed because the observations indicate that in this region the precipitation response is more robust (Fig. A.2).

In the case of positive AMM, both E-CON and P-CON display a similar response. This response can be described as an increase of precipitation north of the climatological precipitation bands and a decrease south of them (Fig. A.6a,d). This precipitation pattern can be interpreted as resulting from a northward shift of the climatology. The displacement of the northern precipitation band is apparent for both E-CON and P-CON; whereas the southern band shift is more distinctive in E-CON due to a more prominent

double band structure in its precipitation climatology. With respect to land precipitation, the two simulations also exhibit similarities with the positive AMM being associated with a north-south precipitation anomaly. This feature is mainly visible in tropical South America and less so over West Africa in agreement with observations, which do not show a robust precipitation response over land in the eastern basin.

The similarity between E-CON and P-CON over the tropical Atlantic and the apparent shift of the precipitation climatology remains true for the negative AMM experiments (Fig. A.6b,e). E-CON and P-CON simulations display enhanced precipitation south of the location of each climatological precipitation band, whereas precipitation decreases towards the north (Fig. A.6c,f). The precipitation response over land is less consistent. E-CON depicts a north-south precipitation anomaly over tropical South America between $10^{\circ}\text{S} - 10^{\circ}\text{N}$, whereas P-CON displays mostly negative anomalies between $0 - 10^{\circ}\text{N}$.

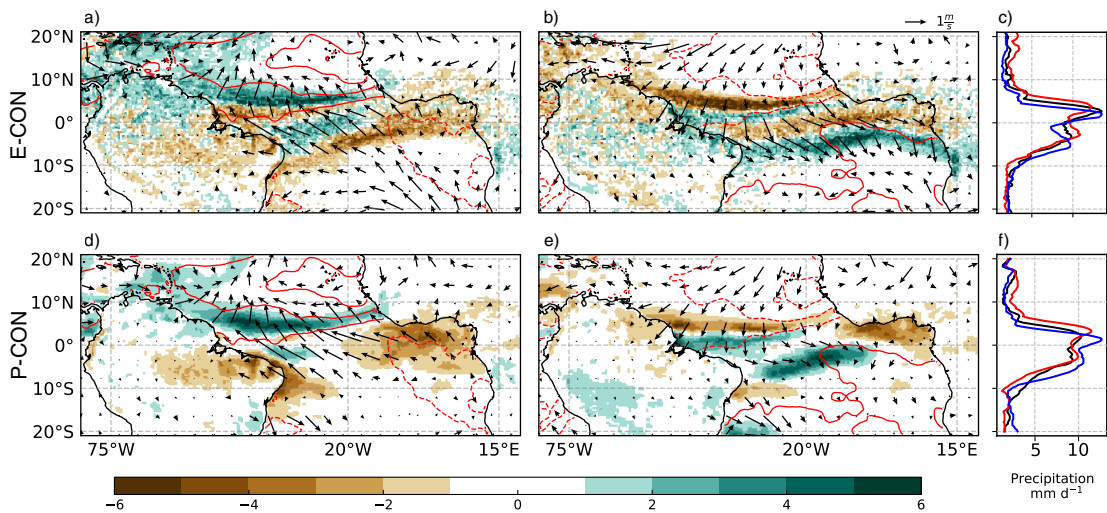


Figure A.6: Precipitation (shaded), SST (contours, intervals each 0.3K starting at 0.2K) and surface wind anomalies related to the (a,d) positive and (b,e) negative AMM for E-CON (upper panels) and P-CON (lower panels) ensemble simulations. The zonal mean precipitation greater than 1 mm d^{-1} over the west Atlantic ($75^{\circ}\text{W} - 20^{\circ}\text{W}$) is displayed for (c) E-CON and (f) P-CON. This threshold is chosen to emphasize regions with larger differences. Solid contours refer to the climatology (black contour), positive (red contour) and negative (blue contour) AMM.

Not only the precipitation response in E-CON and P-CON seems similar, but also the wind pattern response. A cross-equatorial wind flow from 5°S to 5°N in the western Atlantic coincides in both simulations. This picture of precipitation and wind anomalies agree with observations (Fig. A.2). The imprinting of SSTs on boundary layer temperatures, and hence pressure gradients would drive the surface wind anomalies. The resulting cross-equatorial winds can then be interpreted as driving the meridional shift of the precipitation, as suggested by previous studies (e.g. Hastenrath and Greischar, 1993; Chiang et al., 2002; Chiang and Vimont, 2004). This interpretation is also consistent with our simulations.

Even though the overall pattern of the oceanic precipitation response to the AMM is similar between E-CON and P-CON, a more detailed look at Fig. A.6 also reveals localized discrepancies. These are most notable in the west basin. The zonal mean precipitation of P-CON (Fig. A.6f) shows changes in the precipitation intensity in addition to the shift. In particular, the maximum precipitation in P-CON (placed between

0-5°N) increases with respect to the climatology in both positive and negative AMM cases. For E-CON (Fig. A.6c), changes in the maximum precipitation intensity are less clear than in P-CON. Furthermore, the precipitation amount over the whole Atlantic basin are about the same for the climatology, positive and negative AMM; both in E-CON and P-CON. Therefore, the changes in intensity are localized over the rainiest regions, most notably so for P-CON as compared to E-CON.

A second difference between E-CON and P-CON response to the AMM is apparent when comparing the positive and negative AMM responses. In the case of E-CON, the precipitation response to the positive and negative AMM are opposite of one another (Fig. A.6a,b), which, given the symmetry between positive and negative AMM-SST patterns (Figure A.3a), is indicative of a linear response of precipitation to SST. In contrast, with P-CON the response is less symmetric, most notably so in the southern precipitation band (Fig. A.6d,e). In the positive AMM, P-CON keeps the southern band position closer to the South America coast as shown in the climatology (Fig. A.4b). In the negative AMM, the southern precipitation band of P-CON, extends farther east up to 5°W (not shown). This "asymmetric" response to the AMM could be related to the variability of P-CON response. Especially over the south tropical Atlantic, P-CON displayed more inconsistency in the precipitation response among individual simulation members (for all climatology and AMM experiments) in contrast to E-CON, which showed a robust response across all six individual runs (not shown).

A.3.3 *Shift in the climatology*

In section 3b both E-CON and P-CON simulations appeared to predominantly respond to a positive or negative AMM phase by shifting their mean precipitation northward or southward, respectively. This response is consistent with the cross-equatorial winds induced by the inter-hemispheric difference in SST. The SST pattern, however, is not a result of a meridional displacement in the mean state. Instead, the SST anomalies display an asymmetric pattern that favor the northern hemisphere (Fig. A.2). In this section, we explore how much of the response can indeed be interpreted simply as a shift of the observed precipitation climatology, with a main focus on the oceanic ITCZ where the shift is more apparent (both in observations and simulations).

For this purpose, the mean precipitation over the ocean between 10°S - 10°N from the control runs is displaced meridionally in proportion to the grid size (0.36°). Then, the precipitation anomalies obtained from shifting the climatology are compared with those from the AMM runs. A similar procedure is applied to precipitation composites from observations, which were interpolated to the model resolution.

The results show that interpreting the precipitation response to the AMM as an approximately 1° shift in the precipitation climatology, explains a large amount of the precipitation response, with pattern correlations (r) larger than 0.55 for all the simulations and the observations (Fig. A.7). This interpretation works best for E-CON simulations, which depict a correlation of about 0.75 in both positive and negative AMM. For P-CON simulation, a meridional shift in the climatology explains the response of precipitation to the positive AMM ($r=0.75$) much better than the response to the negative AMM ($r=0.55$). Given the known biases of convective parameterizations (Fiedler et al., 2020) and the obvious differences in the precipitation climatology between E-CON and P-CON, it is remarkable that the two simulations exhibit an identical shift of 1°. In the case of observations, most of the precipitation response is also explained by the meridional shift of its climatological position. The maximum correlation is 0.6 for positive AMM and

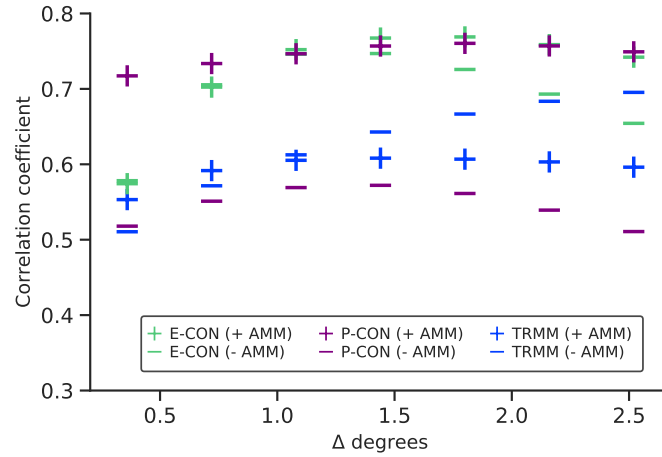


Figure A.7: Correlation of precipitation anomaly maps obtained from shifting the climatology by different degrees in latitude for E-CON (green), P-CON (purple) and observations (TRMM, blue). All data has been interpolated onto the coarser grid of P-CON. Plus (minus) markers indicate positive (negative) AMM case.

about 0.7 for negative AMM. Moreover, the pattern correlation reflects a symmetry in the response for positive and negative AMM at about 1° shift, as it is observed in E-CON.

The analysis of the pattern correlation also highlights the linearity in the meridional shift of precipitation climatology for positive and negative AMM. This is again evident for E-CON and not for P-CON. As explained in the previous section, P-CON displayed an anomalous eastward extension of the southern precipitation band in the negative AMM. This additional change in the precipitation pattern explains the lower correlation obtained in P-CON for the negative AMM ($r=0.55$). In fact, if the pattern correlation is only computed over western basin, a correlation of 0.75 is obtained as in the positive AMM.

To get a more detailed view on the approach of interpreting the precipitation response as a shift, Fig. A.8 shows the precipitation anomalies due to the AMM (shaded) and those obtained from displacing the climatology (contour line) by 1.08° . Overall, there is a very good agreement between the shifted precipitation climatology and the actual response to the AMM for both simulations and observations. This agreement is more apparent in E-CON (Fig. A.8a,b), and to a lesser degree in observations (Fig. A.8e,f), for both positive and negative AMM. In the case of P-CON (Fig. A.8c,d), a shift of the mean precipitation matches the actual precipitation response to the positive and negative AMM principally over the northern basin. South and near the equator discrepancies are more evident. However, as explained in the previous section, P-CON displayed a non-robust precipitation response in the southern Atlantic when comparing across individual members.

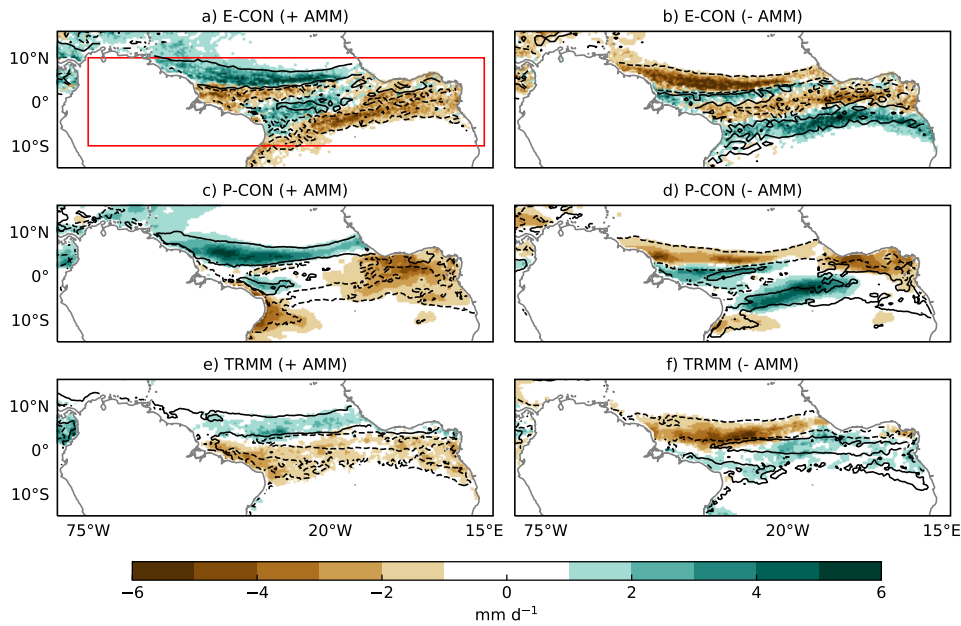


Figure A.8: AMM precipitation anomalies from (a,b) E-CON, (c,d) P-CON and (e,f) observations (shaded). The resulting anomalies from shifting the climatology is displayed as the 1 mm d^{-1} anomaly contour line (positive solid line, negative dashed line). The red box in a) indicates where in the ocean the correlation in Fig A.7 was computed.

A.4 IMPLICATIONS FOR OCEAN-ATMOSPHERE COUPLING

In the previous section we explored how the representation of moist convection influences the precipitation response to positive and negative AMM-SST patterns. This addresses the AMM coupled system from one direction. In this section, we examine whether the atmospheric response to the AMM in explicit versus parameterized convection is indicative of a different coupling to the SSTs. This could happen either via a distinct response of the surface fluxes Vimont, 2010; Martinez-Villalobos and Vimont, 2016; Amaya et al., 2017 and/or of the radiative fluxes Evan et al., 2013; Myers et al., 2018, as both control the surface energy budget. Hohenegger et al. (2020) showed that the surface fluxes are robust to changes in grid spacing, whereas the surface radiation (due to its link to low-level cloudiness) is not. Hence, in the following, we focus our analysis on the response of the surface fluxes and how their distinct response in E-CON and P-CON might amplify or dampen the SST anomaly if the simulations were coupled.

We start by examining the representation of the mean wind in E-CON and P-CON, as changes in the wind speed will strongly impact the surface fluxes. Surface winds are generally faster in E-CON than P-CON simulations (Fig.A.9) regardless of the experiment or the spatial resolution. This difference can be explained by a stronger pressure gradient in E-CON as shown in Fig.A.9, demonstrating that the stronger winds are geostrophically balanced. In particular, along 5°N , the edge of the main precipitation band in the control simulations, we observe a collocation of stronger wind speed and stronger meridional pressure gradient in E-CON as compared to P-CON. North of 5°N , the atmosphere is moister in E-CON than in P-CON below 800hPa, and drier aloft (Fig.A.10). This profile in the humidity distribution favors a stronger radiative cooling by longwave radiation in E-CON north of 5°N , consistent with a colder atmosphere, see the maximum temperature anomaly at about 850hPa north of 5°N in Fig A.10. The resulting difference

in the temperature gradient sets the difference in the surface pressure gradient that in turn, sets the difference in the surface winds. This mechanism follows that proposed by Naumann et al. (2019), which generalized the arguments of Lindzen and Nigam (1987) to emphasize the importance of radiative cooling in supporting near-surface pressure gradients.

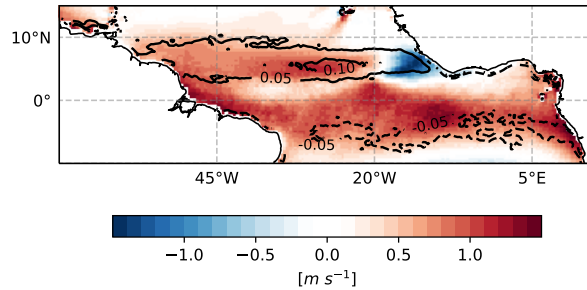


Figure A.9: Surface wind speed (shaded) and meridional pressure gradient (contours) difference between E-CON and P-CON for the control experiments. Units for the pressure gradient are Pa km^{-1} .

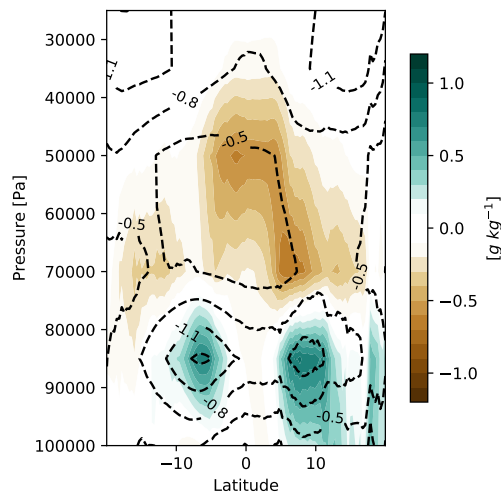


Figure A.10: Meridional cross sections of zonal mean ($75^\circ\text{W} - 15^\circ\text{W}$) specific humidity (shaded) and virtual temperature (contours) difference between E-CON and P-CON for the control experiments. Temperature contour interval is 0.3K .

Differences in the mean state wind speed between E-CON and P-CON translate into different wind speed anomalies as a response to the AMM, with larger anomalies in E-CON (0.3 m s^{-1} to 0.8 m s^{-1} greater in E-CON, not shown). Differences in wind speed will project on the surface enthalpy flux, which will influence the SST, given the constraint of the surface energy budget. Since changes in the surface fluxes influenced by air-sea differences (e.g. Δq) are much less than those influenced by the surface winds (not shown), we focus here on the wind-driven surface enthalpy flux difference $\delta F_h = (\delta V/V) F_h$, where F_h is the surface enthalpy flux (sum of latent and sensible heat flux, defined positive upwards) and V is the wind speed at 10 m. We interpret δF_h as the change in the surface enthalpy flux due to a given change in wind. If we assume no changes in the radiative fluxes and given our sign convention, then negative values in

δF_h would induce an ocean warming.

In a positive AMM case, a negative δF_h would amplify positive SST anomalies in the northern basin (Fig. A.11a,c). The E-CON simulation (Fig. A.11a) suggests most of this amplification over the region $0 - 15^\circ\text{N}$, $60^\circ\text{W} - 30^\circ\text{W}$, which collocates with the prescribed $0.2\text{K} - 0.5\text{K}$ SST anomaly. P-CON also suggests an amplification of SST over that region, but of weaker amplitude, and damping of the SST anomaly over the northeast basin where the SST anomalies are highest ($+0.8\text{K}$). Note here, that according to the observed evolution of the AMM, the importance of wind-induced surface fluxes vary from the subtropical regions (in the preceding boreal winter) towards the southwest equator in boreal spring (Chiang and Vimont, 2004; Amaya et al., 2017). Especially during the peak season of the AMM (MAM), the southwestern edge of the SST anomalies ($0 - 10^\circ\text{N}$, $50^\circ\text{W} - 20^\circ\text{W}$) is where the WES feedback is most strongly expressed (e.g. Chang et al., 2001; Chiang et al., 2002; Hu and Huang, 2006; Foltz et al., 2012; Amaya et al., 2017). It is precisely over this area, that stronger δF_h in E-CON is observed as compared to P-CON (Fig. A.11e). Moreover, this region is also important for convection to occur, since the northern precipitating bands are placed over those latitudes (Fig. A.6a,d). Thus, not only E-CON supports a greater amplification of the SST anomalies, but also sustains convection more strongly than P-CON due to the stronger wind-driven fluxes.

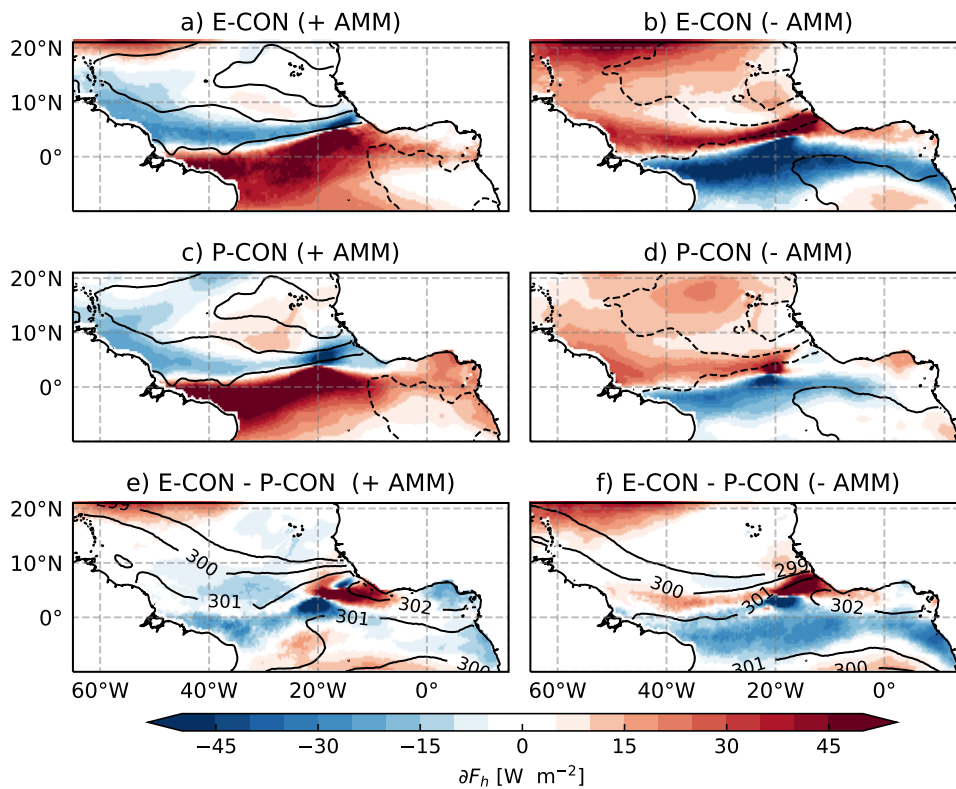


Figure A.11: Wind-driven surface enthalpy flux (shading) for a positive (left panel) and a negative (right panel) AMM, in (a, b) E-CON and (c, d) P-CON simulations. Blue colors denote a reduction of the surface fluxes and suggest an ocean warming; whereas red colors denote an increase of the surface fluxes and suggest an ocean cooling. Prescribed SST anomalies (contours) interval is 0.3K . The difference between E-CON and P-CON simulations are displayed in the bottom panels for (e) positive and (f) negative AMM with its corresponding mean SST (contours).

An amplification of the SST anomalies would also be supported in the negative AMM for both E-CON and P-CON (Fig. A.11b,d). In this case, the northern basin depicts a broadly positive δF_h which is indicative of an ocean cooling. However, differences in δF_h between E-CON and P-CON (Fig. A.11f) reveal again that E-CON would favor a stronger amplification of the SST anomalies over the northwestern tropical Atlantic (0 - 10°N, 50°W - 20°W).

The above mentioned results suggest that simulations with explicit convection would amplify AMM-SST anomalies more strongly than those with parameterized convection in simulations coupled to an interactive ocean. This would have implications in the representation of the AMM development, since the WES feedback is an important driver for sustaining and propagating SST anomalies in the AMM.

A.5 SUMMARY AND CONCLUSIONS

This study investigates the sensitivity of the coupling between precipitation and SST to the representation of convection, being explicit or parameterized, over the tropical Atlantic. We analyze this coupling in the context of the positive and negative phases of the Atlantic Meridional Mode (AMM). The AMM is characterized by a warmer than usual north tropical Atlantic and cooler than usual south tropical Atlantic in its positive phase; whereas opposite conditions occur in its negative phase. We focus first on the response of precipitation over ocean to a positive and a negative AMM-SST pattern as compared to the climatology. Then, we investigate possible implications for the coupling to SST.

To fulfil these goals, we use the ICON atmospheric model with the NWP physics configuration. Numerical experiments are performed using SST composites of the climatological, AMM-positive and AMM-negative conditions, respectively. To select the AMM-SST patterns we first examine observations and define "strong" AMM events as those that exceed one standard deviation of the AMM index. Analysis of individual events show a high degree of similarity among strong AMM events in terms of their SST pattern and associated precipitation response. This analysis supports our methodology approach to build positive and negative AMM composites of strong events. The above mentioned SST patterns are then prescribed to be constant in our simulations integrated from March to May, the season when the AMM is more prominent. Two configurations are applied: one with convective parameterization (P-CON) at a grid spacing of 40 km on a global domain; and one with the convective parameterization turned off (E-CON) at a grid spacing of 5 km over a nested tropical Atlantic domain.

Due to the intensive amount of computation required for the E-CON simulations, they could not be integrated globally like P-CON and only two members were simulated. Such a small number of samples may spuriously affect the results. However, differences between E-CON and P-CON simulations are larger than differences among E-CON and P-CON respective members. In fact, features such as the ITCZ structure, wind speed velocity, vertical profile of temperature and humidity are consistent regardless of the experiment. Moreover, a global simulation conducted with a grid spacing of 20 km revealed similar results than the 20 km nested simulations. Hence, we believe the framework to be informative, despite the small number of simulations.

Based on the analysis of these simulations we address two questions: 1) Does the precipitation response to AMM-SST patterns differ when convection is explicitly resolved as opposed to parameterized convection? and 2) Does the atmospheric response in

explicit and parameterized convection suggest different couplings to the underlying SSTs?

1. We find that the precipitation response to an AMM-SST pattern is robust to the representation of convection. Simulations with explicit and with parameterized convection show a similar response. Both E-CON and P-CON simulations shift the mean position of the ITCZ about one degree towards the warmer tropical Atlantic. Interestingly, this is true even though E-CON and P-CON display a distinct precipitation climatology: P-CON shows a stronger precipitation sensitivity to high SST than E-CON and thus, places an extra peak of precipitation in the eastern basin, coinciding with the maximum SST. Different precipitation patterns are also displayed in response to the AMM, but are the result of shifting the precipitation climatology. The meridional displacement in the precipitation can be explained by the cross-equatorial surface wind anomalies induced by the AMM-SST gradient (e.g. Chiang et al., 2002; Chiang and Vimont, 2004), with the precipitation being shifted towards the region where winds weaken. Our results showed that the latitudinal range where the wind anomalies occur (5°S - 5°N) is about the same for both simulations, which may explain the similar displacement in the Atlantic ITCZ for E-CON and P-CON.

Despite this overall similarity in the precipitation response between E-CON and P-CON, some discrepancies can also be noted. In addition to the meridional shift of precipitation, there are localized changes in the precipitation intensity. These changes are more obvious over the rainiest regions in P-CON as compared to E-CON. Furthermore, our results indicate a linearity in the response of E-CON to the AMM. The meridional shift of the mean precipitation explains about 60% ($r=0.75$) of the precipitation response for both positive and negative AMM in E-CON simulations. In contrast, the precipitation response as explained by the meridional shift in P-CON explains 60% in the positive AMM but only 30% ($r=0.55$) in the negative AMM. Only over the west tropical Atlantic, do we find a symmetry (and hence linearity) in the precipitation shift between positive and negative AMM for P-CON.

2. Analysis of surface flux anomalies lead us to expect a stronger amplification of SST anomalies in simulations with explicit rather than parameterized convection. Our argument is based on the wind speed anomalies in response to an AMM-SST pattern. Surface winds are generally stronger in E-CON due to a stronger pressure gradient, itself related to stronger radiative cooling north of 5°N , a result of a moister boundary layer and drier free atmosphere. The changes in the wind-driven heat fluxes are in consequence, more strongly enhanced in E-CON. Positive SST anomalies in the north tropical Atlantic (positive AMM) would be amplified when the change in the wind-driven surface flux is negative. Therefore, a stronger amplification of the SST anomalies would be induced by a stronger enhancement of the wind-driven heat flux in E-CON as compared to P-CON. In particular, stronger wind-driven fluxes in E-CON than P-CON were visible over the region where the Wind–Evaporation–SST (WES) feedback has been identified by previous studies to play an important role on the development of the AMM (e.g. Amaya et al., 2017). Differences between E-CON and P-CON over this region are mostly evident in the positive AMM case and to a lesser extent in the negative AMM. Based on the mentioned results, we hypothesize that coupled simulations with explicit convection would lead to stronger amplification of the SST anomalies, affecting the development and propagation of the AMM mode, in comparison to coupled simulations with parameterized convection.

ACKNOWLEDGEMENTS

This study was supported by the Max Planck Society for the Advancement of Science. The authors thank Traute Crueger and three anonymous reviewers for their useful and constructive comments on the manuscript. Primary data and scripts used in the analysis that may be useful in reproducing the author's work are archived by the Max Planck Institute for Meteorology and can be obtained via the institutional repository <https://pure.mpg.de>

APPENDIX

Paccini, L., Hohenegger, C. & Stevens, B. (2021). "Atmosphere-ocean coupling related to the Atlantic Meridional Mode in simulations with explicit and parameterized convection"

The contributions of the authors to this paper are as follows:

All authors collaborated in the conceptual experiment design. LP adapted the atmospheric ICON-NWP and the Flake model to a slab-ocean configuration. The simulations, analysis, discussions and writing of the paper was conducted by LP. CH supervised the study, discussed the results and reviewed the manuscript. BS discussed the results.

Atmosphere-ocean coupling related to the Atlantic Meridional Mode in simulations with explicit and parameterized convection

Laura Paccini¹, Cathy Hohenegger¹ and Bjorn Stevens¹

¹Max Planck Institute for Meteorology, Bundesstraße 53, 20146 Hamburg, Germany

We investigate how the representation of convection influence the atmosphere-ocean coupling in the Atlantic Meridional Mode (AMM). We use the atmospheric ICON model coupled to a slab-ocean in two configurations: one with explicit convection (E-CON) at a storm-resolving resolution and one with parameterized convection (P-CON) at a coarser grid spacing. Simulations are performed from mid-April to end of July in order to analyse the evolution of the positive AMM mode towards boreal summer. Our results indicate that the representation of convection interacts differently with the underlying SSTs. First, during the peak signal of the AMM in May, the precipitation response is displaced 1° northward in E-CON simulations whereas P-CON simulations show a displacement of about 2° . Second, during the decay of the AMM, the reduction of SST anomalies is more pronounced in E-CON than in P-CON simulations. Part of this change can be explained by the cooling of wind-driven latent heat flux. In the E-CON simulations, this cooling is between 0.5K-1K greater compared to P-CON. Also, wind-driven latent heat flux anomalies explain up to 67% of the total change of SST anomalies in E-CON and 48% in P-CON, showing a larger imprint of the wind response on the SST change. This result agrees with the hypothesis proposed in Paccini et al., 2021 which based on the wind-driven surfaces fluxes of uncoupled simulations, suggests that the change of SST anomalies would be stronger in simulations with explicit than with parameterized convection.

Ocean-atmosphere interactions are dominant in the tropics and affect the atmospheric circulation and climate variability across different timescales. Over the tropical Atlantic Ocean basin such interactions influence the position of the Intertropical-Convergence Zone (ITCZ, e.g. Xie and Philander, 1994) and play an important role in the development of sea surface temperature (SST) modes of variability like the Atlantic Meridional Mode (AMM) or the Atlantic Niño (e.g. Ruiz-Barradas et al., 2000), which in turn affect the spatial distribution of precipitation. This complex coupled system involves interactions between small-scale processes, such as convection and turbulent fluxes, which are not adequately represented by state-of-the-art climate models, given their coarse grid spacing. Biases in such models stem from both the atmospheric and oceanic components (Richter and Tokinaga, 2020). In this study, we focus on the atmospheric role by investigating the influence of the representation of convection on its coupling to SST anomalies. We use an atmospheric model coupled with a simple representation of the ocean to study the ocean-atmosphere coupling in the context of the AMM.

One of the important mechanisms for the development and sustainment of the AMM is the so-called Wind-Evaporation-SST (WES) feedback (Xie and Philander, 1994; Nobre and Shukla, 1996; Chiang and Vimont, 2004; Mahajan et al., 2009; Amaya et al., 2017). The AMM is triggered during boreal winter by a stochastic atmospheric forcing in the subtropical winds that induces an SST anomaly in the northeast tropical Atlantic (Saravanan and Chang, 2000; Chang et al., 2001; Chiang et al., 2002). The resulting inter-hemispheric difference in SST drives cross-equatorial surface winds towards the warmer hemisphere. For instance, a positive SST anomaly is associated with a weakening of the northern trade winds (i.e. southwesterly wind anomalies), which reduces the latent heat flux (evaporation) and consequently reinforces the surface warming. This positive thermodynamical feedback is maximized during boreal spring and induces a meridional displacement of the ITCZ towards the warmer hemisphere (Hastenrath and Greischar, 1993; Nobre and Shukla, 1996; Chiang and Vimont, 2004). During the transition to boreal summer, the positive SST anomalies reduce and propagate southwest. Latent heat flux anomalies display a dipole where the reduced evaporation co-locates with the displaced positive SST anomaly, while more evaporation coincides with the region of cooling. This feature of latent heat flux and SST indicates that the WES feedback plays an important role towards the decay of the AMM (Hu and Huang, 2006; Amaya et al., 2017).

Among other mechanisms affecting the AMM, radiative and oceanic feedbacks are at play; however, their relative roles are still under debate and are subject of current research. One of these mechanisms is related to changes in the short wave radiation by strato-cumulus clouds, which are tightly related to SST, and can reinforce the AMM-SST-related anomalies, potentially delaying the onset of the decay phase (Hu and Huang, 2006; Evan et al., 2013; Myers et al., 2018). For instance, a positive AMM featuring positive SST anomalies in the north tropical Atlantic would decrease stratocumulus clouds off the equator, which would increase the incoming short-wave radiation and favor the surface warming. Another mechanism involving ocean dynamics, considers the influence of surface winds and latent heat flux anomalies on the depth of the oceanic mixed layer (Rugg et al., 2016; Kataoka et al., 2019). In the case of the positive AMM, weaker winds reduce the turbulent flux while reduced evaporation increases buoyancy in the ocean. As a result, the mixed layer depth gets shallower and allows the short wave radiation to amplify the warming. Therefore, this mechanism can also retard the decay of the AMM.

Most of the studies focusing on the physical mechanisms of the AMM are based on observations and reanalysis products (Chiang and Vimont, 2004; Hu and Huang, 2006; Rugg et al., 2016; Amaya et al., 2017; Myers et al., 2018), or tested in simplified models (Evan et al., 2013; Kataoka et al., 2019). The representation of such mechanisms by coupled climate models, which parameterize convection due to their coarse resolution, have been found either weak or absent (e.g. Amaya et al., 2017; Myers et al., 2018; Kataoka et al., 2019). In a recent study, Paccini et al. (2021) found that the wind response to the AMM is very distinct by comparing explicit against parameterized convection in uncoupled simulations. Based on this result, it was hypothesized that simulations with explicit convection would lead to a stronger change in SST given the greater wind-induced surface fluxes, if simulations were coupled. We test this hypothesis in the present study and for the first time, investigate the ocean - atmosphere coupling related to the AMM with storm-resolving simulations.

This study focuses on the evolution of the AMM from its peak signal in boreal spring towards its decay in boreal summer. We divide the analysis in two parts. First, we look at the precipitation response in May, given the strong signal of the AMM. In Paccini et al. (2021), we found that the precipitation response to the AMM can be interpreted as a meridional shift of the mean-state precipitation by 1° . Also, the same precipitation response was found for explicit and parameterized convection simulations. We test here whether these results are confirmed with coupled simulations. Second, we address the atmosphere-ocean coupling during the decay of the AMM. We define this coupling as the change of SST anomalies per change in the wind-driven latent heat flux. The proposed hypothesis in Paccini et al. (2021) considers the wind response to the AMM averaged from March to May, where weaker winds would potentially increase the positive SST anomaly. In this study we focus on the wind response during the decay of the AMM, from its peak signal in May towards July; therefore, no amplification is expected. Nonetheless, we test the hypothesis of whether stronger changes in the wind response to the cooling of the AMM by storm-resolving simulations, lead to stronger changes in the SST anomalies.

B.2 DATA AND METHODS

B.2.1 Observations

For the initial conditions of the simulations we use analysis data from the European Centre for Medium-Range Weather Forecasts (ECMWF) Integrated Forecast System (IFS). The SST data from the analysis is replaced by composite means from the Hadley Centre Sea Ice and Sea Surface Temperature dataset (HadISST; Rayner et al., 2003) following the methodology described in Paccini et al., 2021.

We also use TRMM-3B42 V7 rainfall product from the Tropical Rainfall Measuring Mission (Huffman et al., 2007) on a 0.25° spatial grid and covering the period 1998-2013, which we take as reference values.

B.2.2 Model and experimental set-up

Simulations are performed with the ICOSahedral Non-hydrostatic (ICON) model (Zängl et al., 2015) in its Numerical Weather Prediction (NWP) configuration, version 2.6.01. The

model settings and experimental design (e.g. grids, external parameters) are as described in Paccini et al., 2021, except for the setting of the ocean surface.

We introduce a simple slab-ocean scheme into the ICON-NWP atmospheric model. For this purpose we adapt the Fresh-water lake model (Flake, Mironov et al., 2010) into a one-layer slab scheme as follows. First, we fix the mixed layer depth to 30m, an average value of the mixed layer depth for the tropical Atlantic basin (Foltz et al., 2013). The depth of the lake is also set equal to the mixed layer depth and invariant over time. The temperature of the mixed layer depth is uniformly distributed in the vertical and is initialized with the surface temperature. This mixed-layer model only considers surface and radiative fluxes from the atmosphere into the water column, and neglects horizontal transport. As a final step, we modify the surface parameters of the initial conditions by re-labeling the ocean regions as lake regions, which now follow the one-layer slab scheme.

Following the experimental design of Paccini et al., 2021, simulations are first performed over a global domain at 40km grid spacing with the convective parameterization scheme turned on ("P-CON" simulations). A one-way nesting approach is then conducted with successive increasing spatial resolution from 20km to 10km and to 5km grid spacing, all with the convective parameterization turned off ("E-CON" simulations). Boundary and initial conditions for E-CON simulations are provided by P-CON simulations.

We perform two experiments for the slab-ocean simulations: a control case with the climatological SST of March-April-May and an AMM case based on the mean composite of strong positive events, as defined and used in Paccini et al. (2021). For each experiment a set of three simulations were performed in order to reduce atmospheric noise. The simulation members are initialized around mid-April and only differ in the initial dates. Simulations are integrated for 100 days and we only consider the last 75 days for analysis.

B.3 MEAN STATE

We analyze first the mean conditions of precipitation, surface winds and SST from the control simulations. Different mean-state features for E-CON and P-CON simulations are shown in Fig. B.1. The surface temperature in E-CON is about 1° colder than P-CON simulations at all latitudes and also has a meridional SST profile closer to observations. This can be explained by less net short-wave radiation at the surface in E-CON consistent with more clouds as compared to P-CON, especially in the eastern basin. In fact, differences in the spatial distribution of SST between E-CON and P-CON are more pronounced zonally over subsidence regions, which are associated with stratocumulus clouds (not shown).

The meridional profile of rainfall shows a prominent precipitation band for both E-CON and P-CON simulations, unlike the uncoupled simulations that displayed a double-band structure (Paccini et al., 2021). The ITCZ profile peaks at about 5°N in E-CON while P-CON depicts a precipitation maximum at about 4°N . The E-CON simulations also exhibit a narrower ITCZ structure by about 20% that of P-CON. Moreover, in agreement with the description of colder temperatures and narrower ITCZ, E-CON displays stronger surface wind speeds than those from P-CON between 5°S and 15°N . This is again a common feature with the uncoupled simulations (Paccini et al., 2021), where E-CON displayed stronger surface winds in all the experiments.

The above mentioned differences between E-CON and P-CON simulations are also displayed in the positive AMM simulations (not shown) with respect to the meridional profiles of SST, rain and wind speeds. Since we focus on the AMM effect relative to the

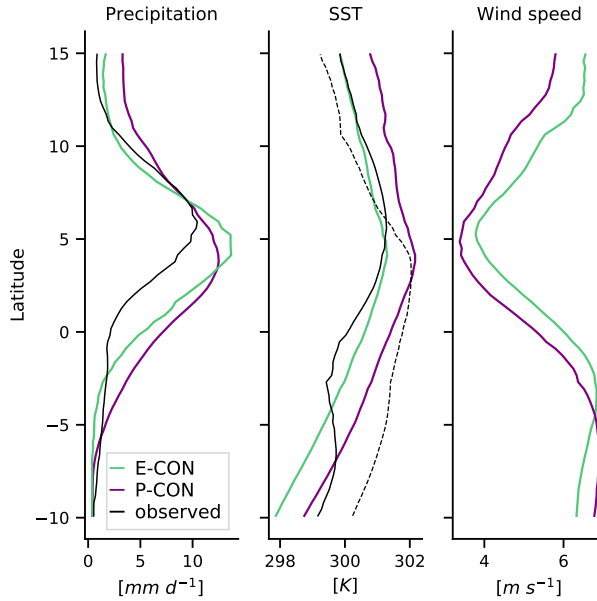


Figure B.1: Zonal mean of SST, precipitation and wind speed of the E-CON (green line) and P-CON (purple line) control simulations. The zonal mean was computed over ocean grid points between 75°W - 15°E from May to July. All simulations were previously interpolated onto the coarser grid spacing (40km). As a reference, May-July 1998-2013 climatology from observations (black lines) are shown for precipitation (TRMM) and SST (HadISST). The zonal mean of the SST used to initialize the simulations (black dashed line) is also shown.

mean state, those differences would not generally impact the anomaly. However, given the non-linear relationship of convection and surfaces fluxes with SST (e.g. Zhang and McPhaden, 1995), the mean state conditions are relevant for these processes and will be taken into consideration for interpreting the results (Section B.4 and B.5).

B.4 ATMOSPHERIC RESPONSE

In this section we describe the atmospheric response to the AMM. We consider the initial response in May, when the SST anomalies are strong in the northeastern basin, up to July when we expect a decay of the SST anomalies.

In May, the SST anomaly remains similar to the initial perturbation (Fig. B.2 a,c) so we can focus on the precipitation response. It is in May when the signal of the AMM dominates, which means that the meridional difference of SST is strong enough to drive a cross-equatorial wind flow towards the warmer hemisphere (e.g. Chiang and Vimont, 2004). Consequently, precipitation is enhanced northward of the mean-state precipitation position in both E-CON and P-CON simulations. This response also agrees with the results of uncoupled simulations (Fig.6 of Paccini et al., 2021), albeit we remind the reader that the seasonal average (March to May) was considered in that case. The distinct characteristic between E-CON and P-CON is that the precipitation and wind anomalies are more zonally homogeneous in the E-CON simulations. By contrast, the P-CON simulations show positive precipitation anomalies over the Caribbean (10°N to 20°N) and over the eastern Atlantic basin from 5°N to 10°N . In the case of the uncoupled simulations, different patterns of precipitation anomalies between E-CON and P-CON

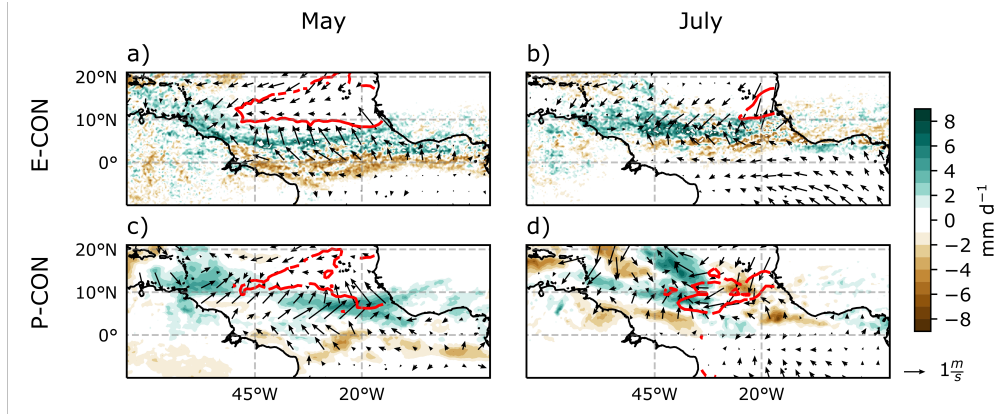


Figure B.2: Precipitation (shaded), SST (0.5K contour) and surface wind anomalies (vectors) from (a,b) E-CON and (c,d) P-CON simulations of the positive AMM for May (left) and July (right).

were the result of shifting the mean-state precipitation, which had a distinct zonal distribution between the two. However, in the coupled simulations the zonal mean-state precipitation looks more similar between E-CON and P-CON, thus the pattern of precipitation anomalies should be more similar in case they exhibit a meridional shift in response to the AMM.

To better illustrate the precipitation response as a meridional displacement we reproduce the analysis of Paccini et al. (2021). First, we obtain the precipitation anomalies from shifting the mean precipitation several degrees northward in proportion to the grid size. Then, we compare these anomalies with the precipitation anomalies from the AMM simulations by calculating their spatial correlation. The correlation coefficients as a function of the northward shift are shown in Fig. B.3 for simulations and TRMM data, which serves as a reference. The results show an optimum displacement of the mean-state precipitation position of about 1°N in E-CON and observations, which is in agreement with the results of Paccini et al. (2021). It is also remarkable how well the E-CON simulations match the observations in this metric after including a simple representation of the ocean in our experimental set-up. By contrast, P-CON shows a maximum correlation of the precipitation displacement at about 2° , which also disagrees with its response in the uncoupled simulations. For larger shifts than 2° of the mean-state precipitation, the correlation remains about the same for P-CON and decreases in E-CON consistently with TRMM data.

The different precipitation response to the AMM between E-CON and P-CON in the coupled simulations might be the result of having different SSTs in the mean-state. Despite of displaying a similar SST anomaly in May, E-CON has cooler SSTs than P-CON as described in Section B.3. In the case of P-CON, SST values are larger than 29°C in the north tropical basin. Given that simulations with parameterized convection tend to co-locate precipitation over high values of SST (e.g. Biasutti et al., 2006; Paccini et al., 2021), it is hypothesized that the larger regions of high SST in P-CON would favor the widening the ITCZ towards the north, in addition to its meridional shift.

Towards boreal summer, precipitation anomalies south of the equator disappear due to the seasonally forced northward displacement of the ITCZ (Fig. B.2 b, d). North of the equator anomalies remain more zonally homogeneous in E-CON (at about 10°) as compared to P-CON, which depicts enhanced precipitation in the central basin between

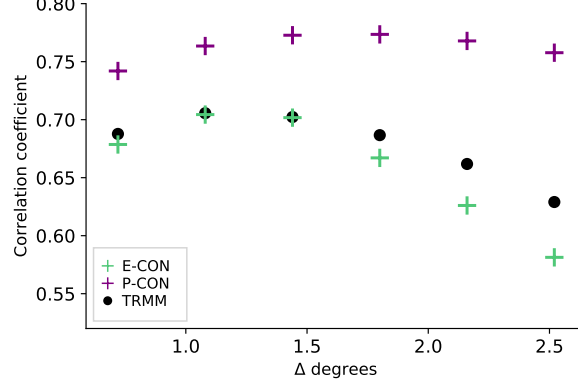


Figure B.3: Correlation of precipitation anomaly maps in May obtained from shifting the mean-state precipitation by different degrees in latitude for E-CON (green), P-CON (purple), and observations (blue). All data have been interpolated onto the coarser grid of P-CON.

5°N-20°N. Similarly, surface winds show mostly an enhancement of the northeasterlies in E-CON, whereas for P-CON wind anomalies look rather uneven in agreement with the precipitation pattern. Analysis of the individual members show larger variability in the patterns of surface winds, especially north of 10°N. However, the magnitude of surface winds remain

Finally, as the AMM signal vanishes, SST anomalies are expected to reduce (Amaya et al., 2017). This response is more evident in E-CON simulations where the 0.5° isoline only reaches up to 25°W. In contrast, the same contour line in P-CON extends up to 40°W. We further explore the SST response in the following section.

B.5 DECAY OF SST ANOMALIES AND THE ROLE OF WIND-DRIVEN LATENT HEAT FLUX

As depicted in Fig.B.2 (b,d), SST anomalies (δSST) are more reduced in E-CON than P-CON simulations. In this section we examine such changes in δSST by analyzing the heat budget in the slab-ocean experiments, which is given by:

$$\partial(\delta SST_{total}) = (\delta LHF + \delta SHF + \delta LW + \delta SW) \frac{\partial t}{h\rho C_p} \quad (\text{B.1})$$

where $\partial(\delta SST_{total})$ is the total change in time of SST anomalies (δSST) from July with respect to May and is the result of the anomalies in the latent heat flux (δLHF), sensible heat flux (δSHF), net long-wave radiation at the surface (δLW) and net short-wave radiation (δSW) at the surface, all of which are averaged from May to July [W/m^2]; $h = 30\text{m}$ is the mixed layer depth, ∂t is the time in seconds from May to July, and ρC_p is the volumetric heat capacity of water [$\text{J}\text{K}^{-1}\text{m}^{-3}$]. We refer anomalies as the difference between the positive AMM and control simulations.

The total change in δSST is then decomposed by its change due to the "non-solar" component, Q_s ($\delta LHF + \delta SHF + \delta LW$), and the solar component I_s (δSW) as displayed in Fig.B.4. Since the changes of δSST as observed in Fig. B.2 are pronounced from 10°N to 20°N and 45°W to 15°W, we focus the analysis on this region.

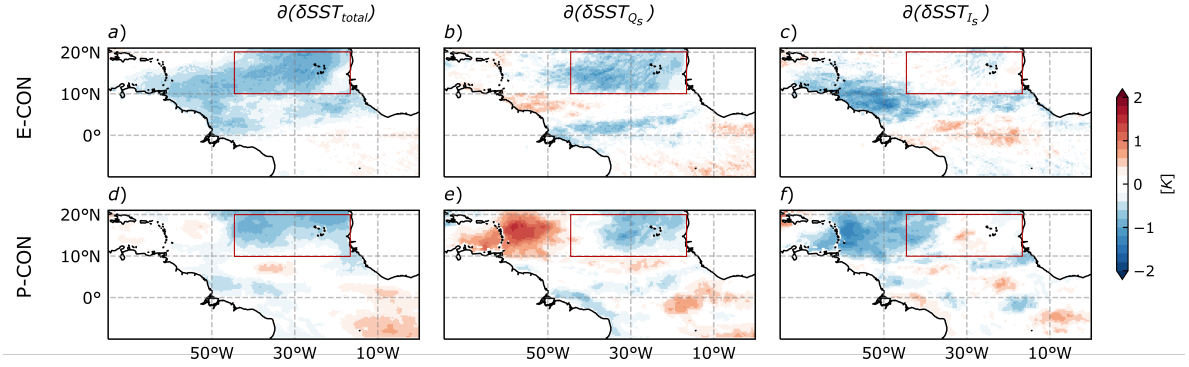


Figure B.4: (a, d) Total change of SST anomalies ($\partial(\delta SST_{total})$) in July with respect to May for E-CON (upper row) and P-CON (lower row) simulations. (b, e) The change of SST anomalies due to the non-solar component ($\partial(\delta SST_{Q_s})$) represents the sum of anomalies in the latent heat flux, sensible heat flux and net long-wave radiation at the surface averaged from May to July. (c, f) The change of SST anomalies due to the solar component ($\partial(\delta SST_{I_s})$) is the anomaly of net short-wave radiation at the surface averaged from May to July. The anomalies represent the difference of the positive AMM and control experiments and the change in SST anomalies refers to time difference between July and May. The red-outlined box shows the region of analysis.

A stronger cooling in the E-CON simulations is observed when comparing the total change of δSST with that of P-CON (Fig. B.4 a, d). This difference becomes more evident when we look at the changes in δSST due to the non-solar component (Fig. B.4 b, e). This is because the cooling in E-CON is mostly explained by the Q_s component; whereas in P-CON, it is explained by Q_s between $35^\circ W$ - $15^\circ W$ and by I_s between $45^\circ W$ - $35^\circ W$. Despite of the overall differences between E-CON and P-CON, we can note that in both cases the Q_s component explains the cooling in the west coast of Africa between $35^\circ W$ - $15^\circ W$. This is consistent with Amaya et al., 2017, who based on observations and reanalysis showed that a reduction of latent heat flux anomalies (i.e. Q_s) off the west African coast ($10^\circ N$ - 20° , $30^\circ W$ - $15^\circ W$) could explain the cooling of SST in that region from boreal spring to summer with good approximation.

Given that great part of the δSST change is explained by Q_s and our interest in the interaction of the atmospheric response with the SST, we focus on the changes due to the non-solar part $\partial\delta SST_{Q_s}$. Among the three terms in Q_s the largest component is δLHF (note the similarity between Fig. B.4 b, e and Fig. B.5 a, d). According to the conventional bulk formula, LHF is influenced by the wind speed and the vertical difference in humidity between the sea surface and the air above (Δq). We also assume here that changes in aerodynamic resistance are negligible. Following the analysis in Paccini et al. (2021), we estimate the anomalies in LHF as $\delta LHF = (\delta V/V)LHF + (\delta\Delta q/\Delta q)LHF$, where V is the mean wind speed at 10m from the control experiment and δV is the anomaly between the AMM and control experiment, all averaged from May to July; Δq is the difference between the specific humidity at the surface and at the air 2m above. We are particularly interested in the wind-driven change because of its relevance for interpreting the coupling with SST. However, we also present the changes in Δq because of the varying SST, unlike the uncoupled simulations in Paccini et al. (2021), may yield different effects by this term. Finally, we calculate $\partial(\delta SST)$ due to δLHF and its components according to Eq.B.1 (Fig. B.5).

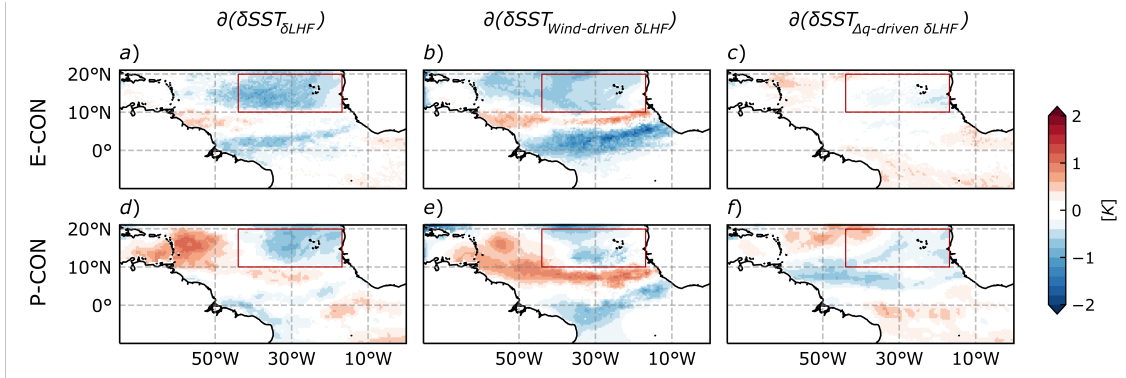


Figure B.5: (a, d) Change of the SST anomalies due to the anomaly in the latent heat flux ($\partial(\delta SST_{\delta LHF})$) averaged from May to July and its decomposition by (b, e) the wind-driven ($\partial(\delta SST_{wind-driven \delta LHF})$) and (c, f) Δq -driven terms ($\partial(\delta SST_{\Delta q-driven \delta LHF})$). Note that the sum of wind-driven and Δq -driven terms does not match exactly the change by the total δLHF given our approximations in the bulk formula (see text for details).

By decomposing changes in δSST due to δLHF , it results evident that the cooling is particularly stronger in E-CON than P-CON simulations in the wind-driven component (Fig. B.5b, e). The difference between the E-CON and P-CON wind-driven δLHF is about 1.5K west of 35°W and about 0.5K east of 35°W. The relative influence of the wind-driven δLHF component to the total change of δSST (Fig. B.4 a, d) is also important to note. We estimate that the cooling by the wind-driven δLHF represents about 67% of $\partial(\delta SST_{total})$ in the E-CON simulations, and about 48% in P-CON over the region of interest (10°N - 20°N; 45°W - 15°W).

It is also interesting to note the relative contributions of the Δq -driven terms in contrast to the wind-driven terms. In E-CON, the Δq -driven term is very small (Fig. B.5 c), hence the influence of the wind-driven term dominates the changes of δSST due to δLHF . By contrast, while the wind-driven term is large in P-CON, so it is the Δq -driven term (Fig. B.5 f). In particular, over the region of interest (10°N - 20°N; 45°W - 15°W), the Δq -driven term explains about 50% of the cooling in the changes of δSST due to δLHF . The greater influence of the Δq -driven term in P-CON can be explained by the higher values of SST in the mean state compared to E-CON. It has been previously found that changes in LHF due to humidity difference increase with high SST (Zhang and McPhaden, 1995). This is the case of P-CON simulations which have SST values greater than 29°C north of 10°N (not shown).

Our results suggest a stronger coupling with SST in E-CON than P-CON simulations, given that the imprint of the wind response in the total change of δSST is larger in the storm-resolving simulations.

B.6 CONCLUSIONS AND FINAL REMARKS

The aim of this study was to investigate the sensitivity of atmosphere-ocean coupling to the representation of convection, in relation to the Atlantic Meridional Mode (AMM). We interpret the coupling as the change in the SST anomalies per change of the wind-driven latent heat flux. Our interest in this component of the surface flux is motivated by

the relevance of the wind-evaporation-SST feedback for the development of the AMM (Amaya et al., 2017).

In order to address this coupling we used slab-ocean simulations at a coarse resolution of 40km with the convective parameterization switched on (P-CON simulations), and storm-resolving simulations at a resolution of 5km with the convection scheme switched off (E-CON simulations). Our results show that explicit and parameterized convection simulations display a different precipitation response to the AMM and a different coupling with SST. In more detail we found:

- In May, the precipitation response to the AMM exhibits a northward displacement of about 1° in simulations with explicit convection, which is consistent with the results of uncoupled simulations in Paccini et al. (2021). By contrast, a northward shift of about 2° is observed in simulations with parameterized convection. This is the month when SST anomalies are maximum in the northeastern tropical Atlantic. The associated cross-equatorial flow and meridional SST gradient enhance the ITCZ displacement towards the warmer hemisphere, which is observed in both simulations and in agreement with observations. However, the precipitation response to the AMM in simulations with explicit convection is more robust. This also suggests that the sensitivity of resolved convection to SST anomalies is less than that of parameterized convection but closer to observations.

It is hypothesized that the distinct precipitation response to the AMM between E-CON and P-CON simulations, as a result of the coupling, can be explained by their distinct mean-state SSTs. Simulations with parameterized convection tend to co-locate precipitation over high SST (e.g. Biasutti et al., 2006). The P-CON simulations exhibit temperatures larger than 29°C which would favor larger areas for convection and thus a widening of the ITCZ.

- The decay of SST anomalies towards boreal summer is more pronounced in simulations with explicit convection. This larger change of the SST anomalies is more evident when looking at the wind-driven latent heat flux, which cools off the SST more efficiently in E-CON from 0.5K to 1.5K greater than P-CON simulations. The wind-driven cooling represents in average about 67% of the total cooling in E-CON simulations and about 48% in P-CON simulations. The relative contributions to the total SST change evidences the stronger influence of the wind response on the latent heat flux and consequently on the SST anomaly change in the E-CON simulations. Hence, suggesting a stronger coupling with SST in storm-resolving simulations than in simulations with parameterized convection.

These results agree with the hypothesis proposed in Paccini et al., 2021, which is based on the surface wind response to the AMM in uncoupled simulations and suggests that the change of SST anomalies would be stronger when explicit convection is allowed. This hypothesis also suggests that the positive SST anomalies would be more enhanced, but this estimate considered the change between March and May. As previously exposed, the AMM has a strong signal in boreal spring. This constitutes the pattern imposed as initial conditions, where SST anomaly is at its peak. Therefore, no amplification is expected and we focus on the decay of SST anomalies.

A comparison with the observed evolution of the SST anomalies in the AMM reveals that our simulations (E-CON and P-CON) produce a faster cooling than in observations.

By the end of May, there is already a cooling of about 0.5K in the west coast of Africa (not shown). This is a region of strato-cumulus clouds, whose radiative effect has been found to delay the Newtonian cooling of SST by about 40% (Evan et al., 2013). Both the E-CON and P-CON simulations failed in representing such effects, but still point out their relevance for a realistic representation of the AMM evolution. Processes like the mixed layer dynamics, which were not considered in this study, could also contribute to delay the decay of the SST anomalies (Rugg et al., 2016; Kataoka et al., 2019).

APPENDIX

Paccini, L., Stevens, B. & Hohenegger, C. (2021). "Value of storm-resolving simulations for the representation of Amazon rainfall", *In preparation*.

Value of storm-resolving simulations for the representation of Amazon rainfall

Laura Paccini¹, Bjorn Stevens¹ and Cathy Hohenegger¹

¹Max Planck Institute for Meteorology, Bundesstraße 53, 20146 Hamburg, Germany

The Amazon basin is a region of substantial importance for the global hydro-climate and biodiversity, over which state-of-the-art climate models have large and systematic precipitation biases given their coarse-grid spacing. In recent years, the increased use of kilometer-scale simulations over large domains have achieved progress in the representation of precipitation. In this study we investigate whether improvements in the representation of Amazon precipitation by storm-resolving simulations are associated with the representation of organized convection systems in the Amazon basin. We perform a set of simulations with the ICON model at both coarse-resolution, wherein convection is parameterized by the modified-Bechtold scheme (P-CON) and storm-resolving (E-CON) simulations covering the entire Amazon. We identify that the greatest improvements in the representation of rain by E-CON, are the distribution of precipitation intensity and the diurnal cycle. Light and high-intensity rain rates, misrepresented by P-CON, show a close similarity between E-CON and observations. The storm-resolving simulations are also able to reproduce the spatially heterogeneous diurnal cycle over the Amazon, unlike P-CON, which shows a rather homogeneous distribution. We also show that the similarity between E-CON and observations increases when only considering organized convective systems in terms of the precipitation intensity and diurnal cycle. Organized convective systems in E-CON reproduce well the overnight precipitation peaking between 1h-6h, especially in the central and northeast Amazon. Diurnal variations of the size and intensity of organized convective systems in E-CON also agree with their observed life cycle. Our results show the value of storm-resolving simulations on linking the representation of interactive physical processes systems with improvements on the representation of Amazon precipitation.

B.1 INTRODUCTION

The Amazon basin is the largest rainforest in the Earth, of great relevance for the global hydro-climate and biodiversity (Marengo, 2006; Phillips et al., 2008). This important region is still one of the largest in the tropics where precipitation is misrepresented by climate models regarding its spatio-temporal variability across different scales (e.g. Yin et al., 2013; Fiedler et al., 2020). However, the increased use of kilometer-scale "storm-resolving" simulations have demonstrated systematic improvements in representing precipitation (e.g. Stevens et al., 2020). In this study, we use these models to investigate how the simulation of precipitation characteristics in the Amazon relates to the representation of organized convective systems.

The Amazon is a unique region for the development of moist convection (Betts et al., 2009). Local-to-meso scales processes modulate the diurnal cycle in the Amazon, which displays a heterogeneous spatial variability (e.g. Angelis et al., 2004; Janowiak et al., 2005; Tanaka et al., 2014; Ghate and Kollias, 2016). For instance, during its dry season, local land-atmosphere interactions influence the daytime precipitation; whereas elevated topography induce thermally-driven circulations that favor nocturnal precipitation peaks over downslope regions, such as the eastern flank of the Andes (Chavez and Takahashi, 2017; Junquas et al., 2018). Likewise, temperature contrasts between rivers and land induce circulations that suppress convection during the day and favor nocturnal convection near the Amazonian rivers (Tanaka et al., 2014; Wu et al., 2021).

Another atmospheric process that influences the diurnal cycle of rain in the Amazon is the occurrence of organized convective systems (Ghate and Kollias, 2016). These can be understood as a congregation of clouds that covers hundreds of kilometers (Houze Jr, 2018). Amazon organized convective systems owe their development to large-scale circulations (Carvalho et al., 2002; Rehbein et al., 2018) and surface-induced circulations at smaller scales (e.g. Angelis et al., 2004). One example is the coastal convective systems that originate due to land-sea contrasts over the northeast region of Brazil (e.g. Greco et al., 1990). Near the coast, convection initiates rapidly during the day, progressively develops to deep convection in the afternoon (15h-18h) and organizes into convective clusters that propagate towards the Amazon basin overnight (e.g. Greco et al., 1990; Garstang et al., 1994; Burleyson et al., 2016). Convective systems generated inland typically form around 17h-18h whereas its dissipation typically begins around midnight (Rehbein et al., 2018). Nocturnal precipitation from these systems also affect the following-day convection by cooling and drying from stratiform precipitation and blocking solar radiation due to morning cloud cover (Rickenbach, 2004).

Organized convective systems in the Amazon have been largely described in terms of their spatial structure, duration and propagation thanks to observational field campaigns (e.g. Carvalho et al., 2002; Angelis et al., 2004; Tanaka et al., 2014; Ghate and Kollias, 2016) and satellite based observations (Greco et al., 1990; Garstang et al., 1994; Garreaud and Wallace, 1997; Rehbein et al., 2018; Anselmo et al., 2021). Moreover, organized precipitation remain missed by climate models, affecting the representation of interactive processes between convection and its environment. The advantages of high-resolution storm-resolving simulations enable the representation of such interactions. How much do the improvements in the representation of rain relate to the better representation of atmospheric phenomena (e.g. organized convective systems) is not evident and needs further research, which is the aim of this study.

B.2 DATA AND METHODOLOGY

B.2.1 Observations

We use the Climate Prediction Center Morphing Method (CMORPH; Xie et al., 2017) dataset for the period from 2010 to 2020. This product estimates precipitation based on passive microwave instruments. The main advantages of CMORPH data are its high temporal (30min) and spatial (8km) resolutions. Previous studies have also validated its good performance over the Amazon region (e.g. Janowiak et al., 2005; Fitzjarrald et al., 2008). We also compared the analysis with other high-resolution datasets but similar results were obtained; therefore we chose the CMORPH data.

B.2.2 CMIP6

We use simulations from the Coupled Model Inter-comparison Project: Phase 6 (CMIP6; Eyring et al., 2016). Multi-model ensemble means are used from the historical simulations of the 21th century (2000-2014) and are the same used in Fiedler et al. (2020). We use daily and 3-hourly data available from 14 and 13 models, respectively. Simulations were spatially interpolated to the common T63 grid (about 180km), the native grid of MPI-ESM low-resolution configuration. For a detailed list of the models, the reader is referred to the supplementary material of Fiedler et al. (2020).

B.2.3 ICON-NWP

We use the Icosaedral Nonhydrostatic (ICON) atmospheric model (Zängl et al., 2015) in the numerical weather prediction (NWP) configuration. Among the applied physical parameterizations by these model, the parameterization of moist convection is only used for the coarser grid spacing in our experiments. It consists of a bulk mass-flux (Bechtold, 2017), one of the latest implementations in the NWP of European meteorological services.

As initial conditions for the simulations we use the operational analysis data from the European Centre for Medium-Range Weather Forecasts (ECMWF) and Integrated Forecast System (IFS), and from the Hadley Centre Sea Ice and Sea Surface Temperature Center HadISST; Rayner et al., 2003 for SST. Grids and external parameters (e.g. land properties, topography) are retrieved from the Online Grid Generator tool from the German Meteorological Service (DWD).

B.2.3.1 Experimental set-up

We conduct a set of simulations using the same approach as Paccini et al. (2021). Global simulations, at 40km grid spacing (P-CON simulations), serve as initial and boundary conditions to the one-way nested domains at finer grid spacing. The three inner domains have the convective parameterization turned off (E-CON simulations) and comprise the same regions as described in Paccini et al. (2021). The horizontal resolution is successively increased from 20km to 10km and to 5km, with the finest grid spacing covering the tropical Atlantic sector (85°W-25°E; 25°S-25°N). In all domains the vertical resolution includes 90 levels, with the model top at 75km

We start 8 simulations at the beginning of March, with different atmospheric states but with the same fixed SST, which does not vary over time. Simulations are integrated for

40 days and the analysis is performed over the last 31 days, representing the simulation of March.

We conduct another set of simulations using an updated version of ICON (v2.6.01) with an additional inner domain, at a grid spacing of 2.5km, that bounds the region: 81°W-36°W; 21°S-11°N. Given the high computational demands, only 2-member simulations are performed.

In our analysis we compare the 8-member ensemble of P-CON, E-CON at 5km and 2-member ensemble E-CON at 2.5km. Although from different members, the E-CON simulations at 2.5km and 5km lead to same results as the E-CON 2.5km and 5km from the 2-member ensemble. We present the results of the 8-member E-CON simulations due to more robust statistics.

All data and simulation outputs are regridded to the resolution of the P-CON experiments (about 40km) except for the CMIP6 ensemble which keeps the grid spacing of about 180km. The CMIP6 data only serves as a reference of how state-of-the-art climate models, representing the average convective parameterizations, simulate Amazon precipitation.

B.3 REPRESENTATION OF PRECIPITATION

B.3.1 Geographic distribution

One of the basic metrics when evaluating the representation of rainfall is the mean amount and its spatial pattern. The prevailing known bias in most climate models is the underestimation of rain in the Amazon, especially during the wet season (Fiedler et al., 2020). The associated spatial pattern depicts enhanced rain over the eastern region of Brazil and insufficient rain in the central Amazon (Fig. C.1, e), a long-standing bias that has also been documented in models with prescribed SST (Richter and Xie, 2008).

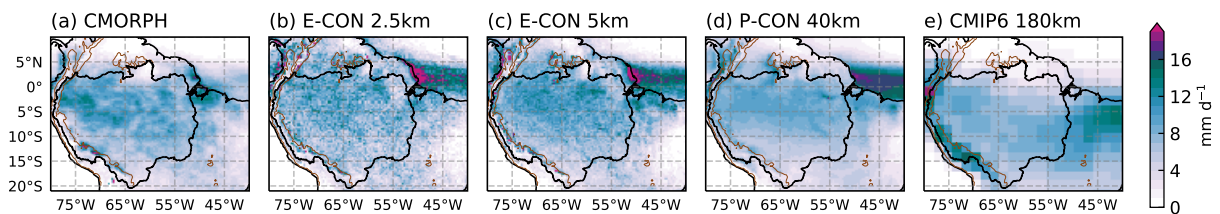


Figure C.1: Mean precipitation in March from (a) CMORPH observations, simulations with explicit (E-CON) convection at (b) 2.5km, (c) 5km, parameterized convection (P-CON) at (d) 40km and the (e) CMIP6 multi-model ensemble mean. Data is regridded to 40km except for CMIP6 models which were interpolated to a common grid of about 180km and only serves as a reference. The Amazon basin is defined as black contours and the topography at 1000m, in brown contours.

By contrasting observations with a set of simulations, a better representation of the mean spatial pattern is apparent with both the E-CON and P-CON simulations (Fig. C.1, b, c, d). Although a broader precipitation band depicts enhanced rainfall north of the Amazon basin in the E-CON and P-CON simulations (probably related to the invariable SST), the spatial patterns over the Amazon basin and south of it remain even more similar to that of CMORPH than the CMIP6 pattern. The P-CON simulation, which uses the modified-Bechtold convective scheme, shows improvements in the geographic

Table C.1: Averaged precipitation over the Amazon Basin (AB) and the ratio of Amazon and tropical South America (SA, 20°S-10°N; 80°W-38°W) rain rates. Values in parenthesis are the averages over regions where topography is below 1000m. For these calculations, observations and output simulations were spatially interpolated onto the CMIP6 grid (180km).

Dataset	Mean precipitation [mm d ⁻¹]	
	Amazon Basin (AB)	Ratio AB/SA
CMORPH	7.85 (8.07)	1.28
E-CON 2.5km	7.71 (7.85)	1.17
E-CON 5km	8.16 (8.40)	1.20
P-CON 40km	7.33 (7.52)	1.18
CMIP6 180km	7.82 (7.41)	1.08

distribution of rain over tropical South America, meaning more rain over central Amazon and less so over eastern Brazil (Fig. C.1, d). Likewise, the E-CON simulations maximize precipitation over the central Amazon. Both the 2.5km and 5km experiments, albeit from different ensemble members, display a very similar pattern.

A quantitative comparison is presented in Tab. C.1. Precipitation is averaged over the Amazon basin and over the continental region comprised by 20°S-10°N; 80°W-38°W. The observations and all simulations, except for CMIP6, display an increase of the mean precipitation in the Amazon when omitting regions with elevated topography. The E-CON simulations show a mean value closer to CMORPH than P-CON and CMIP6. Moreover, Amazon precipitation is about 1.2 greater than precipitation over the whole tropical continent in observations, the E-CON and P-CON simulations. In contrast, the CMIP6 ensemble displays a ratio closer to 1 which might be related to the enhanced precipitation over high topography and over the eastern coast of Brazil.

In general, the E-CON and P-CON simulations show a good performance in the representation of the spatial pattern of Amazon rainfall. A closer look at the spatial characteristics of rainfall, however, reveals some discrepancies. For instance, along the eastern flank of the Andes, the Amazon comprises some of the rainiest places in the region, known as "precipitation hot spots" (e.g. Chavez and Takahashi, 2017). The E-CON simulations exhibit a good representation of such precipitation hot spots, showing places with precipitation amounts higher than 12mm d⁻¹ near the 1000m isoline, south of 10°S (Fig. C.1). The P-CON simulation shows a weaker gradient in the horizontal precipitation near the hot spots and misses the intense precipitation in the southern tip of the Amazon.

Another pronounced difference between the E-CON and P-CON simulations is found in the coastal precipitation over northeastern coast of Brazil. There is a lack of precipitation over this region in simulations with parameterized convection, (P-CON as well as CMIP6) unlike the E-CON simulations. This difference between E-CON and P-CON simulations might suggest that processes related to land-sea interactions depend mostly on the representation of convection (e.g. Hohenegger et al., 2015). Having an adequate representation of the coastal precipitation is important for the Amazon, due to organized convective systems that originate there and displace inland (e.g. Greco et al., 1990). The E-CON simulations show an improvement in representing the coastal precipitation

which might be related to the better representation of Amazon rainfall, as it will be discussed in next sections.

B.3.2 Frequency and intensity

The E-CON simulations show a notable improvement in the estimated frequency and distribution of precipitation intensity in the Amazon basin (Figs. C.2 and C.3). As in observations, the frequency of daily precipitation follows the spatial pattern of the mean precipitation, featuring regions where it rains up to 80% of the days (Fig. C.2). Despite of some differences in the spatial distribution of precipitation frequency, it is possible to identify common places where the frequency is larger than 50%, such as the equatorial (5°S-0°N) coasts of South America, the central Amazon and the eastern flank of the Andes. The E-CON simulations also distinguish more frequency of rain over land areas than rivers, like the Amazon river mouth and the Tapajos river (Fig.C.2 b, c), although details are smoothed by the interpolation.

A very different picture is displayed by simulations with parameterized convection, both CMIP6 and P-CON, which tend to overestimate the frequency of rain (Dai, 2006) regardless of the spatial resolution (Fig. C.2 d,e). Regions where the mean precipitation is greater or equal than 5mm d^{-1} show a frequency greater than 90-95%, indicating that the mean precipitation amount is related to the persistence of rainy days.

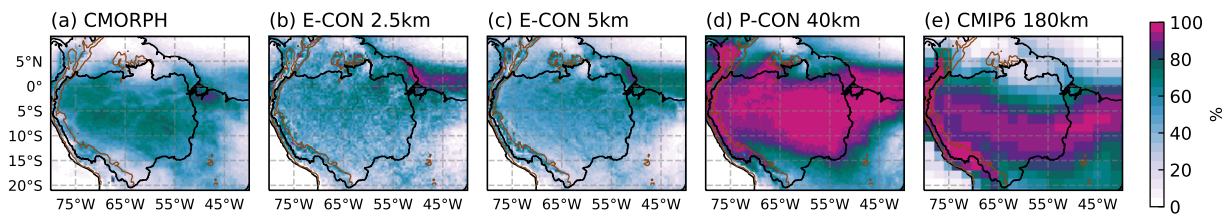


Figure C.2: Frequency (%) of daily precipitation greater than 1mm d^{-1} in March from (a) CMORPH observations and simulations with explicit (E-CON) convection at (b) 2.5km, (c) 5km, parameterized convection (P-CON) at (d) 40km and the (e) CMIP6 multi-model ensemble mean. Data is regridded to 40km except for CMIP6 models which were interpolated to a common grid of about 180km and only serves as a reference. The Amazon basin is defined as black contours and the topography at 1000m, in brown contours.

To have a broader view of the frequency spectra, Figure C.3 displays the distribution of precipitation intensity over the Amazon basin. The E-CON simulations show an important improvement in the representation of this precipitation feature as compared to simulations with parameterized convection. This appears to be a robust attribute of the E-CON simulations that is mainly determined by the treatment of convection rather than the experimental set-up (global versus nested, not shown) and spatial resolution. In a recent comparison study, Judt and Rios-Berrios (2021) showed that simulations with full convective parameterization run at about 4km grid spacing displayed the same distribution of precipitation intensity as those at 100km.

Overall there are two intensity ranges with the most pronounced differences. First, the interval between 2mm d^{-1} to 20mm d^{-1} (light-to-moderate rain) shows a larger frequency in the rainfall distribution of simulations with parameterized convection than observations and E-CON simulations. The second range covers values higher than

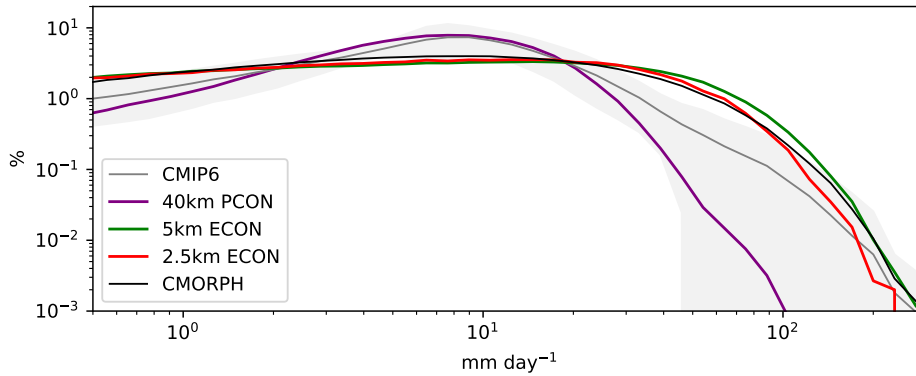


Figure C.3: Distribution (%) of daily precipitation intensity greater than 0 mm over the Amazon basin for observations (black line) and simulations (colored lines). Values are binned in a logarithmic scale. The gray shading represents the standard deviation of 14-models of the CMIP6 ensemble.

25mm d^{-1} (high intensity rain) and displays scarce intense precipitation especially in P-CON, compared to observations and E-CON simulations. In the case of CMIP6 models the inter-model variability considerably increases in this range, showing a multi-model ensemble mean above the P-CON simulations but still below what is observed. This confirms to be an intrinsic feature of simulations with parameterized convection: too frequent and weak rain, something that persists despite of the great development in convective schemes (Flato et al., 2014; Fiedler et al., 2020; Judt and Rios-Berrios, 2021).

The distribution of rain intensity by the E-CON simulations is very close to observations, especially in the high intensity range. The 2.5km E-CON ensemble (red line) matches the observations in the range of 20 mm d^{-1} to 100 mm d^{-1} , which gives an indication of improvement with increasing spatial resolution in the E-CON simulations. Values larger than 100mm d^{-1} are less frequent and might be related to the smaller member size of 2.5km-ECON (2×31 days) as compared to the 5km-ECON ensemble (8×31 days) and observations (21×31 days).

B.3.3 Diurnal cycle

The diurnal cycle of rainfall over the Amazon is not spatially homogeneous. In order to illustrate this feature, we compute the hourly mean for each grid point and then select the time when rainfall is maximum (Fig. C.4). Although great part of the Amazon region shows a precipitation maximum in the afternoon (15-18 hrs), as expected from daytime heating, there are several other places where the precipitation peaks overnight (Garreaud and Wallace, 1997; Yang and Slingo, 2001; Rickenbach, 2004; Janowiak et al., 2005; Tanaka et al., 2014). For instance, the northeast extreme of the Amazon basin exhibits a coast-parallel band of consecutive peaking times in CMORPH data (Fig.C.4,a) that is very well reproduced in the E-CON simulations (Fig.C.4, b and c). Different times of maximum precipitation can be associated to different types of convection and their transition. Near the coast, precipitation maximizes close to midday (12-14hrs) which is typical for shallow convection; later peaks in the day (15-18hrs) are consistent with deep convection, and the consecutive overnight peaking times have been associated to convective systems called squall lines (e.g. Garstang et al., 1994). The representation of such progressive peaking times suggests that the E-CON simulations are able to reproduce a realistic

transition of convection. Other places displaying nocturnal precipitation peaks are not as pronounced in the E-CON simulations as in observations, but can be distinguished more inland between 65°W-75°W, 5°S-0°W and over the southeast Amazon (50°W-55°W, 15°S-10°S). It is interesting to note that many of the nocturnal precipitation peaks collocate with the Amazon river and its tributaries, suggesting an adequate representation of local processes (e.g. Fitzjarrald et al., 2008; Tanaka et al., 2014; Wu et al., 2021). Finally, overnight precipitation along the eastern flank of the Andes is less pronounced in the 5km E-CON simulations north of 10°S. The 2.5km E-CON simulations show a better representation of the nocturnal phase.

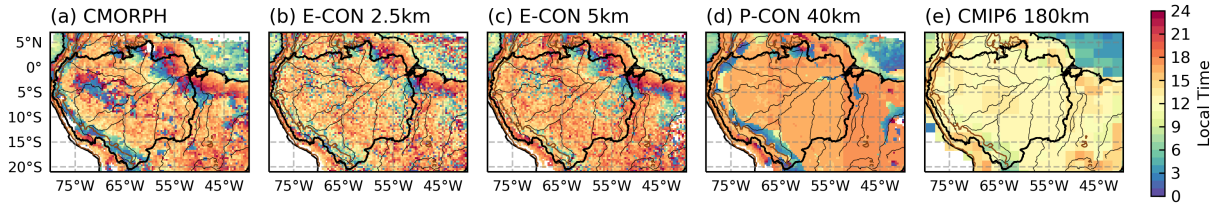


Figure C.4: Time of maximum diurnal precipitation in March from (a) CMORPH observations and simulations with explicit (E-CON) convection at (b) 2.5km, (c) 5km, parameterized convection (P-CON) at (d) 40km and the (e) CMIP6 multi-model ensemble mean. Data is regridded to 40km except for CMIP6 models which were interpolated to a common grid of about 180km and only serves as a reference. The Amazon basin is defined as black contours as well as the rivers, and the topography at 1000m is shown in brown contours.

The P-CON simulations are able to reproduce the time of maximum precipitation in the afternoon (Fig.C.4, d), unlike the CMIP6 (Fig.C.4, e) which still tend to precipitate too early during the day (Fiedler et al., 2020; Tang et al., 2021). Also, the time of precipitation peak overnight near elevated terrain is reproduced in P-CON, probably related to a better representation of topography. Nonetheless, P-CON displays a rather homogeneous spatial distribution in the diurnal cycle. Precipitation peaking overnight in the central and northeast Amazon are completely missed by P-CON.

The representation of the diurnal cycle in the Amazon basin confirms to be another major difference between simulations with parameterized convection and those that resolve convection explicitly.

B.4 ORGANIZED CONVECTIVE SYSTEMS

In section B.3 we compared precipitation characteristics between observations and a set of simulations, differing in their treatment of convection and spatial resolution. The main improvements in the representation of Amazon precipitation are found in the E-CON simulations regarding the distribution of precipitation intensity and the spatial heterogeneity in the diurnal cycle. These precipitation features can be related to organized convective systems, which tend to develop during the day and can last overnight generating intense rainfall episodes (e.g. Garreaud and Wallace, 1997; Rickenbach, 2004; Pereira Filho et al., 2015).

In this section we analyze whether the representation of the precipitation intensity and diurnal cycle by the E-CON simulations are related to the representation of organized

convective systems in the Amazon. Since simulations with parameterized convection fail in reproducing such precipitation features, we exclude them from further analysis.

We define organized convective systems following an object-based approach. First, precipitation is filtered out as those grid cells with hourly rain rate equal to or greater than 2mm h^{-1} . Precipitation objects are then identified as contiguous grid cells (8-way connection) with a minimum area of 10000km^2 (equivalent to 6 grid cells). These values are chosen based on previous studies of observed organized systems in the Amazon (Pereira Filho et al., 2015; Rehbein et al., 2018; Anselmo et al., 2021), although they are based on brightness temperature. Tests with other different thresholds for size and intensity yield similar results.

We examine precipitation characteristics of the built precipitation objects and compare them with the non-organized precipitation.

B.4.1 Size and intensity

Figure C.5 (a) shows the distribution of area corresponding to the precipitation objects. The E-CON simulations generally show smaller precipitation objects than those identified in CMORPH data. The median area for E-CON simulations is $14\ 411\text{km}^2$ and for CMORPH is $19\ 223\text{km}^2$. Despite of the differences in the number of members between the 2.5km and 5km E-CON ensembles, they both agree with the size distribution of precipitation objects, which are mostly below $100\ 000\text{km}^2$.

We further explore the distribution of precipitation intensity by separating that belonging to our defined organized convective systems ("*ob*") from the non-organized precipitation ("*non-ob*"). By comparing Fig.C.5 (b) with Fig.C.3 one can notice that the distribution of precipitation is more similar between the E-CON simulations and observations when only considering the organized convective systems, especially for rates lower than 30mm d^{-1} . For higher intensities, the improvement is most apparent with the 5km which agrees remarkably well with observations.

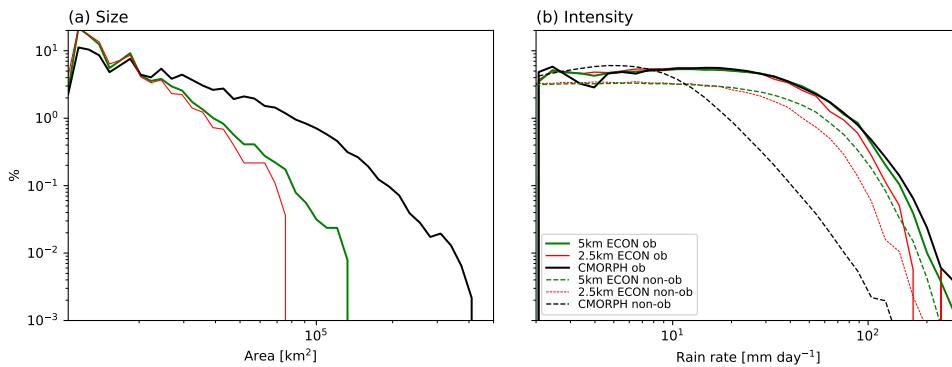


Figure C.5: Distribution (%) of the (a) size of defined organized convective systems over the Amazon basin, and, (b) daily rainfall intensity greater than 0mm d^{-1} for organized convective systems ("*ob*", solid lines) and non-organized precipitation ("*non-ob*", dashed lines). Observations are displayed in black and the E-CON simulations are displayed in green (5km) and red (2.5km) colors. Values are binned in a logarithmic scale.

The intensity distributions of non-organized precipitation show apparent differences between the E-CON simulations and observations. The distribution of "*non-ob*" CMORPH

precipitation misses intensities above 100mm d^{-1} and resembles much more like the P-CON distribution in Fig.C.3. By contrast, the "non-ob" 2.5km-5km E-CON precipitation ensembles still display intensities around 200mm d^{-1} . The intensity distribution of "non-ob" E-CON simulations are more similar to that in Fig.C.3, as compared to "non-ob" CMORPH, which evidence the tendency of E-CON on producing high-intensity rain rates. This is a known deficiency from simulations with explicit convection at kilometer-scale resolutions given that convection is not fully resolved (Prein et al., 2015; Kendon et al., 2021).

The relative contribution of organized convective systems to the total rainfall can be partly associated with the distributions of precipitation intensity. Most of the very intense precipitation ($>50\text{mm d}^{-1}$) belongs to the organized systems in observations, then a significant part (about 50%, not shown) of the total rain in observations comes from organized systems. In the case of the E-CON simulations, this contribution is reduced (about 30%) because high intensity rates are also present in the non-organized precipitation.

B.4.2 Diurnal cycle

Another important precipitation feature that the E-CON simulations were able to reproduce is the spatial variability of the diurnal cycle. Consecutive precipitation peaking times not only suggest a transition of different types of convection, but they could be associated with organized convective systems. Here we examine whether the diurnal cycle of organized precipitation is related to the spatial heterogeneity in the diurnal cycle.

The spatial distribution of the diurnal cycle of organized convective systems is consistent with the geographic distribution of "mesoscale" convective systems in climatological studies (Rehbein et al., 2018; Anselmo et al., 2021; Feng et al., 2021) both in E-CON and observations. Regions with overnight precipitation that peaks from 1h-6h are more pronounced when considering organized precipitation (Fig. C.6 a, b, c). The coast-parallel band of consecutive peaking times is also more evident within the organized convective systems and could be associated with the so-called "coastal occurring systems" or squall lines (e.g. Greco et al., 1990; Garstang et al., 1994; Rickenbach, 2004).

Non-organized precipitation mostly features daytime peaks ranging from 12h to 20h (Fig. C.6 d, e, f), which also remain very similar between E-CON and observations. Moreover, E-CON displays scattered nocturnal peaks in the central Amazon, which could be associated with very intense rain rates (Fig.C.5, b) from isolated convective cells. The location of such isolated nocturnal rainfall is placed near the rivers. In the case of CMORPH, peaks at about midnight are also co-located over the Amazon river and its tributaries.

The similarity of the spatial distribution in the diurnal cycle between non-organized precipitation and the total precipitation in E-CON indicates that the organized convective systems do not dominate the overall diurnal cycle as in observations. However, the times of maximum precipitation at night associated with organized convective systems do explain most of the overnight precipitation in observations, and these are captured by E-CON.

A more detailed view of the diurnal cycle in terms of the size and intensity of the organized convective systems is presented in Fig.C.7. Changes in the size and intensity of are shown as the anomalies with respect to the diurnal mean, given the distinct characteristics of such properties as detailed in section 4.1. Apart from differences in

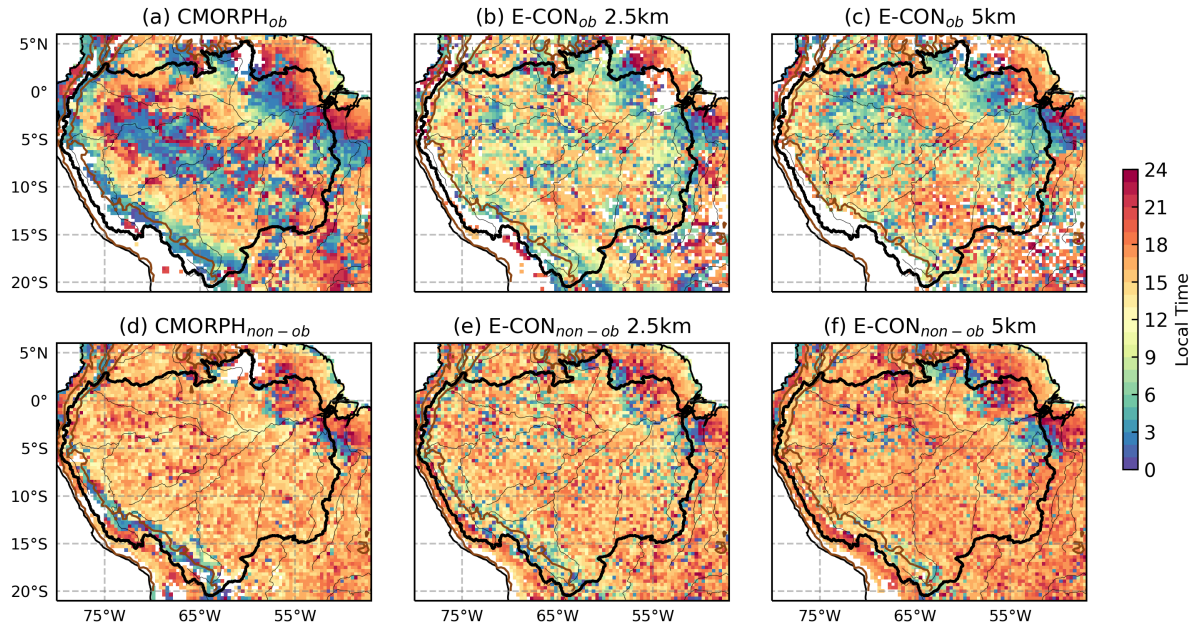


Figure C.6: Time of maximum diurnal precipitation for (a,b,c) organized convective systems ("ob") and (d, e, f) non-organized precipitation ("non-ob") for (a, d) CMORPH, (b, e) 5km E-CON and (c, f) 2.5km E-CON simulations. Only in this case precipitation objects were identified over tropical South America. The Amazon basin is defined as black contours as well as the rivers, and the topography at 1000m is shown in brown contours.

the size (Fig.C.5 a), the mean precipitation from objects is nearly twice in the E-CON simulations (about 10mm h^{-1} in both 2.5km and 5km ensembles) than in observations (about 5mm h^{-1}).

The biggest convective systems occur during early morning (3h-8h), with the maximum peak in size coinciding with the minimum peak in intensity (Fig.C.7). By contrast, the smallest convective systems occur during the afternoon and coincide with the most intense rain rates, albeit later in observations (20h) than in the E-CON simulation (18h). Despite of some discrepancies in the precipitation peaking times, the E-CON simulations are able to distinguish additional features of the convective systems providing a good representation of their evolution. Intense precipitation associated with deep convection features the genesis of organized convective systems in the afternoon; while in the mature phase, they reach the maximum size and less intense, stratiform precipitation dominates (Rickenbach, 2004; Rehbein et al., 2018).

B.5 SUMMARY AND CONCLUSION

This study investigates whether the improvement of the representation of Amazon rainfall by storm-resolving simulations, in contrast to conventional simulations with parameterized convection. We use the ICON-NWP atmospheric model and perform simulations at a coarse grid spacing of 40km wherein convection is parameterized (P-CON) and storm-resolving simulations that enable the explicit representation of convection (E-CON) at 2.5km and 5km grid spacing.

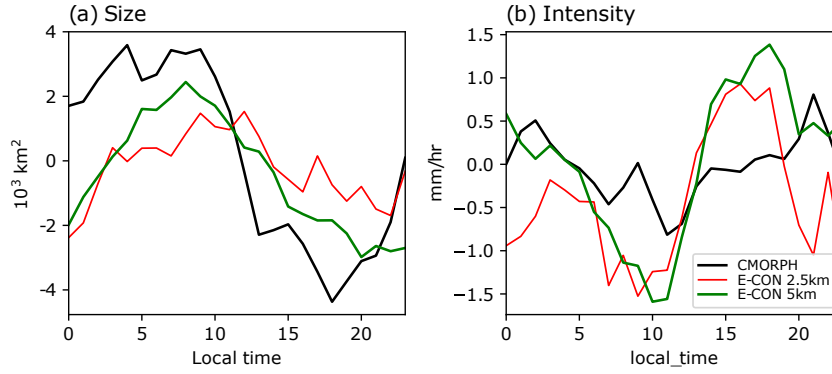


Figure C.7: Diurnal variations of the (a) size and (b) mean of organized convective systems with respect to their diurnal means. Observations are displayed in black and the E-CON simulations are displayed in green (5km) and red (2.5km) colors.

As a first step, we compare our set of simulations with CMORPH observations and the latest generation of CMIP models. The latter only serves as reference of average convective parameterizations, whereas the P-CON simulations symbolizes a state-of-the-art convective scheme. We identified that the major improvements in the E-CON simulations are shown in the distribution of precipitation intensity and the spatial variability of the diurnal cycle in the Amazon. Such improvements agree with many previous studies that assessed the representation of precipitation by storm-resolving simulations (e.g. Stevens et al., 2020; Judt and Rios-Berrios, 2021). Light-to-moderate precipitation 2 mm d^{-1} to 20 mm d^{-1} and high intensity rain rates ($>25 \text{ mm d}^{-1}$) in E-CON are very close to observations; whereas P-CON and CMIP persist on intensity biases. The spatial heterogeneous diurnal cycle is also well captured by the E-CON simulations. The P-CON simulations are able to reproduce the afternoon peak of maximum precipitation over most of the Amazon and nocturnal rain near elevated topography, unlike the CMIP6 ensemble. However, its distribution is rather homogeneous and misses the nocturnal precipitation over the central and northeast Amazon.

In the second part, we associate these two precipitation characteristics with the representation of organized convective systems. Given the persistent biases of simulations with parameterized convection, we exclude them for further analysis. We found some differences between E-CON and observations. The E-CON simulations tend to produce smaller convective systems than observed. The median area for CMORPH is $19\,223 \text{ km}^2$, whereas for E-CON is $14\,411 \text{ km}^2$. Also, organized precipitation in the E-CON simulations displays more intense rain than observations. The mean value intensity per area is about twice in E-CON than CMORPH.

Despite of these differences, we found a better similarity between E-CON and observations regarding the distribution of precipitation intensity and diurnal cycle, when only considering the organized convective systems.

The distribution of precipitation intensity shows a remarkable agreement between E-CON and observations for most of the intensity rain rates (5 mm d^{-1} to 100 mm d^{-1}). The precipitation maximum occurring between 1h-6h is well captured by E-CON, especially over the central and northeast Amazon. Analysis of the diurnal variations in the size and intensity of organized convective systems, suggests a good representation of their life cycle. The maximum intensity is shown in the afternoon, when precipitation begins to organize and its covers a relatively small area. Hours later, overnight, the organized

systems have reached a mature stage showing a maximum peak in size, and start the dissipation phase featuring less intense rain (e.g. Rickenbach, 2004; Rehbein et al., 2018).

We conclude that the realistic representation of the intensity and diurnal variations of organized convective systems, contribute to the improvement of the overall representation of such precipitation features in the Amazon basin.

BIBLIOGRAPHY

- Adler, Robert F, George J Huffman, Alfred Chang, Ralph Ferraro, Ping-Ping Xie, John Janowiak, Bruno Rudolf, Udo Schneider, Scott Curtis, David Bolvin, et al. (2003). "The version-2 global precipitation climatology project (GPCP) monthly precipitation analysis (1979–present)". *Journal of Hydrometeorology* 4.6, pp. 1147–1167. DOI: [10.1175/1525-7541\(2003\)004<1147:TVGPCP>2.0.CO;2](https://doi.org/10.1175/1525-7541(2003)004<1147:TVGPCP>2.0.CO;2).
- Amaya, Dillon J, Michael J DeFlorio, Arthur J Miller, and Shang-Ping Xie (2017). "WES feedback and the Atlantic meridional mode: Observations and CMIP5 comparisons". *Climate Dynamics* 49.5, pp. 1665–1679.
- Angelis, Carlos F, Glenn R McGregor, and Chris Kidd (2004). "Diurnal cycle of rainfall over the Brazilian Amazon". *Climate Research* 26.2, pp. 139–149.
- Anselmo, Evandro M, Luiz AT Machado, Courtney Schumacher, and George N Kiziladis (2021). "Amazonian mesoscale convective systems: Life cycle and propagation characteristics". *International Journal of Climatology*.
- Anselmo, Evandro M, Courtney Schumacher, and Luiz AT Machado (2020). "The Amazonian Low-level Jet and its Connection to Convective Cloud Propagation and Evolution". *Monthly Weather Review* 148.10, pp. 4083–4099.
- Arakawa, Akio (2004). "The cumulus parameterization problem: Past, present, and future". *Journal of Climate* 17.13, pp. 2493–2525.
- Bechtold, Pedro, J-P Chaboureaud, A Beljaars, AK Betts, M Köhler, M Miller, and J-L Redelsperger (2004). "The simulation of the diurnal cycle of convective precipitation over land in a global model". *Quarterly Journal of the Royal Meteorological Society: A journal of the atmospheric sciences, applied meteorology and physical oceanography* 130.604, pp. 3119–3137.
- Bechtold, Peter (2017). "Atmospheric Moist Convection". *Meteorological Training Course Lecture Series*, pp. 1–78. URL: <https://www.ecmwf.int/node/16953>.
- Betts, AK, G Fisch, C Von Randow, MAF Silva Dias, JCP Cohen, R Da Silva, and DR Fitzjarrald (2009). "The Amazonian boundary layer and mesoscale circulations". *Amazonia and global change. Geophysical monograph* 186.
- Betts, Alan K and Christian Jakob (2002). "Study of diurnal cycle of convective precipitation over Amazonia using a single column model". *Journal of Geophysical Research: Atmospheres* 107.D23, ACL–25.
- Biasutti, M, AH Sobel, and Y Kushnir (2006). "AGCM precipitation biases in the tropical Atlantic". *Journal of climate* 19.6, pp. 935–958.
- Boyle, W Alice, Elsie H Shogren, and Jeffrey D Brawn (2020). "Hygic niches for tropical endotherms". *Trends in Ecology & Evolution*.
- Burleyson, Casey D, Zhe Feng, Samson M Hagos, Jerome Fast, Luiz AT Machado, and Scot T Martin (2016). "Spatial variability of the background diurnal cycle of deep convection around the GoAmazon2014/5 field campaign sites". *Journal of Applied Meteorology and Climatology* 55.7, pp. 1579–1598.
- Carvalho, Leila MV, Charles Jones, and Maria AF Silva Dias (2002). "Intraseasonal large-scale circulations and mesoscale convective activity in tropical South America during the TRMM-LBA campaign". *Journal of Geophysical Research: Atmospheres* 107.D20, LBA–9.

- Chang, Ping, Link Ji, and R Saravanan (2001). "A hybrid coupled model study of tropical Atlantic variability". *Journal of climate* 14.3, pp. 361–390. DOI: [10.1175/1520-0442\(2001\)013<0361:AHCMS0>2.0.CO;2](https://doi.org/10.1175/1520-0442(2001)013<0361:AHCMS0>2.0.CO;2).
- Chang, Ping, Ramalingam Saravanan, Link Ji, and Gabriele C Hegerl (2000). "The effect of local sea surface temperatures on atmospheric circulation over the tropical Atlantic sector". *Journal of Climate* 13.13, pp. 2195–2216. DOI: [10.1175/1520-0442\(2000\)013<2195:TEOLSS>2.0.CO;2](https://doi.org/10.1175/1520-0442(2000)013<2195:TEOLSS>2.0.CO;2).
- Chavez, Steven P and Ken Takahashi (2017). "Orographic rainfall hot spots in the Andes-Amazon transition according to the TRMM precipitation radar and in situ data". *Journal of Geophysical Research: Atmospheres* 122.11, pp. 5870–5882.
- Chiang, John CH, Yochanan Kushnir, and Alessandra Giannini (2002). "Deconstructing Atlantic Intertropical Convergence Zone variability: Influence of the local cross-equatorial sea surface temperature gradient and remote forcing from the eastern equatorial Pacific". *Journal of Geophysical Research: Atmospheres* 107.D1, ACL–3. DOI: [10.1029/2000JD000307](https://doi.org/10.1029/2000JD000307).
- Chiang, John CH and Daniel J Vimont (2004). "Analogous Pacific and Atlantic meridional modes of tropical atmosphere–ocean variability". *Journal of Climate* 17.21, pp. 4143–4158.
- Colin, Maxime, Steven Sherwood, Olivier Geoffroy, Sandrine Bony, and David Fuchs (2019). "Identifying the sources of convective memory in cloud-resolving simulations". *Journal of the Atmospheric Sciences* 76.3, pp. 947–962.
- Dai, Aiguo (2006). "Precipitation characteristics in eighteen coupled climate models". *Journal of climate* 19.18, pp. 4605–4630. DOI: [10.1175/JCLI3884.1](https://doi.org/10.1175/JCLI3884.1).
- Deser, Clara, Michael A Alexander, Shang-Ping Xie, and Adam S Phillips (2010). "Sea surface temperature variability: Patterns and mechanisms". *Annual review of marine science* 2, pp. 115–143.
- Evan, Amato T, Robert J Allen, Ralf Bennartz, and Daniel J Vimont (2013). "The modification of sea surface temperature anomaly linear damping time scales by stratocumulus clouds". *Journal of climate* 26.11, pp. 3619–3630.
- Eyring, Veronika, Sandrine Bony, Gerald A Meehl, Catherine A Senior, Bjorn Stevens, Ronald J Stouffer, and Karl E Taylor (2016). "Overview of the Coupled Model Intercomparison Project Phase 6 (CMIP6) experimental design and organization". *Geoscientific Model Development* 9.5, pp. 1937–1958.
- Feng, Zhe, L Ruby Leung, Nana Liu, Jingyu Wang, Robert A Houze Jr, Jianfeng Li, Joseph C Hardin, Dandan Chen, and Jianping Guo (2021). "A Global High-Resolution Mesoscale Convective System Database Using Satellite-Derived Cloud Tops, Surface Precipitation, and Tracking". *Journal of Geophysical Research: Atmospheres* 126.8, e2020JD034202.
- Fiedler, Stephanie, Traute Crueger, Roberta D'Agostino, Karsten Peters, Tobias Becker, David Leutwyler, Laura Paccini, Jorg Burdanowitz, Stefan Buehler, Alejandro Cortes, et al. (2020). "Simulated tropical precipitation assessed across three major phases of the Coupled Model Intercomparison Project (CMIP)". *Monthly weather review* 148.9, pp. 3653–3680.
- Fitzjarrald, David R, Ricardo K Sakai, Osvaldo LL Moraes, Raimundo Cosme de Oliveira, Otávio C Acevedo, Matthew J Czikowsky, and Troy Beldini (2008). "Spatial and temporal rainfall variability near the Amazon-Tapajós confluence". *Journal of Geophysical Research: Biogeosciences* 113.G1.
- Flato, Gregory, Jochem Marotzke, Babatunde Abiodun, Pascale Braconnot, S Chan Chou, William Collins, Peter Cox, Fatima Driouech, Seita Emori, Veronika Eyring, et al.

- (2014). "Evaluation of climate models". In: *Climate change 2013: the physical science basis. Contribution of Working Group I to the Fifth Assessment Report of the Intergovernmental Panel on Climate Change*. Cambridge University Press, pp. 741–866.
- Foltz, Gregory R, Michael J McPhaden, and Rick Lumpkin (2012). "A strong Atlantic meridional mode event in 2009: The role of mixed layer dynamics". *Journal of Climate* 25.1, pp. 363–380. DOI: [10.1175/JCLI-D-11-00150.1](https://doi.org/10.1175/JCLI-D-11-00150.1).
- Foltz, Gregory R, Claudia Schmid, and Rick Lumpkin (2013). "Seasonal cycle of the mixed layer heat budget in the northeastern tropical Atlantic Ocean". *Journal of Climate* 26.20, pp. 8169–8188.
- Fontaine, Bernard and Serge Janicot (1996). "Sea surface temperature fields associated with West African rainfall anomaly types". *Journal of climate* 9.11, pp. 2935–2940.
- Gao, Liping, Bo Tao, Yunxuan Miao, Lihua Zhang, Xia Song, Wei Ren, Liyuan He, and Xiaofeng Xu (2019). "A global data set for economic losses of extreme hydrological events during 1960–2014". *Water Resources Research* 55.6, pp. 5165–5175.
- Garreaud, René D and John M Wallace (1997). "The diurnal march of convective cloudiness over the Americas". *Monthly Weather Review* 125.12, pp. 3157–3171.
- Garstang, Michael, Harold L Massie Jr, Jeffrey Halverson, Steven Greco, and John Scala (1994). "Amazon coastal squall lines. Part I: Structure and kinematics". *Monthly Weather Review* 122.4, pp. 608–622.
- Ghate, Virendra P and Pavlos Kollias (2016). "On the controls of daytime precipitation in the Amazonian dry season". *Journal of Hydrometeorology* 17.12, pp. 3079–3097.
- Giannini, A, R Saravanan, and P Chang (2004). "The preconditioning role of tropical Atlantic variability in the development of the ENSO teleconnection: Implications for the prediction of Nordeste rainfall". *Climate Dynamics* 22.8, pp. 839–855.
- Gill, Adrian E (1980). "Some simple solutions for heat-induced tropical circulation". *Quarterly Journal of the Royal Meteorological Society* 106.449, pp. 447–462.
- Greco, Steven, Robert Swap, Michael Garstang, Stanley Ulanski, Mark Shipham, RC Harriss, R Talbot, MO Andreae, and Pedro Artaxo (1990). "Rainfall and surface kinematic conditions over central Amazonia during ABLE 2B". *Journal of Geophysical Research: Atmospheres* 95.D10, pp. 17001–17014.
- Hastenrath, Stefan and Lawrence Greischar (1993). "Circulation mechanisms related to northeast Brazil rainfall anomalies". *Journal of Geophysical Research: Atmospheres* 98.D3, pp. 5093–5102.
- Hirota, Nagio, Yukari N Takayabu, Masahiro Watanabe, and Masahide Kimoto (2011). "Precipitation reproducibility over tropical oceans and its relationship to the double ITCZ problem in CMIP3 and MIROC5 climate models". *Journal of climate* 24.18, pp. 4859–4873. DOI: [10.1175/2011JCLI4156.1](https://doi.org/10.1175/2011JCLI4156.1).
- Hohenegger, Cathy, Luis Kornbluh, Daniel Klocke, Tobias Becker, Guido Cioni, Jan Frederik Engels, Uwe Schulzweida, and Bjorn Stevens (2020). "Climate Statistics in Global Simulations of the Atmosphere, from 80 to 2.5 km Grid Spacing". *Journal of the Meteorological Society of Japan. Ser. II*. DOI: [10.2151/jmsj.2020-005](https://doi.org/10.2151/jmsj.2020-005).
- Hohenegger, Cathy, Linda Schlemmer, and Levi Silvers (2015). "Coupling of convection and circulation at various resolutions". *Tellus A: Dynamic Meteorology and Oceanography* 67.1, p. 26678.
- Holloway, CE, SJ Woolnough, and GMS Lister (2012). "Precipitation distributions for explicit versus parametrized convection in a large-domain high-resolution tropical case study". *Quarterly Journal of the Royal Meteorological Society* 138.668, pp. 1692–1708. DOI: [10.1002/qj.1903](https://doi.org/10.1002/qj.1903).

- Holloway, Christopher E, Steven J Woolnough, and Grenville MS Lister (2013). "The effects of explicit versus parameterized convection on the MJO in a large-domain high-resolution tropical case study. Part I: Characterization of large-scale organization and propagation". *Journal of the Atmospheric Sciences* 70.5, pp. 1342–1369.
- Houze Jr, Robert A (2018). "100 years of research on mesoscale convective systems". *Meteorological Monographs* 59, pp. 17–1.
- Hu, Zeng-Zhen and Bohua Huang (2006). "Physical processes associated with the tropical Atlantic SST meridional gradient". *Journal of climate* 19.21, pp. 5500–5518. DOI: [10.1175/JCLI3923.1](https://doi.org/10.1175/JCLI3923.1).
- Huffman, George J, David T Bolvin, Eric J Nelkin, David B Wolff, Robert F Adler, Guojun Gu, Yang Hong, Kenneth P Bowman, and Erich F Stocker (2007). "The TRMM Multisatellite Precipitation Analysis (TMPA): Quasi-global, multiyear, combined-sensor precipitation estimates at fine scales". *Journal of Hydrometeorology* 8.1, pp. 38–55.
- Jakob, Christian (2010). "Accelerating progress in global atmospheric model development through improved parameterizations: Challenges, opportunities, and strategies". *Bulletin of the American Meteorological Society* 91.7, pp. 869–876.
- Janowiak, John E, Vernon E Kousky, and Robert J Joyce (2005). "Diurnal cycle of precipitation determined from the CMORPH high spatial and temporal resolution global precipitation analyses". *Journal of Geophysical Research: Atmospheres* 110.D23.
- Jones, Todd R and David A Randall (2011). "Quantifying the limits of convective parameterizations". *Journal of Geophysical Research: Atmospheres* 116.D8.
- Judt, Falko and Rosimar Rios-Berrios (2021). "Resolved Convection Improves the Representation of Equatorial Waves and Tropical Rainfall Variability in a Global Nonhydrostatic Model". *Geophysical Research Letters*.
- Junquas, Clémentine, Ken Takahashi, Thomas Condom, J-C Espinoza, Steven Chávez, J-E Sicart, and Thierry Lebel (2018). "Understanding the influence of orography on the precipitation diurnal cycle and the associated atmospheric processes in the central Andes". *Climate dynamics* 50.11, pp. 3995–4017.
- Kalnay, Eugenia, Masao Kanamitsu, Robert Kistler, William Collins, Dennis Deaven, Lev Gandin, Mark Iredell, Suranjana Saha, Glenn White, John Woollen, et al. (1996). "The NCEP/NCAR 40-year reanalysis project". *Bulletin of the American meteorological Society* 77.3, pp. 437–472. DOI: [10.1175/1520-0477\(1996\)077<0437:TNYRP>2.0.CO;2](https://doi.org/10.1175/1520-0477(1996)077<0437:TNYRP>2.0.CO;2).
- Kataoka, Takahito, Masahide Kimoto, Masahiro Watanabe, and Hiroaki Tatebe (2019). "Wind-mixed layer-SST feedbacks in a tropical air-sea coupled system: Application to the Atlantic". *Journal of Climate* 32.13, pp. 3865–3881.
- Kendon, EJ, AF Prein, CA Senior, and A Stirling (2021). "Challenges and outlook for convection-permitting climate modelling". *Philosophical Transactions of the Royal Society A* 379.2195, p. 20190547.
- Kent, Chris, Robin Chadwick, and David P Rowell (2015). "Understanding uncertainties in future projections of seasonal tropical precipitation". *Journal of Climate* 28.11, pp. 4390–4413.
- Kiladis, George N and Klaus M Weickmann (1992). "Circulation anomalies associated with tropical convection during northern winter". *Monthly weather review* 120.9, pp. 1900–1923.
- Klocke, Daniel, Matthias Brueck, Cathy Hohenegger, and Bjorn Stevens (2017). "Rediscovery of the doldrums in storm-resolving simulations over the tropical Atlantic". *Nature Geoscience* 10.12, pp. 891–896.
- Lindzen, Richard S and Sumant Nigam (1987). "On the role of sea surface temperature gradients in forcing low-level winds and convergence in the tropics". *Journal of the*

- Atmospheric Sciences* 44.17, pp. 2418–2436. DOI: [10.1175/1520-0469\(1987\)044<2418:OTROSS>2.0.CO;2](https://doi.org/10.1175/1520-0469(1987)044<2418:OTROSS>2.0.CO;2).
- Love, Barnaby S, Adrian J Matthews, and Grenville MS Lister (2011). “The diurnal cycle of precipitation over the Maritime Continent in a high-resolution atmospheric model”. *Quarterly Journal of the Royal Meteorological Society* 137.657, pp. 934–947.
- Lucena, Daisy Beserra, Jacques Servain, and Manoel Francisco Gomes Filho (2011). “Rainfall response in Northeast Brazil from ocean climate variability during the second half of the twentieth century”. *Journal of Climate* 24.23, pp. 6174–6184. DOI: [10.1175/2011JCLI4194.1](https://doi.org/10.1175/2011JCLI4194.1).
- Mahajan, Salil, R Saravanan, and Ping Chang (2009). “The role of the wind-evaporation-sea surface temperature (WES) feedback in air-sea coupled tropical variability”. *Atmospheric research* 94.1, pp. 19–36.
- Manabe, Syukuro and Robert F Strickler (1964). “Thermal equilibrium of the atmosphere with a convective adjustment”. *Journal of the Atmospheric Sciences* 21.4, pp. 361–385.
- Marengo, Jose Antonio (2006). “On the hydrological cycle of the Amazon Basin: A historical review and current state-of-the-art”. *Revista brasileira de meteorologia* 21.3, pp. 1–19.
- Marengo, José Antonio and Jhan Carlo Espinoza (2016). “Extreme seasonal droughts and floods in Amazonia: causes, trends and impacts”. *International Journal of Climatology* 36.3, pp. 1033–1050.
- Marshall, John H, Nick S Dixon, Luis Garcia-Carreras, Grenville MS Lister, Douglas J Parker, Peter Knippertz, and Cathryn E Birch (2013). “The role of moist convection in the West African monsoon system: Insights from continental-scale convection-permitting simulations”. *Geophysical Research Letters* 40.9, pp. 1843–1849.
- Martinez-Villalobos, Cristian and Daniel J Vimont (2016). “The role of the mean state in meridional mode structure and growth”. *Journal of Climate* 29.10, pp. 3907–3921.
- Masson-Delmotte, V., P. Zhai, A. Pirani, S. L. Connors, C. Péan, S. Berger, N. Caud, Y. Chen, L. Goldfarb, M. I. Gomis, M. Huang, K. Leitzell, E. Lonnoy, J.B.R. Matthews, T. K. Maycock, T. Waterfield, O. Yelekçi, R. Yu, B. Zhou, and (eds.) (2021). “IPCC: Climate Change 2021: The Physical Science Basis”. *Cambridge University Press. In Press. Sixth Assesment Report*, p. 42. URL: <https://www.ipcc.ch/report/ar6/wg1/>.
- Mironov, Dmitrii, Erdmann Heise, Ekaterina Kourzeneva, Bodo Ritter, Natalia Schneider, and Arkady Terzhevik (2010). “Implementation of the lake parameterisation scheme FLake into the numerical weather prediction model COSMO”.
- Mori, Shuichi, Hamada Jun-Ichi, Yudi Iman Tauhid, Manabu D Yamanaka, Noriko Okamoto, Fumie Murata, Namiko Sakurai, Hiroyuki Hashiguchi, and Tien Sribimawati (2004). “Diurnal land-sea rainfall peak migration over Sumatera Island, Indonesian Maritime Continent, observed by TRMM satellite and intensive rawinsonde soundings”. *Monthly Weather Review* 132.8, pp. 2021–2039.
- Myers, Timothy A, Carlos R Mechoso, and Michael J DeFlorio (2018). “Importance of positive cloud feedback for tropical Atlantic interhemispheric climate variability”. *Climate Dynamics* 51.5, pp. 1707–1717.
- Naumann, Ann Kristin, Bjorn Stevens, and Cathy Hohenegger (2019). “A moist conceptual model for the boundary layer structure and radiatively driven shallow circulations in the trades”. *Journal of the Atmospheric Sciences* 76.5, pp. 1289–1306.
- Nobre, Paulo and John Shukla (1996). “Variations of sea surface temperature, wind stress, and rainfall over the tropical Atlantic and South America”. *Journal of climate* 9.10, pp. 2464–2479.

- Oueslati, Boutheina and Gilles Bellon (2015). “The double ITCZ bias in CMIP5 models: interaction between SST, large-scale circulation and precipitation”. *Climate dynamics* 44.3-4, pp. 585–607. DOI: [10.1007/s00382-015-2468-6](https://doi.org/10.1007/s00382-015-2468-6).
- Paccini, Laura, Cathy Hohenegger, and Bjorn Stevens (2021). “Explicit versus parameterized convection in response to the Atlantic Meridional Mode”. *Journal of Climate* 34.9, pp. 3343–3354.
- Penny, Ann Loiuise, Shelley Templeman, Madeline McKenzie, Daniela Tello Toral, and Erin Hunt (2020). *State of the Tropics*. Tech. rep. James Cook University. URL: <https://www.jcu.edu.au/state-of-the-tropics/publications/state-of-the-tropics-2020-report>.
- Pereira Filho, Augusto J, Richard E Carbone, John D Tuttle, Hugo A Karam, et al. (2015). “Convective rainfall in Amazonia and adjacent tropics”. *Atmospheric and Climate Sciences* 5.02, p. 137.
- Peters, Karsten, Cathy Hohenegger, and Daniel Klocke (2019). “Different representation of mesoscale convective systems in convection-permitting and convection-parameterizing NWP models and its implications for large-scale forecast evolution”. *Atmosphere* 10.9, p. 503.
- Phillips, Oliver L, Simon L Lewis, Timothy R Baker, Kuo-Jung Chao, and Niro Higuchi (2008). “The changing Amazon forest”. *Philosophical Transactions of the Royal Society B: Biological Sciences* 363.1498, pp. 1819–1827.
- Prein, Andreas F, Wolfgang Langhans, Giorgia Fosser, Andrew Ferrone, Nikolina Ban, Klaus Goergen, Michael Keller, Merja Tölle, Oliver Gutjahr, Frauke Feser, et al. (2015). “A review on regional convection-permitting climate modeling: Demonstrations, prospects, and challenges”. *Reviews of geophysics* 53.2, pp. 323–361.
- Rayner, NAA, De E Parker, EB Horton, Chris K Folland, Lisa V Alexander, DP Rowell, EC Kent, and A Kaplan (2003). “Global analyses of sea surface temperature, sea ice, and night marine air temperature since the late nineteenth century”. *Journal of Geophysical Research: Atmospheres* 108.D14. DOI: [10.1029/2002JD002670](https://doi.org/10.1029/2002JD002670).
- Rehbein, Amanda, Tercio Ambrizzi, and Carlos Roberto Mechoso (2018). “Mesoscale convective systems over the Amazon basin. Part I: climatological aspects”. *International Journal of Climatology* 38.1, pp. 215–229.
- Richter, Ingo and Hiroki Tokinaga (2020). “An overview of the performance of CMIP6 models in the tropical Atlantic: mean state, variability, and remote impacts”. *Climate Dynamics* 55.9, pp. 2579–2601.
- Richter, Ingo and Shang-Ping Xie (2008). “On the origin of equatorial Atlantic biases in coupled general circulation models”. *Climate Dynamics* 31.5, pp. 587–598. DOI: [10.1007/s00382-008-0364-z](https://doi.org/10.1007/s00382-008-0364-z).
- Rickenbach, Thomas M (2004). “Nocturnal cloud systems and the diurnal variation of clouds and rainfall in southwestern Amazonia”. *Monthly Weather Review* 132.5, pp. 1201–1219.
- Rugg, Allyson, Gregory R Foltz, and Renellys C Perez (2016). “Role of mixed layer dynamics in tropical North Atlantic interannual sea surface temperature variability”. *Journal of Climate* 29.22, pp. 8083–8101.
- Ruiz-Barradas, Alfredo, James A Carton, and Sumant Nigam (2000). “Structure of interannual-to-decadal climate variability in the tropical Atlantic sector”. *Journal of Climate* 13.18, pp. 3285–3297.
- Saravanan, R and Ping Chang (2000). “Interaction between tropical Atlantic variability and El Niño-Southern Oscillation”. *Journal of Climate* 13.13, pp. 2177–2194.

- Satoh, Masaki, Bjorn Stevens, Falko Judt, Marat Khairoutdinov, Shian-Jiann Lin, William M Putman, and Peter Düben (2019). "Global Cloud-Resolving Models". *Current Climate Change Reports*, pp. 1–13. DOI: [10.1007/s40641-019-00131-0](https://doi.org/10.1007/s40641-019-00131-0).
- Schumacher, Courtney, Robert A Houze Jr, and Ian Kraucunas (2004). "The tropical dynamical response to latent heating estimates derived from the TRMM precipitation radar". *Journal of the Atmospheric Sciences* 61.12, pp. 1341–1358.
- Senf, Fabian, Daniel Klocke, and Matthias Brueck (2018). "Size-resolved evaluation of simulated deep tropical convection". *Monthly Weather Review* 146.7, pp. 2161–2182.
- Sherwood, Steven C, Sandrine Bony, and Jean-Louis Dufresne (2014). "Spread in model climate sensitivity traced to atmospheric convective mixing". *Nature* 505.7481, pp. 37–42.
- Siongco, Angela Cheska, Cathy Hohenegger, and Bjorn Stevens (2015). "The Atlantic ITCZ bias in CMIP5 models". *Climate Dynamics* 45.5-6, pp. 1169–1180. DOI: [10.1007/s00382-014-2366-3](https://doi.org/10.1007/s00382-014-2366-3).
- Siongco, Angela Cheska, Cathy Hohenegger, and Bjorn Stevens (2017). "Sensitivity of the summertime tropical Atlantic precipitation distribution to convective parameterization and model resolution in ECHAM6". *Journal of Geophysical Research: Atmospheres* 122.5, pp. 2579–2594. DOI: [10.1002/2016JD026093](https://doi.org/10.1002/2016JD026093).
- Stevens, Bjorn, Claudia Acquistapace, Akio Hansen, Rieke Heinze, Carolin Klinger, Daniel Klocke, Harald Rybka, Wiebke Schubotz, Julia Windmiller, Panagiotis Adamidis, et al. (2020). "The added value of large-eddy and storm-resolving models for simulating clouds and precipitation". *Journal of the Meteorological Society of Japan. Ser. II*.
- Stevens, Bjorn and Sandrine Bony (2013). "What are climate models missing?" *Science* 340.6136, pp. 1053–1054.
- Stevens, Bjorn, Masaki Satoh, Ludovic Auger, Joachim Biercamp, Christopher S Bretherton, Xi Chen, Peter Düben, Falko Judt, Marat Khairoutdinov, Daniel Klocke, et al. (2019). "DYAMOND: the DYNAMICS of the Atmospheric general circulation Modeled On Non-hydrostatic Domains". *Progress in Earth and Planetary Science* 6.1, pp. 1–17.
- Tanaka, LM d S, Prakki Satyamurty, and Luiz Augusto Toledo Machado (2014). "Diurnal variation of precipitation in central Amazon Basin". *International Journal of Climatology* 34.13, pp. 3574–3584.
- Tang, Shuaiqi, Peter Gleckler, Shaocheng Xie, Jiwoo Lee, Min-Seop Ahn, Curt Covey, and Chengzhu Zhang (2021). "Evaluating the Diurnal and Semidiurnal Cycle of Precipitation in CMIP6 Models Using Satellite-and Ground-Based Observations". *Journal of Climate* 34.8, pp. 3189–3210.
- Tanimoto, Youichi and Shang-Ping Xie (2002). "Inter-hemispheric decadal variations in SST, surface wind, heat flux and cloud cover over the Atlantic Ocean". *Journal of the Meteorological Society of Japan. Ser. II* 80.5, pp. 1199–1219.
- Taylor, Michael A, David B Enfield, and A Anthony Chen (2002). "Influence of the tropical Atlantic versus the tropical Pacific on Caribbean rainfall". *Journal of Geophysical Research: Oceans* 107.C9, pp. 10–1.
- Tiedtke, MICHAEL (1989). "A comprehensive mass flux scheme for cumulus parameterization in large-scale models". *Monthly Weather Review* 117.8, pp. 1779–1800. DOI: [10.1175/1520-0493\(1989\)117<1779:ACMFSF>2.0.CO;2](https://doi.org/10.1175/1520-0493(1989)117<1779:ACMFSF>2.0.CO;2).
- Vimont, Daniel J (2010). "Transient growth of thermodynamically coupled variations in the tropics under an equatorially symmetric mean state". *Journal of climate* 23.21, pp. 5771–5789.

- Vimont, Daniel J and James P Kossin (2007). "The Atlantic meridional mode and hurricane activity". *Geophysical Research Letters* 34.7.
- Wang, Jiande and James A Carton (2003). "Modeling climate variability in the tropical Atlantic atmosphere". *Journal of climate* 16.23. [https://doi.org/10.1175/1520-0442\(2003\)016<3858:MCVITT>2.0.CO;2](https://doi.org/10.1175/1520-0442(2003)016<3858:MCVITT>2.0.CO;2), pp. 3858–3876. DOI: 10.1175/1520-0442(2003)016<3858:MCVITT>2.0.CO;2.
- Wu, M, J-E Lee, D Wang, and M Salameh (2021). "Suppressed Daytime Convection over the Amazon River". *Journal of Geophysical Research: Atmospheres*, e2020JD033627.
- Xie, Pingping, Robert Joyce, Shaorong Wu, Soo-Hyun Yoo, Yelena Yarosh, Fengying Sun, and Roger Lin (2017). "Reprocessed, bias-corrected CMORPH global high-resolution precipitation estimates from 1998". *Journal of Hydrometeorology* 18.6, pp. 1617–1641.
- Xie, Shang-Ping and James A Carton (2004). "Tropical Atlantic variability: Patterns, mechanisms, and impacts". *Earth Climate: The Ocean-Atmosphere Interaction, Geophys. Monogr* 147, pp. 121–142. DOI: 10.1029/147GM07.
- Xie, Shang-Ping and S George H Philander (1994). "A coupled ocean-atmosphere model of relevance to the ITCZ in the eastern Pacific". *Tellus A* 46.4, pp. 340–350. DOI: 10.1034/j.1600-0870.1994.t01-1-00001.x.
- Yang, Gui-Ying and Julia Slingo (2001). "The diurnal cycle in the tropics". *Monthly Weather Review* 129.4, pp. 784–801.
- Yin, Lei, Rong Fu, Elena Shevliakova, and Robert E Dickinson (2013). "How well can CMIP5 simulate precipitation and its controlling processes over tropical South America?" *Climate Dynamics* 41.11-12, pp. 3127–3143.
- Zängl, Günther, Daniel Reinert, Pilar Ripodas, and Michael Baldauf (2015). "The ICON (ICOsahedral Non-hydrostatic) modelling framework of DWD and MPI-M: Description of the non-hydrostatic dynamical core". *Quarterly Journal of the Royal Meteorological Society* 141.687, pp. 563–579.
- Zhang, Guang Jun and Michael J McPhaden (1995). "The relationship between sea surface temperature and latent heat flux in the equatorial Pacific". *Journal of climate* 8.3, pp. 589–605.

VERSICHERUNG AN EIDES STATT

Hiermit versichere ich an Eides statt, dass ich die vorliegende Dissertation mit dem Titel: "Sensitivity of resolved convection to ocean and land surfaces in the tropical Atlantic and Amazon basin" selbstständig verfasst und keine anderen als die angegebenen Hilfsmittel – insbesondere keine im Quellenverzeichnis nicht benannten Internet-Quellen – benutzt habe. Alle Stellen, die wörtlich oder sinngemäß aus Veröffentlichungen entnommen wurden, sind als solche kenntlich gemacht. Ich versichere witerhin, dass ich die Dissertation oder Teile davon vorher weder im In- noch im Ausland in einem anderen Prüfungsverfahren eingereicht habe und die eingereichte schriftliche Fassung der auf dem elektronischen Speichermedium entspricht.

Hamburg, October 2021

Laura Giulianna Paccini Peña

Hinweis / Reference

Die gesamten Veröffentlichungen in der Publikationsreihe des MPI-M
„Berichte zur Erdsystemforschung / Reports on Earth System Science“,
ISSN 1614-1199

sind über die Internetseiten des Max-Planck-Instituts für Meteorologie erhältlich:
<http://www.mpimet.mpg.de/wissenschaft/publikationen.html>

*All the publications in the series of the MPI -M
„Berichte zur Erdsystemforschung / Reports on Earth System Science“,
ISSN 1614-1199*

*are available on the website of the Max Planck Institute for Meteorology:
<http://www.mpimet.mpg.de/wissenschaft/publikationen.html>*

